Structure and Timing of the Austerfjord Thrust and Related Shear Zones, Hinnøy, North Norway: Implications for Late-stage Caledonian Tectonic Evolution

by

Thomas Brandon Key

A thesis submitted to the Graduate Faculty of
Auburn University
in partial fulfillment of the
requirements for the Degree of
Master of Science

Auburn, Alabama
August 9, 2010

Approved by

Mark G. Steltenpohl, Chair, Alumni Professor of Geology
Willis E. Hames, Professor of Geology
Ashraf Uddin, Associate Professor of Geology

Abstract

The Austerfjord thrust on central Hinnøy, north Norway is reexamined in its context as the structurally lowest Caledonian thrust preserved in the arctic Norwegian Caledonides. The discovery of the Vassvika group metasedimentary sequence in central Hinnøy, which connects the Austerfjord thrust to the even more internal, and, thus, structurally lower Gullesfjord shear zone 8 km to the west, results in the recognition of the Gullesfjord-Austerfjord shear zone (GASZ). The GASZ is a tops-east-directed thrust duplex that incorporates metasedimentary cover rocks and slivers of granitic basement gneiss. The GASZ has decapitated the domal crest of the Austerfjord antiform, implying that the latter is a pre-Caledonian structure that controlled the somewhat odd geometry of this segment of the basal Caledonian thrust.

A high-temperature, tops-west shear zone, the Sørfjorden shear zone (SSZ) is recognized as a counterpart to a macroscopic northwest-vergent sheath-style back fold that affected the upper and lower plates of the GASZ. ^{40}Ar/^{39}Ar thermochronology reveals that muscovite from the tops-east GASZ records cooling from 420-380 Ma (Scandian), and muscovite from the tops-west SSZ records cooling from 380-370 Ma (Devonian extension). This temporal relationship documents that Caledonian contraction was followed closely by extensional movement in this area of north Norway. Connection to the synchronously developed tops-east Øse thrust requires reassessment of Devonian extension here in the northernmost terminus of the orogen-wide system of Devonian

extensional faults. Observations and data presented herein strongly support that Devonian extension in Lofoten-Vesterålen was accommodated by gravity-driven, foreland- and hinterland-directed movement away from a thermal dome created beneath over-thickened Caledonian crust.

Acknowledgments

I would like to thank my parents for their continual encouragement and financial support throughout my undergraduate and graduate studies. I also thank Dr. Mark Steltenpohl for his special interest in me when I was enrolled in his Structural Geology class, a mentorship that led to my eventual field studies in north Norway and my entry into the graduate program at Auburn. Without funding through research grants, this project would not have been possible; thanks to the College of Science and Mathematics for awarding me an Undergraduate Research Fellowship; to Rob Hargett and Jacob Dunstan for sponsoring an Undergraduate Field-based Mapping Project Grant, which I was awarded; to the Geological Society of America and the Auburn University Graduate School, both of which awarded me Grants-In-Aid of Research; and grants to support travel to conferences to present my research findings were provided by GSA, as well as the Alabama Geological Society. I am also very thankful for Dr. Arild Andresen's (University of Oslo) intellectual, logistical, and financial assistance; for Einar Tveten's (NGU, retired) wealth of knowledge and data, with which he so generously supplied me; and to Aksel Akselsen and Bjørn Gunnar Holand for providing me with field lodging, especially Aksel, who came to my rescue after an unfortunate, field season-ending injury during my second summer on Hinnøy.

Table of Contents

List of Tables

List of Figures

Introduction

<u>Tectonic Setting</u>

The Scandinavian Caledonides formed during the Siluro-Devonian collision and partial subduction of the Baltic margin beneath Laurentia. Deep levels of erosion have exposed Precambrian basement rocks in Lofoten-Vesterålen, north Norway (Fig. 1), that had once occupied the deepest structural positions within the core of the mountain belt. The stack of allochthonous nappes (Lower, Middle, Upper, and Uppermost Allochthons) is preserved mostly on the mainland to the east. The basal thrust to the nappe stack has been variably reported to be exposed somewhere on the eastern part of the island of Hinnøy (Bartley, 1980; Hodges et al., 1982; Björklund, 1987; Rykkelid, 1992). West of the allochthonous rocks, the Lofoten-Vesterålen area is dominated by Archean migmatite gneisses and Proterozoic plutonic rocks of predominantly intermediate to felsic composition. Isolated blocks of metasedimentary and metasupracrustal rocks also occur together with the basement gneisses (Griffin et al., 1978).

This study is focused on the rocks and structures exposed in the area around Gullesfjorden in the central part of Hinnøy (Fig. 1A). The purpose is to reexamine the Austerfjord thrust and Gullesfjord shear zone (Hakkinen, 1977, and Rykkelid, 1992, respectively; Fig. 1B) and several metasedimentary sequences of uncertain origin (Fig. 2). Three highly disparate interpretations have been proposed for the Austerfjord thrust: (1) a Caledonian suture between Baltica and a microcontinental block, that is, the Lofoten

1
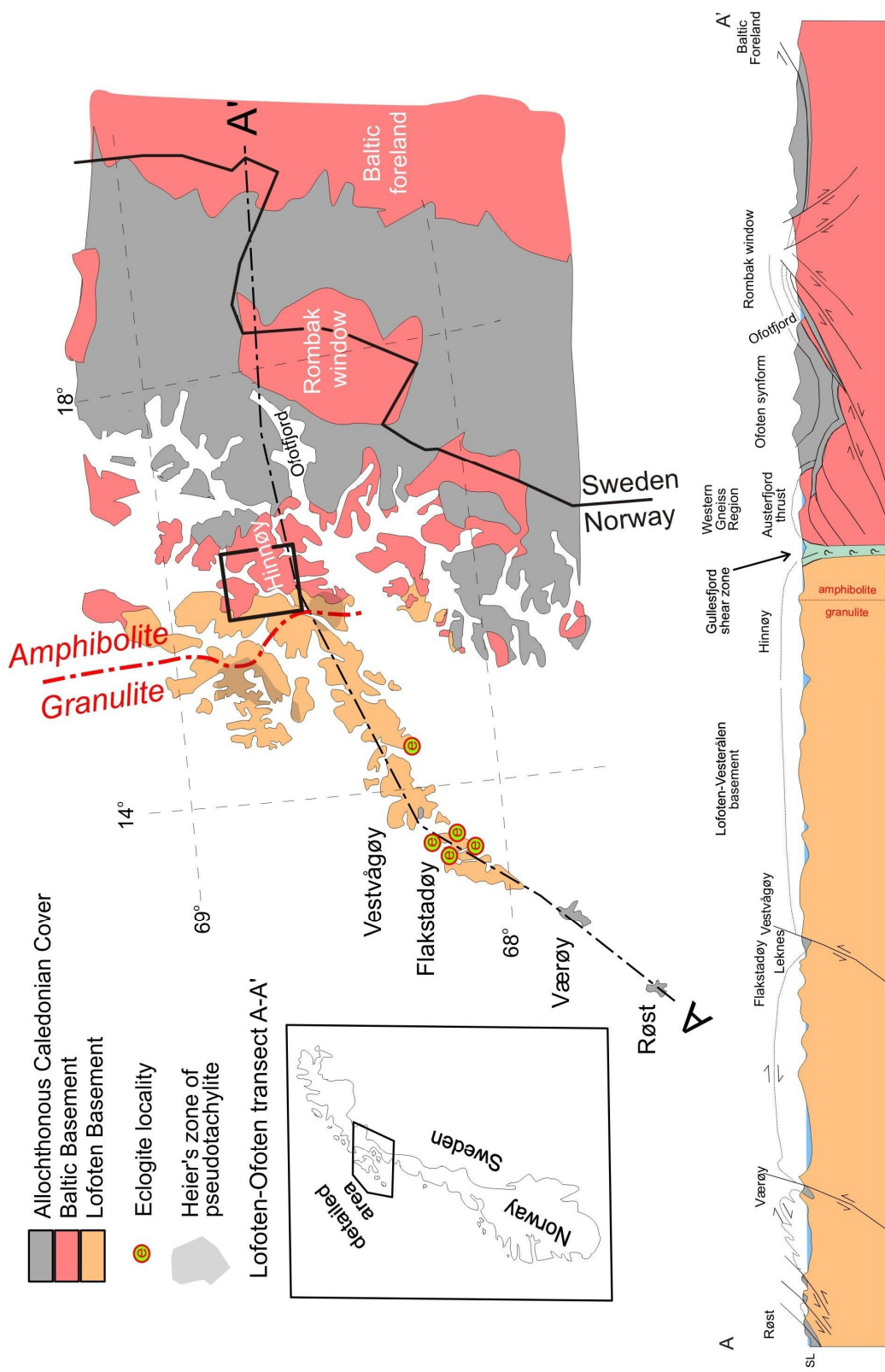
Figure 1. Upper diagram: Generalized tectonic map of Lofoten – Sweden transect showing basement terranes and Caledonian cover. Study area on Hinnøy designated by black box. Lower diagram: Cross-section A-A' shows position of Gullesfjord shear zone and Austerfjord thrust in the area between Baltic and Lofoten basement. (From Steltenpohl et al., 2006).

2

Figure 2. Lithologic map highlighting the three packages of metasedimentary and metasupracrustal rocks in the study area. Gullesfjord and Vassvika groups modified from Tveten (1978, and personal communication 2007). Austerfjord group modified from Hakkinen (1977), Rykkelid (1992), and Tveten (personal communication 2007). Asterisk marks location of sample of Gullesfjord group quartzite from which detrital zircons were separated for U/Pb analysis (discussed below). Geographic names shown on map are referred to throughout the text.

terrane (Hakkinen, 1977); (2) a late fault internal to Baltica that cut the original subduction zone boundary (Hodges et al., 1982; Rykkelid, 1992); or (3) a simple westward continuation of Lower and Middle Allochthon thrusts exposed in the Swedish foreland (Gustavson, 1974; Björklund, 1987). Rykkelid (1992) recognized the Gullesfjord shear zone and interpreted it to be similar in age to the Austerfjord thrust based on parallelism of the structures, similar tops-to-the-east shear fabric, and syn- to post-kinematic amphibolite facies metamorphism. Nothing else is reported about it, however, and no modern studies have documented the absolute timing of either shear zone.

Large volumes of metasedimentary and metasupracrustal rocks in the study area are the Austerfjord group (Hakkinen, 1977), Gullesfjord group (Tveten, 1978), and "Vassvika group" (Tveten, personal communication 2007) (Fig. 2). Their contact relations with the adjacent gneisses have been variably reported as intrusive, faulted, and/or depositional. The convergence of the Austerfjord thrust and Gullesfjord shear zone and these lithologies in this relatively small area (~175 km^2) on central Hinnøy makes this an ideal place to examine (1) how the shear zones interact with one another and with the metasedimentary and metasupracrustal sequences, and (2) the possible origins and correlations of these rocks. Determining the scale and timing of these structures may aid in gaining a better understanding of their significance for tectonic evolution of the northern Scandinavian Caledonides.

Geologic Context

The oldest rocks on central Hinnøy are partially migmatized gneisses that occur mostly in the western part of the study area, and granodioritic gneiss in the central and

eastern parts (Fig. 3). Griffin et al. (1978) reported a Pb/Pb secondary isochron with an age of 2685 ± 65 Ma for quartzofeldspathic migmatites from four localities on northwest Hinnøy, interpreted to indicate an important crustal accretion event around this time. Corfu (2007) reported a U/Pb upper intercept age of 2638 ± 6 Ma on collinear monazite and zircon analyses from a leucosomal portion of the migmatite ca. 5 km west of the area in Figure 2. Corfu (2007) interpreted this date to correspond to the terminal phase of the partial melting event.

The most abundant rock type in the study area is granitic to granodioritic gneiss (Fig. 3). Geochronologic and petrologic studies have indicated that, though local compositional variations in the gneisses range from granitic to granodioritic, there appears to be an older granodiorite gneiss and a younger granitic gneiss (Hakkinen, 1977; Griffin et al., 1978; Corfu, 2004b). However, as Figure 3 illustrates, there is disagreement between workers as to the placement of the contact between the two gneisses. Hakkinen (1977) described and named the Gullesfjord granodiorite gneiss from exposures in his study area (Fig. 3F). Griffin et al. (1978) reported an Rb/Sr whole rock age of ca. 2600 Ma for the Gullesfjord gneiss (northernmost sample in Fig. 3D). Vogt (1941) first described and named the Lødingen granite for exposures on southeast Hinnøy near the town of Lødingen (Fig. 3C). Several attempts to date the Lødingen granite using Rb/Sr whole rock methods yielded ages between 1380 and 1640 Ma (Heier and Compston, 1969; Griffin et al., 1974 and 1978; Taylor, 1974; Andresen and Tull, 1983; Wade, 1985). U/Pb analyses of zircon and titanite from a sample of the Lødingen granite (Fig. 3A) yielded an upper intercept age of 1873 ± 2 Ma (Corfu, 2004b). This age established a temporal link between the Lødingen granite and the earlier of two phases of the anortho-
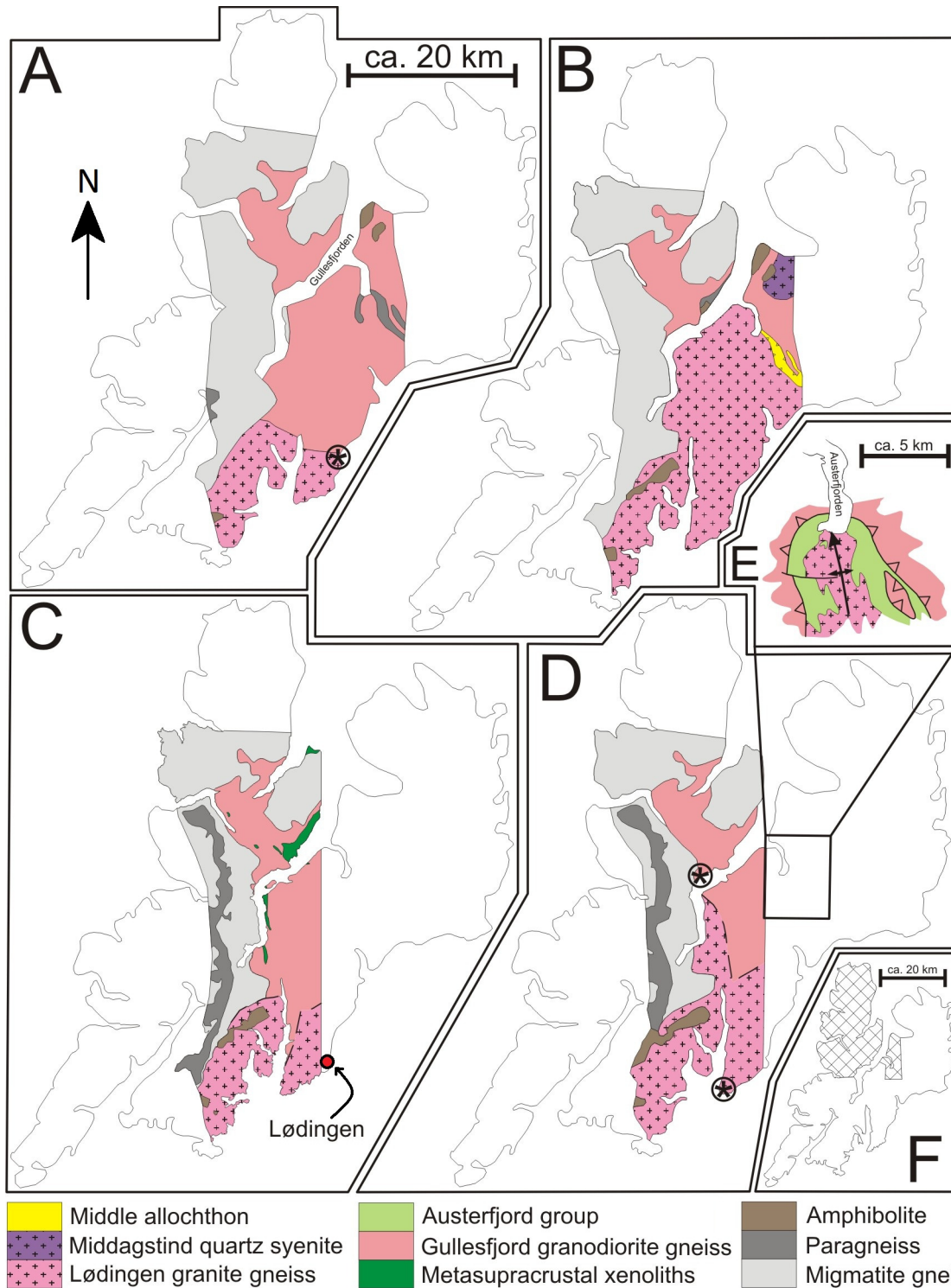
Figure 3. Geologic maps of central Hinnøy with conflicting interpretations of the distribution of crustal rocks, particularly the extent of granodiorite and granite gneisses. (A) Corfu, 2004b; (B) Kautsky, 1987; (C) Tveten, 1978; (D) Griffin et al., 1978; and (E) Bartley, 1980 (simplified from Hakkinen, 1977). (F) Cross-hatching shows map area of Hakkinen (1977). Asterisks in A and D mark geochronological sample locations from previous studies discussed in the text.

6

site-mangerite-charnockite-granite (AMCG) plutonic suite that intruded the Lofoten basement at ca. 1870-1860 Ma; the later, dominant phase of the AMCG suite intruded Lofoten at ca. 1800-1790 Ma (Corfu, 2004b). The younger, 1380-1640 Ma Rb/Sr dates likely reflect isotopic disturbances related to Caledonian overprinting (Corfu, 2004b). High-grade regional metamorphism accompanied the intrusion of the AMCG suite, producing amphibolite-facies assemblages in rocks of the present study area and granulite-facies assemblages to the west, separated by an orthopyroxene isograd (Fig. 1: Griffin et al., 1978; Corfu, 2007).

Also exposed on Hinnøy are several packages of metasedimentary and metasupracrustal rocks that have been interpreted in a variety of ways (Table 1). Relative age determinations have been suggested for several of the packages based on interpreted intrusive or depositional contacts, but tectonic overprinting has rendered most original contact relations equivocal. Many of these groups of rocks are interpreted to have formed prior to Archean or Proterozoic magmatism and thus occur as xenoliths, whereas others are interpreted to correlate with allochthonous Caledonian nappes (Table 1).

The main Scandian phase of Caledonian deformation and metamorphism in the area of Lofoten-Ofoten peaked between ca. 425 and 432 Ma as recorded by lower and upper intercept ages from U/Pb analyses and $^{40}Ar/^{39}Ar$ mineral cooling ages (Coker et al., 1995; Hames and Andresen, 1996; Northrup, 1997; Steltenpohl et al., 2004; Corfu, 2004b and 2007). However, $^{40}Ar/^{39}Ar$ and U/Pb analyses on rocks from farther west on the islands of Vestvågøy and Flakstadøy (Fig. 1), show evidence for Middle-Ordovician, pre-Scandian metamorphism (Steltenpohl et al., 2003b; Corfu, 2004a). Following Scandian, syn-peak metamorphic thrusting, was a phase of south-vergent cross-folding about axes

Lithologic Package	Type Locality	Lithologies	Contacts		Interpretations/ correlations
			Upper(?)	Lower(?)	
Storvann Group[4] (SG)	Northeastern shore of Storvann	-Marble, -quartzite/ meta-arkose, -garnet-quartz-mica schists ± kyanite, -amphibolite (minor)[4]	Thrust[4]	Depositional[4]	-Correlative with Late Proterozoic-Cambrian cover sequence in the Baltic foreland in Sweden[4] -Allochthonous rocks of the Caledonian nappe stack[5,6]
Hesjevann assemblage[4] (HA)	Near Hesjevatn, ca. 3 km northwest of Storvann	-Amphibolite, -quartzite, -calc-silicate marble, -calc-silicate -hornfels(?), -quartz-mica schists[4]	Intrusive[4], thrust[5]	Intrusive[4], depositional[5,6]	-Xenoliths within Proterozoic basement possibly correlative with Gullesfjord group rocks near Flesnes[4] -Autochthonous cover, correlative with Baltic cover in foreland of Sweden, over-thrust by Caledonian allochthon[5,6]
Kvæfjord group[4] (KG)	The head of Kvæfjorden	-Hbl-epidote paragneisses, -semipelitic paragneisses and schists, -rare calc. schists and marbles[4]	Intrusive[4]	Intrusive[4]	-Possibly correlative with early Proterozoic supracrustals of Lofoten[4]
Austerfjord group[1] (AG)	South of Austerfjord (Austerdalen & Aspenesdalen)	-Amphibolite ± garnet, -mica schist ± garnet ± kyanite, -marble, -quartzite[1]	Thrust[1,6]	Intrusive[1], depositional[6]	-Xenolith intruded by 1.8 Ga pluton[1] -Autochthonous cover, correlative with Baltic cover in foreland of Sweden, over-thrust by Caledonian allochthon[6]
Gullesfjord group[3] (GG)	All along Gullesfjorden	-Biotite schist, -quartzite, -amphibolite, -marble[1,3]	Fault[6], intrusive[2,3]	Intrusive[2,3]	-Xenoliths within Archean (2.7 Ga) Gneisses[2,3]
Vassvika group[7] (VG)	Ridge east of Vassvika	-Biotite schist, -amphibolite[7]	Fault[7]	Fault[7]	-Correlative with amphibolite and biotite schist units of Austerfjord group[7]

Table 1. Metasedimentary packages and problems related to their various interpretations and correlations. See Figure 2 for locations of AG, GG, and VG. SG, HA, and KG occur outside of the study area. [1]Hakkinen, 1977; [2]Griffin et al., 1978; [3]Tveten, 1978; [4]Bartley, 1980; [5]Björklund, 1987; [6]Rykkelid, 1992; [7]Tveten, personal communication 2007.

transverse to the trend of the mountain system that Steltenpohl and Bartley (1988) interpreted to relate to sinistral shearing. Northwest-vergent back-folds (Steltenpohl and Bartley, 1988) and westward-directed backsliding along the reactivated basal thrust (Fossen and Rykkelid, 1992) represent the first stages of late- to post-orogenic extension that affected rocks in the area from the Early to Middle Devonian through the Permian. Absolute timing of uplift and extension is recorded by $^{40}Ar/^{39}Ar$ cooling ages for hornblende and muscovite (Coker et al., 1995; Steltenpohl et al., 2004; Key et al., 2007; Steltenpohl et al., 2009). Brittle faulting related to Mesozoic rifting and Eocene continental separation appear to be the latest tectonic events to have affected rocks of the Lofoten region (Bergh et al., 2007a; Steltenpohl et al., 2009) prior to extensive glaciation that exposed the current structural levels in the area.

Previous Work and Justification

The Austerfjord thrust was first recognized by Tull (1973), and subsequently described in detail by Hakkinen (1977). Hakkinen (1977) interpreted it to have emplaced the Gullesfjord granodiorite gneiss above the Austerfjord group metasedimentary package, which is exposed in a granite-cored, north-plunging anticline at the head of Austerfjorden (Fig. 3E). The base of the Austerfjord group was interpreted to have been intruded by the granite, which Hakkinen (1977) reported as continuous with the Lødingen granite ca. 30 km to the south. Later, Rykkelid (1992) interpreted the basal Austerfjord group contact to be depositional, thereby requiring at least the lowest unit of the metasedimentary package to be autochthonous cover.

Hakkinen (1977) interpreted the contact between the Gullesfjord granodiorite (structurally above) and Lødingen granite (structurally below) at the extreme southern end of his map area as a thrust fault (Figs. 3E and F). Tveten (1978) also inferred a late fault to have overprinted the original contact between the two gneisses, though he placed the boundary much further to the south (Fig. 3C). The nature of this boundary is not specifically addressed elsewhere, and the presence of a fault along the contact between similar granites might prove to be difficult to recognize in the field.

Hakkinen (1977) interpreted the Austerfjord thrust as the east-directed (tops toward the foreland) Caledonian suture between the western Baltic margin and a micro-continental fragment that now represents the basement exposed in the Lofoten islands (Fig. 1). Hodges et al. (1982), on the other hand, interpreted the Austerfjord thrust as a late-stage, lower-plate-rooted thrust that imbricated the original subduction zone boundary as part of their A-type subduction model (Fig. 4A). In this model, faults formed subsequent to initial plate convergence propagate successively in a foreland direction from within the down-going plate. Rykkelid (1992) also inferred the timing of movement along the Austerfjord thrust as having succeeded the basal Caledonian thrust, cutting it from a hinterland direction in an out-of-sequence fashion (Fig. 4B). The models of both Hodges et al. (1982) and Rykkelid (1992) place the Austerfjord thrust within the Baltic plate, such that Lofoten basement is the western edge of Baltica. Gustavson's (1974) and Björklund's (1987) models correlate the Austerfjord thrust to the Lower and Middle Allochthon thrusts exposed in the Swedish foreland, requiring that they are continuous beneath the Caledonian nappe stack to the east.
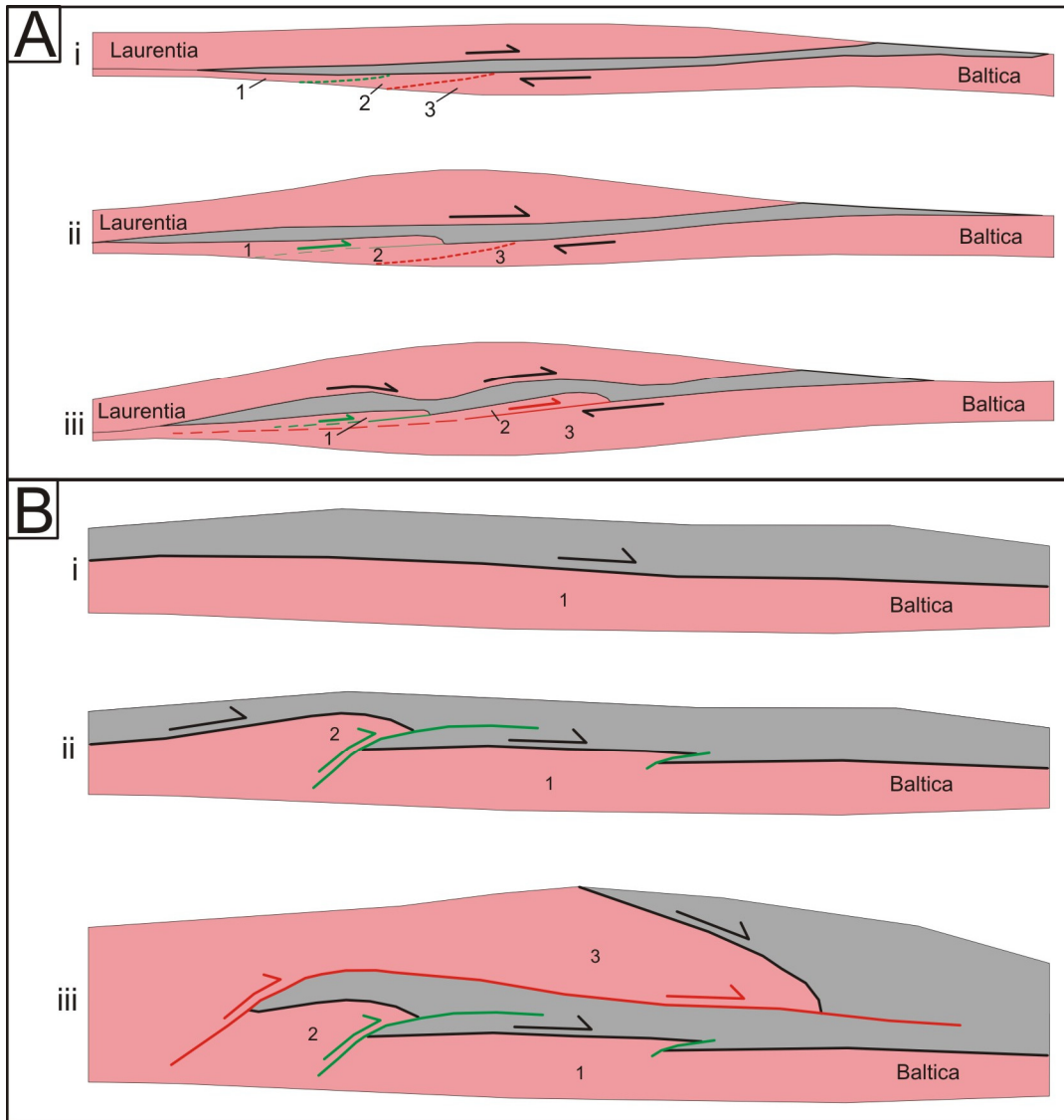
Figure 4. Cartoon drawings of the evolution of (A) A-type subduction model (from Hodges et al., 1982) and (B) out-of-sequence thrust model (after Rykkelid, 1992). Pink represents continental basement and gray represents accretionary rocks in the subduction zone. Green lines represent the first faults to form after emplacement of accretionary rocks. Red lines represent the last faults to form. Numbers indicate the sequence of lower-plate imbrication.

The Gullesfjord shear zone (Rykkelid, 1992), which approximately parallels the north-south trending arm of Gullesfjorden, is located near the Austerfjord thrust and, thus, similarly has been implicated as the transitional boundary between Lofoten and Baltic basement (Steltenpohl et al., 2006; Fig. 1: cross-section). Early workers interpreted the metasedimentary units in the Gullesfjord shear zone, the Gullesfjord group (Fig. 2), as supracrustal xenoliths within the Archean-Palaeoproterozoic basement complex (Griffin et al., 1978; Tveten, 1978). Rykkelid (1992) agreed with the interpretation that the Gullesfjord group rocks were xenoliths; however, he interpreted the present-day upper (eastern) contact of the Gullesfjord group south of Forøya (Fig. 2) as an east-dipping ductile extensional shear zone. The contacts of the Gullesfjord group north of Gullesfjorden near Flesnes (Fig. 2) have been reported as either intrusive (Tveten, 1978) or as intrusive with later fault movement having overprinted the primary igneous relations (Hakkinen, 1977). Hakkinen (1977) provided no estimates as to the magnitude or sense of movement along the contacts.

Recent LA-ICP-MS U/Pb isotopic analysis of detrital zircon populations from a sample of orthoquartzite from the Gullesfjord group southwest of Flesnes (Fig. 2) is dominated, surprisingly, by 1100 and 1350 Ma ages (~90%) with older, much less abundant ages of 1850, 2500, and 2700 Ma (Steven Braun, Vanderbilt University; Steltenpohl et al., 2010). Lofoten, therefore, clearly cannot be the source of most of the detrital zircons; and, though ~1100 Ma ages (Early Sveconorwegian) have been documented in southwest Norway (Bingen et al., 2008), the source of ~90% of these zircons must have been must have been much more proximal to the depocenter than such a correlation would require. The 1100 Ma population (Grenvillian) necessitates

Neoproterozoic or younger deposition of the quartz sandstone protolith, and combined with the 1350 Ma population (similar ages exist in the Laurentian of Scotland and the Hebrides; e.g., Cawood et al., 2003), it appears to be of Laurentian origin. The quartzite and associated marbles could correlate with rocks in the cover nappe stack in the Ofoten synform to the east, where the Uppermost Allochthon has been suggested to have originated from the Laurentian margin (Stephens et al., 1993; Roberts, 2003; Steltenpohl et al., 2003a and 2003b). If this is the case then a tremendous thickness of rock is missing across the contact between the quartzite and the Lofoten basement.

Mapping performed in conjunction with this study, as well as data from Tveten (personal communication, 2007), has revealed previously undescribed metasedimentary units in this area, referred to here as the Vassvika group. Their location and lithologic similarities to certain units of the Austerfjord group present significant implications for resolving current models for the Austerfjord thrust. The structural and geographic position of the Vassvika group relative to the Gullesfjord and Austerfjord groups serve as further impetus for reevaluation of age relations, provenance, and correlations of the metasedimentary sequences.

Field studies during summers 2007 and 2008 demonstrated that most of the conflicting interpretations for geologic relations exposed in central Hinnøy partly result from tenuously documented and contradicting field interpretations. Also, during the 2007 field season, we discovered an enormous, high temperature shear zone, herein called the Sørfjord shear zone (Fig. 2), that interacts with the Austerfjord thrust. The Sørfjord shear zone is marked by a distinctive L-tectonite, and it plunges to the southeast beneath the Vassvika group south of Gullesfjorden. This thesis study aims to constrain the

relationship between the Austerfjord thrust, the Sørfjord and Gullesfjord shear zones, and the various packages of metasedimentary rocks in this area based on structural and petrographic investigation and ^{40}Ar/^{39}Ar isotopic analyses.

Thesis Objectives and Methods of Investigation

Three objectives of the present study in the Austerfjord-Gullesfjord area are as follows: (1) to map and describe structures reported or suspected to be of Caledonian age; (2) to sample and describe the units composing metasedimentary sequences; and (3) to constrain the relative and absolute timing of fabric development and thermal history of major structures.

Geologic mapping was performed using 1:50,000 scale topographic base maps in the areas where discrepancies among previous maps and interpretations exist, and to characterize contact relationships of lithologic units and the kinematics and geometries of their structures. A Brunton compass was used for structural data collection. A handheld GPS unit was used to record the UTM coordinates of field stations. Structural data collected during the 2007 and 2008 field seasons were compiled with existing data from Hakkinen (1977) and Tveten (pers. comm. 2007 and 2008) to produce contoured lower-hemisphere stereoplots (using Rockware® and Stereowin®), a structural form line map for an analysis of dominant trends of the orientations of planar fabric elements, and a compilation geologic map.

Sample collecting for laboratory analysis focused on metasedimentary units and rocks defining major mylonitic shear zones. Of particular interest were mylonitic rocks that might contain meso- and microstructural indicators of shear sense and conditions of

deformation, and those containing muscovite that could be analyzed using ^{40}Ar/^{39}Ar isotopic methods for dating purposes.

Thin sections were commercially made of oriented structural samples and otherwise general lithologic samples. Petrographic microscopes at Auburn University were used to perform microstructural and kinematic analyses of oriented samples, and mineralogical and textural analyses of representative suites of metasedimentary and metaplutonic basement gneiss samples. Microstructural analyses were performed in order to characterize the modes and degrees of deformation experienced by the rocks and their constituent minerals. Kinematic analyses were performed in order to determine sense of movement along shear zones. Petrographic analyses of representative lithologies from the field area were performed for the purpose of comparison and correlation among units. To this end, the author's own observations and descriptions of the basement gneiss and units of the Gullesfjord and Vassvika groups were compared to those of the Gullesfjord granodiorite gneiss and Austerfjord group, respectively, made by Hakkinen (1977).

Muscovite grains were separated from mylonitized samples of rock from within the Austerfjord thrust, and Gullesfjord and Sørfjord shear zones. They were dated using ^{40}Ar/^{39}Ar Single Crystal Total Fusion methods in the Auburn Noble Isotope Mass Analysis Lab (ANIMAL) at Auburn University, under the supervision of Dr. W.E. Hames. The analyses were performed in an attempt to constrain the timing of movement and cooling history of the shear zones.

Rock Units

<u>Introduction</u>

Rock units in the study area traditionally have been summarized as follows: Archean migmatites, Archean gneisses and supracrustal xenoliths, Proterozoic felsic plutonic rocks, and Caledonian allochthonous rocks comprising sequences of metasediments and interleaved basement gneiss. Figure 5 is a lithologic map of the study area. Table 2 provides a general outline of the crustal evolution of rocks in this region as the author has established by the integration of age determinations (Hakkinen, 1977; Griffin et al., 1978; Bartley, 1981; Corfu, 2004b; Steven Braun, Vanderbilt University, personal communication 2009) with field relationships.

Three large areas of metasedimentary sequences on central Hinnøy, the Austerfjord, Vassvika, and Gullesfjord groups, have been previously mapped and described. The sequences have been subdivided into distinct units by Hakkinen (1977), Tveten (personal communication 2008), and the present author. Plastic deformation has resulted in the attenuation and/or excision of many of these units along strike. Gullesfjorden parallels and masks many units from surface exposure. Exposures are also lacking in many large marshy areas. Distinctive lithologies were delineated within each package of metasedimentary rocks. Lithologic associations and sequences within each of the groups were also established as criteria that might aid in correlation.
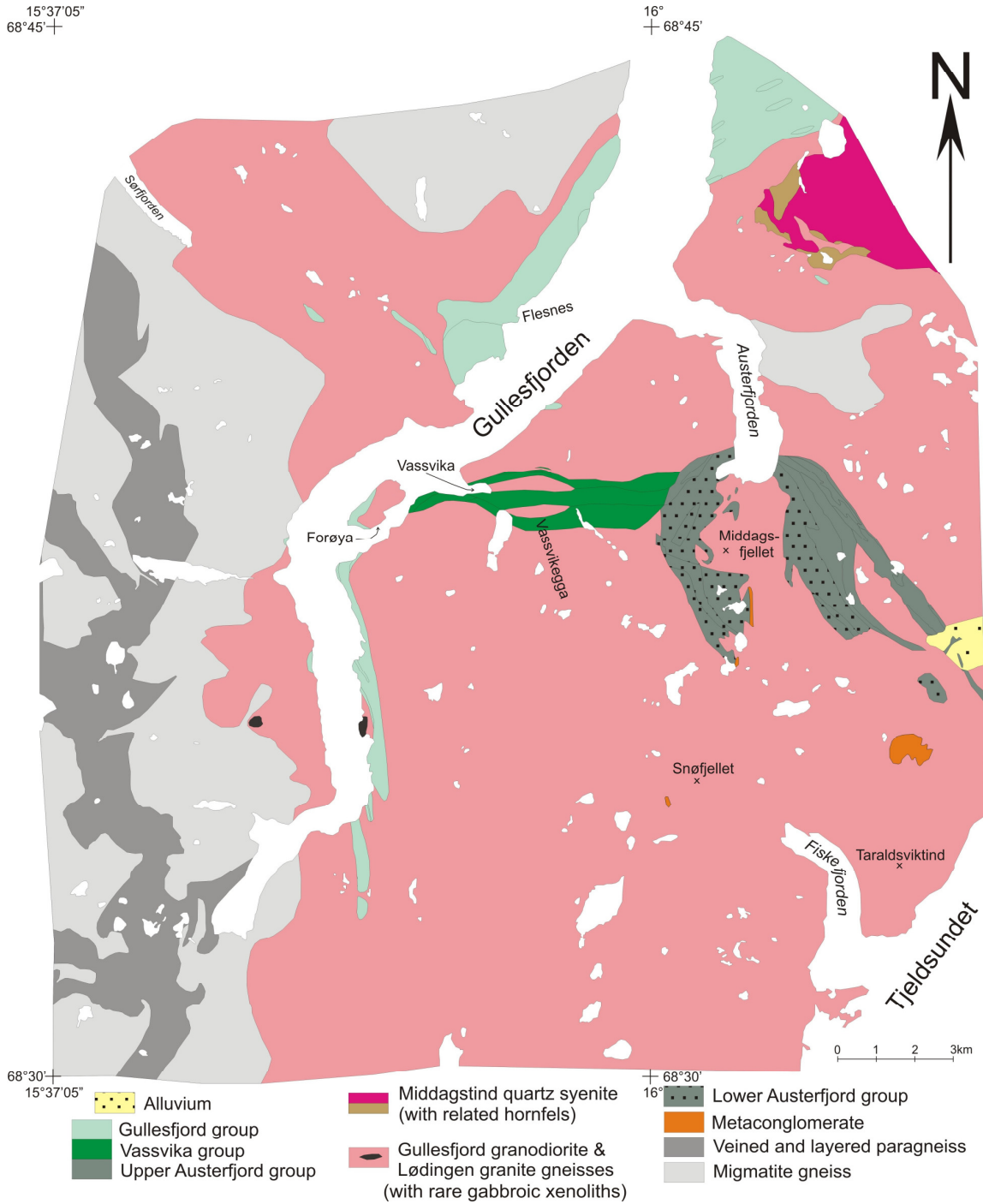
Figure 5. Generalized lithologic map of central Hinnøy showing the major rock units and metasedimentary packages. Modified from Hakkinen (1977), Rykkelid (1992), Tveten (personal communication 2008), and the present study.

Major Rock Units		
Gullesfjord group including quartzite at Flesnes[3]	< 1100 Ma[7]	Layers of (garnet) mica schist, biotite gneiss, marble, amphibolite, quartzite and lenses of sheared granite. Schistosity parallels compositional layering.[3,8]
Vassvika group	?	Layers of amphibole-biotite schist with marble, quartzite, garnet mica schist, amphibolite, biotite gneiss and lenses of sheared granite. Schistosity parallels compositional layering.[8]
Upper Austerfjord group	?	Layers of (garnet) mica schist amphibolite, marble, and quartzite. Ubiquitous schistosity parallel to compositional layering.[1]
Middagstind quartz syenite[4]	1726 ± 97 Ma[4]	Massive, unfoliated pluton with associated hornfels[4]
Lødingen granite gneiss	1873 ± 2 Ma[6]	Fine to coarse-grained, weakly to well foliated granitic gneiss.[1,5] Microcline porphyroblasts(?) up to a few cm in diameter.[5]
Gullesfjord granodiorite gneiss[1]	ca. 2600 Ma (based on low $^{87}Sr/^{86}Sr$)[2]	Granodiorite gneiss with multiple foliations resulting in outcrops of heterogeneous textural character[1]
Lower Austerfjord group	Intruded by Lødingen(?) granite[1,8]	Layers of biotite schist (± chlorite, kyanite, and garnet) with schistosity parallel to compositional layering[1]
Veined and layered paragneiss[1]	>ca. 2640 Ma[6]	Finely layered, fine grained gneiss with numerous pegmatitic stringers. Contains thin iron-rich and calcareous-rich layers.[1]
Migmatite gneiss[1]	ca. 2700 Ma[2]	Heterogeneous, coarse-grained migmatites and banded gneisses[1]

Table 2. Relative sequence of crustal evolution of basement lithologies adapted from [1]Hakkinen (1977) with additional data from [2]Griffin et al. (1978), [3]Tveten (1978), [4]Bartley (1981), [5]Andresen and Tull (1983), [6]Corfu (2004b), [7]Steven Braun (personal communication 2009), and [8]the present study. Relative positions of the Gullesfjord, Vassvika, and upper Austerfjord groups are conjectural, as their absolute ages are undetermined.

Since a main objective of this project was the focused mapping of key structures and related rocks, the author has relied on existing reports that address rock units not found to be directly involved with the formation of structures in the area; some previously reported descriptions, therefore, are briefly summarized. The reader is directed to those works for further petrographic and geochemical information; specifically, the migmatite gneiss (Hakkinen, 1977; Griffin et al., 1978), the veined and layered paragneiss (Hakkinen, 1977), the Lødingen granite (Hakkinen, 1977; Andresen and Tull, 1983), the Middagstind quartz syenite (Bartley, 1981), and the Austerfjord group (Hakkinen, 1977).

Migmatite and Veined and Layered Gneisses

The migmatite gneiss is found mostly in the western part of the map area and in small areas in the north and east (Fig. 5). The veined and layered paragneiss is found only in association with the western exposures of migmatite (Fig. 5).

The migmatite gneiss is typically gray (white when weathered), and generally granodioritic to quartz monzonitic in composition (Hakkinen, 1977). The rocks have a variable grain size and mafic mineral content, and range in overall texture from chaotically migmatitic to broadly banded. Small, discontinuous layers of amphibolite and marble may occur in this unit (Hakkinen, 1977). Geochemical studies indicate that these migmatites are the lower-grade, amphibolite-facies equivalent of the granulite-facies migmatites found west of the field area on Langøy (Griffin et al., 1978).

The veined and layered paragneiss is predominantly composed of quartz, plagioclase, and biotite with little to no potassium feldspar (Hakkinen, 1977). Hakkinen

(1977) inferred what little potassium feldspar is present within the rocks to have originated in microcline-rich pegmatites and aplite dikes observed to have intruded the unit. The dikes are most abundant near the contacts with the migmatite gneiss. This rock type is differentiated from the migmatite gneiss by its finer grain size, finer and more continuous laminations, and more distinct segregation of mafic and felsic minerals. Hakkinen (1977) interpreted the presence of iron-rich and calcareous layers to suggest a sedimentary origin (paragneiss), but geochemical studies indicate a volcanogenic origin (Krogh, 1976) with calc-alkaline affinity (Griffin et al. 1978).

Griffin et al. (1978) interpreted the veined and layered paragneiss to be the primary cover to the migmatite protolith. The contact between the two is predominantly a diffuse zone thought to have been caused by the latest phase of *in situ* anatectic remobilization in the migmatite, which resulted in the incorporation of blocks of the veined and layered gneiss within the migmatite (Hakkinen, 1977).

Gullesfjord Granodiorite and Lødingen Granite Gneisses

The 2.6 Ga Gullesfjord granodiorite and 1.8 Ga Lødingen granite gneisses compose roughly 75% of the map area, yet there is confusion as to where one stops and the other begins (Fig. 5). Both the Gullesfjord and Lødingen gneisses are enormous intrusive bodies, and variability of original magmatic compositions likely accounts for the compositional heterogeneity observed within each of these units. There is a high degree of compositional overlap between the two, such that the rocks can be mineralogically identical, which has complicated attempts to delineate a distinct field boundary between these two bodies of vastly different aged plutonic rock. Textural

variations in both gneisses range from massive, nearly igneous-looking to progressively more gneissic/mylonitic with proximity to shear zones. Workers have interpreted the aerial extents of the two gneisses on central Hinnøy in many different ways without much consensus (see Fig. 3). A fairly representative suite of samples of granitic gneiss from across the map area collected during this study was petrographically analyzed (Fig. 6). Findings are combined with those of Hakkinen (1977) and Andresen and Tull (1983) to more thoroughly characterize the granitic rocks. Discussions of the Gullesfjord granodiorite and Lødingen granite gneisses are, therefore, presented together.

Hakkinen (1977) described exposures of the Gullesfjord granodiorite gneiss from north of Gullesfjorden, along the southern shore of the fjord, and from the Austerfjord area (Fig. 2). These rocks are medium- to coarse-grained, pinkish-colored with microcline porphyroblasts slightly larger than the equigranular quartz, plagioclase, microcline, biotite matrix, which is consistent with findings from the present study. Throughout these areas, the rock type varies texturally from weakly foliated to highly schistose with a prominent muscovite foliation (Hakkinen, 1977), to an L-tectonite with an intense rodding lineation defined by aggregates of quartz and microcline (Fig. 7).

Modal analysis of samples of the Gullesfjord gneiss (Hakkinen, 1977) indicates volumetric compositions of 26.5 to 38.5% quartz, 27 to 57% plagioclase, and 4.5 to 40% microcline (Fig. 8). Hakkinen (1977, p. 31) classified the gneiss as a granodiorite based on the fact that for most samples plagioclase was usually dominant over "potash" feldspar, but he stated that "the difference in percentage between the two mineral constituents is so slight that the rock is essentially a granite." In fact, the average of quartz (Q), alkali feldspar (A), and plagioclase (P) values determined from his modal

21
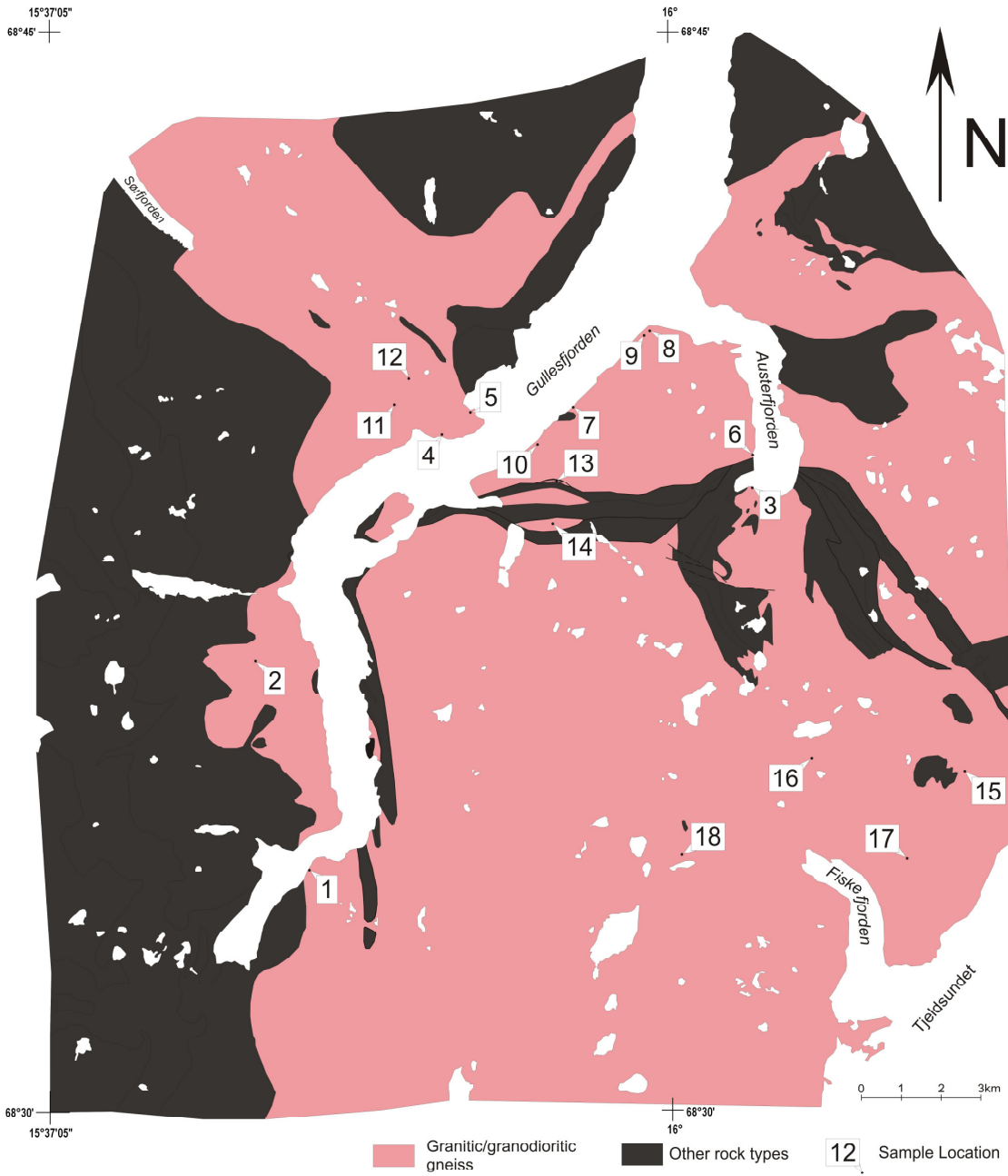
Figure 6. Locations of samples of gneiss that were petrographically analyzed.

Figure 7. Orthogonally slabbed and polished L-tectonite from the core of the Sørfjord shear zone (Fig. 2). The two right-hand faces are cut parallel to the pencil lineation, and the view on the perpendicular face shows the complete lack of a planar fabric within the rock.
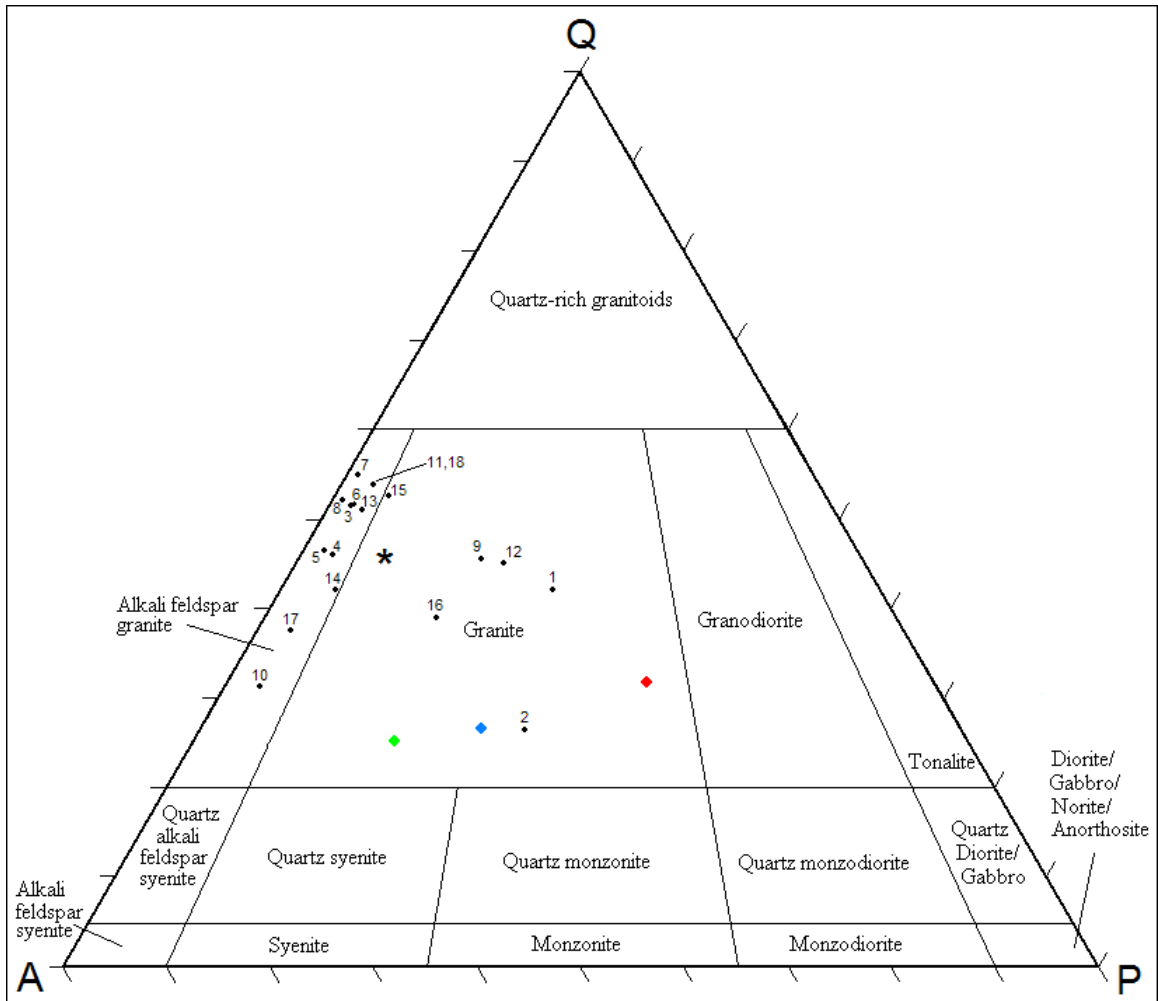
Figure 8. Ternary diagram of quartz (Q), alkali feldspar (A), and plagioclase (P) content of 18 samples of granitic gneiss. Volumetric percentages were visually estimated and normalized to 100%. Numbers correspond to sample locations in Figure 6. Asterisk is the average composition of the 18 samples that were analyzed for this study. Red diamond is the average composition of samples of Gullesfjord granodiorite determined from modal analysis performed by Hakkinen (1977). Green diamond is the average composition of samples of Lødingen granite reported by Andresen and Tull (1983). Blue diamond is the average composition of the granite south of Austerfjorden that Hakkinen (1977) correlated with the Lødingen granite. Diagram modified from original created with Tri-plot (Graham and Midgley, 2000).

analysis plots in the 'granite' field of the IUGS Q-A-P ternary diagram for intrusive rocks (Fig. 8).

Hakkinen (1977) and Griffin et al. (1978) interpreted an Rb-Sr whole rock age of ca. 2600 Ma as the time of intrusion for the Gullesfjord granodiorite into the migmatite gneiss (northern sample locality in Fig. 3D). The low initial $^{87}Sr/^{86}Sr$ ratio of <0.700 was interpreted to indicate intrusion of a primitive magma rather than one derived from anatexis of ancient crustal rocks (Griffin et al., 1978).

Vogt (1941) first described the Lødingen granite gneiss for exposures near the town of Lødingen on southeast Hinnøy, about 10 km south of the present study area (Fig. 3C). Hakkinen (1977) correlated the white to gray, medium- to coarse-grained granitic gneiss forming the core of the Austerfjord anticline (Fig. 3E) with the Lødingen granite gneiss ca. 30 km to the south. South of Austerfjorden, the granite gneiss comprises 25 to 30% quartz, 25 to 30% plagioclase and 40 to 45% microcline (Hakkinen, 1977; Fig. 8). Field and petrographic findings of Andresen and Tull (1983) led them to interpret the Lødingen granite to extend from Lødingen as far north as Fiskefjorden. Their petrographically determined compositions for ten samples of weakly- to well-foliated, fine- to medium-grained Lødingen granite gneiss averaged 24 to 29% quartz, 13 to 29% plagioclase, and 47 to 63% microcline (Fig. 8: Andresen and Tull, 1983). A distinctive characteristic of the gneiss from this area are large (up to 2 cm) flesh-colored potassium feldspar megacrysts (Andresen and Tull, 1983). The present author observed similar rocks in the areas between Fiskefjorden and exposures of the Austerfjord group metasediments to the north, and along the north-south trending ridge directly east of the southern exposures of the Gullesfjord group metasediments (Fig. 5). As illustrated in

25

Figure 3, the rocks in these areas have been reported as either or both the Gullesfjord gneiss and the Lødingen gneiss.

Given the similar field and mineralogical characteristics of the Gullesfjord and Lødingen gneisses, a comprehensive analysis of the geochemical nature of the granitic rocks across the study area would be required to separate them, but such an approach was outside the scope of the present study. No distinct boundary between the gneisses was observed by the author, so results from petrographic analysis of samples of granitic rocks from across central Hinnøy are plotted together in Figure 8. Visual estimations (i.e., no point counts were performed) of the major mineralogical constituents (i.e., quartz, microcline, and plagioclase) of 18 samples from this study yielded 26 to 55% quartz, 22 to 65% microcline, and 1 to 32% plagioclase, compositions that plot in the granite and alkali feldspar granite fields (Fig. 8). These compositions are much more quartz-rich than has been previously reported. This might be an artifact, however, caused by the difficulty in identifying plagioclase when grains are not twinned. In many cases, plagioclase was identified in thin section based on the observation of concentric zonation and/or clouding of grains due to saussuritization or sericitization (e.g., samples 1, 2, 9, 12, and 16; Fig. 8). There does not appear to be much correlation between geographic location and modal composition. Justifications of previous workers' interpretations of the location of the boundary between the two gneisses are, therefore, considered with the new structural data to better clarify the extent of the two distinctly different aged gneisses.

Hakkinen (1977) recognized a major thrust fault in the southern part of his map area (Fig. 3E), the Austerfjord thrust, and interpreted it to have emplaced the Gullesfjord and migmatite gneisses above the Austerfjord group metasedimentary rocks and the

Lødingen granite that had intruded them. South of the metasediments in the western limb of the Austerfjord anticline, a contact between two separate gneisses has not been observed. The paucity of evidence to support Hakkinen's (1977) interpretation of a thrust contact along the western limb of the anticline south of the intersection of the Vassvika and Austerfjord group rocks (Fig. 5) calls into question the actual existence of two different rock types in this area. Tveten (1978) inferred a late tectonic contact south of the present study area (Fig. 3C) to have overprinted an original intrusive relationship between the 2.6 Ga Gullesfjord and 1.8 Ga Lødingen gneisses. Griffin et al. (1978) also place the contact to the southeast of Gullesfjorden (Fig. 3D), but they do not describe the nature of the boundary. The lack of data supporting the interpretation for a fault defining the western limb of the Austerfjord anticline, coupled with the recognition of the Vassvika group rocks extending westward from the nose of the anticline, implies continuity of the granitic rocks south of the Vassvika group metasediments. The strongly deformed metasediments and basement slivers of the Gullesfjord group, the Vassvika group, and the upper units of the Austerfjord group must represent a significant tectonic boundary across central Hinnøy (discussed below), and the present author interprets it to be the most likely contact between the Gullesfjord and Lødingen gneisses (Fig. 9).

Middagstind Quartz Syenite

A massive, unfoliated pluton in the northeast corner of the map area, the Middagstind quartz syenite, has a hornsfelsic contact aureole and cuts structures in Gullesfjord gneiss, Kvæfjord group, and Hesjevann assemblage wall rocks (Bartley, 1981; Fig. 9). This rather homogeneous pluton is generally pink to tan with rounded dark
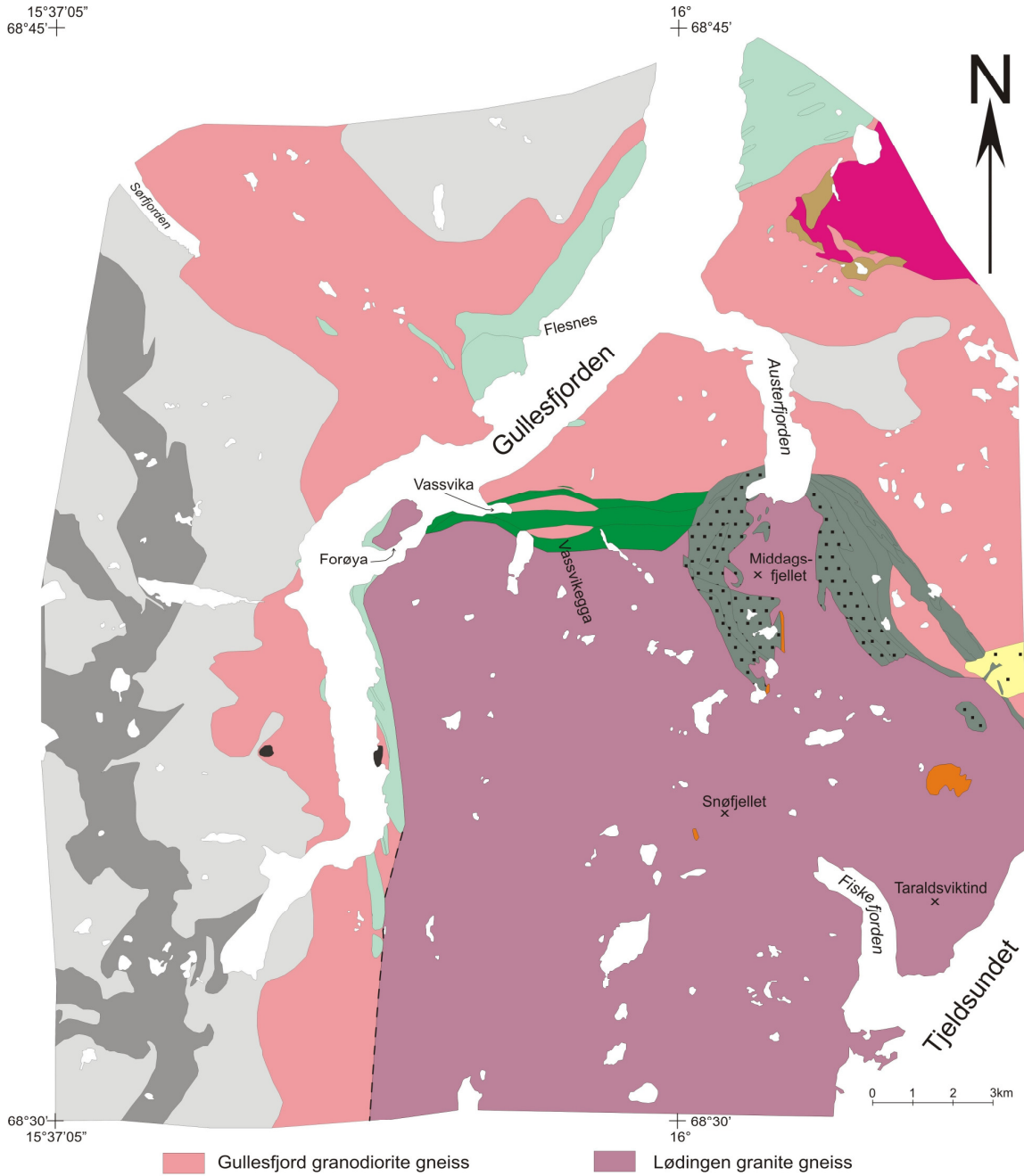
Figure 9. Lithologic map of central Hinnøy illustrating the hypothesized extents of the Gullesfjord granodiorite and Lødingen granite gneisses. The zone of strongly deformed Gullesfjord, Vassvika, and upper Austerfjord group metasediments is interpreted as the most likely contact between the two gneisses. Other lithologic symbols are the same as in Figure 5. Modified from Hakkinen (1977), Rykkelid (1992), Tveten (personal communication 2008), and the present study.

clusters of mafic minerals (biotite and amphibole) ca. 5 mm across. The syenite comprises 50 to 70% perthitic microcline, 15 to 35% plagioclase, and minor quartz. Bartley (1981) reported an Rb/Sr whole rock age of 1726 ± 97 Ma, which he interpreted to reflect the time of initial igneous crystallization. This age is compatible with the dominant phase of the AMCG suite that intruded the Lofoten-Vesterålen basement. The occurrence of the Middagstind quartz syenite has been interpreted to extend the Lofoten terrane farther east to contact the Caledonian allochthons, arguably supporting its pre-Caledonian continuity with Baltic basement (Bartley, 1981).

Caledonian Allochthonous Rocks

Three sequences of metasedimentary rocks that occur in the study area are interpreted to have been emplaced along Caledonian thrust faults or at least to have been deformed in Caledonian shear zones (Fig. 9). They include the Gullesfjord group (Tveten, 1978), the Vassvika group (Tveten, personal communication 2007), and the upper units of the Austerfjord group (Hakkinen, 1977); Table 3 lists the units of these groups. Direct lithologic correlation between the groups is hindered by structural complexities and their discontinuous nature. Table 3 is organized to suggest possible relationships between the three groups based on lithology, both of individual units and those typically found in association with them, and on horizons within each sequence along which variably tectonized lenses of granitic rocks are found.

Gullesfjord Group – Units of the Gullesfjord group crop out discontinuously along the shores of Gullesfjorden (Fig. 5) and have previously been interpreted as metasedimentary

Metasedimentary Sequences		
Gullesfjord group	**Vassvika group**	**Austerfjord group**
Quartzite	Quartzite	Quartzite Quartzofeldspathic schist Fine-grained biotite schist
	Granite sliver	
Amphibolite with layers of tremolite-bearing marble	Amphibolite	Iron-stained amphibolite
	Amphibole-bearing biotite schist with layers of tremolite-bearing marble	Tremolite-bearing marble Calcareous schist Biotite-rich amphibolite
	Granite sliver	
	Amphibolite intercalated with marble	
Slivers of granite		
Amphibolite Amphibole-bearing biotite schist Marble Biotite gneiss Micaceous quartzite Garnet-mica schist	Micaceous quartzite	Garnet muscovite schist Biotite schist, minor amphibolite Sericite quartzite
	Garnet muscovite biotite schist	
Schistose amphibolite	Biotite gneiss	Garnet amphibolite intercalated with marble
Quartzite		
		Chlorite biotite schist
		Kyanite garnet biotite schist Biotite schist, finely laminated
		Metaconglomerate

Table 3. Metasedimentary packages in the map area that are interpreted as having been emplaced along Caledonian thrust faults. Thick black lines represent surfaces interpreted as faults. The three lowest units previously assigned to the Austerfjord group are excluded from the allochthonous sequences based on lithology and contact relations discussed in the text. Austerfjord group units from Hakkinen (1977) and Rykkelid (1992). Heights of boxes do not imply any vertical scale.

xenoliths within the Archean Gullesfjord granodiorite gneiss (Griffin et al., 1978; Tveten, 1978; Rykkelid, 1992). A majority of the sequence is hidden from view beneath Gullesfjorden, and the units are best exposed near Flesnes and along the eastern shoreline south of Forøya, which trends parallel to strike. The sequence was not sampled extensively for petrographic studies, though a summary of lithologies can be found in Tveten (1978). Structural analysis (see below) indicates that the southern part of the sequence has been overturned to its current steeply east-dipping orientation. The units are described, therefore, from what is presumed to be the original stratigraphic bottom to top.

The lowest and most continuous unit of the sequence is a large (~6 km along strike and up to 450 m thick) body of light tan to white, medium-grained orthoquartzite that crops out along the northwest shore of Gullesfjorden near Flesnes (Fig. 9). Hakkinen (1977) interpreted "quartz-rich inclusions" within the adjacent Gullesfjord granodiorite gneiss near the contact to indicate its original igneous contact relations with the gneiss. Definitive intrusive relationships have not been observed along the contact, however, and plastic interfingering with basement gneisses along the basal thrust has been documented elsewhere at this latitude (Van Winkle et al., 1996). In fact, Hakkinen (1977) interpreted micaceous zones at the base of the quartzite to indicate tectonic movement along the boundary; no estimates were provided, however, as to the amount or sense of displacement.

Above the quartzite is a finely-banded amphibolite comprising ~60% idioblastic hornblende, ~25% quartz, and ~10% plagioclase. The remainder of the rock is composed of clinozoisite, chlorite, and rutile. The contact between the quartzite and amphibolite is a meter-thick zone of impure quartzite with a higher content of biotite and hornblende

(Hakkinen, 1977). This unit strikes into the fjord, but is present on the small islands near Flesnes (Tveten, personal communication 2008).

The upper section of the Gullesfjord group is most continuously exposed in the northeast corner of the map area. There, Tveten (personal communication 2010) reported mica schist with layers of amphibolite, marble, quartzite, and garnet-mica schist identical to the lithologies present near Vassvika. To the southeast, these units are overlain by Gullesfjord gneiss. The contact is poorly exposed, but is most likely tectonic in nature, as the gneiss is mylonitic near the boundary and the fabrics of the two rock types are concordant where it has been observed (Bartley, 1981; Tveten, personal communication 2010).

To the south, the stratigraphically lowest (easternmost) unit of the overturned section of the Gullesfjord group sequence is a weakly to moderately banded, fine-grained, salt-and-pepper-colored biotite gneiss. The overturned contact between the biotite gneiss and the Lødingen granite gneiss is exposed on the southern shore of Forøya and is characterized by a mylonitic fabric in the granitic gneiss near the boundary. South of there, the biotite gneiss is found along the eastern shore of Gullesfjorden. The gneiss contains discontinuous lenses of micaceous quartzite near its base. In zones ca. 200 m west of the base of the unit, a distinct rock has abundant, randomly oriented porphyroblasts of zoisite roughly 1 cm in length.

Stratigraphically above the biotite gneiss is an amphibole-bearing biotite schist that has a lepidoblastic texture defined by alignment of biotite and hornblende grains. Within this unit are discontinuous lenses of amphibolite. Thin layers of marble separate the biotite schist and biotite gneiss. Tracing these units to the south was difficult as they

32

strike into a low, marshy valley, but a few exposures were found in a creek (UTM33, E534181 N7606702). This geomorphic depression might have resulted from the lower resistance to weathering of the metasediments than the adjacent granitic gneiss, which likely also holds for the Gullesfjord itself.

Above the schist are tectonically emplaced slivers of granite, a style clearly reminiscent of the basement-cover contact on the mainland (Gustavson, 1974; Hodges et al., 1982; Steltenpohl, 1987; Van Winkle et al., 1996). The mylonitic fabric of the granitic lenses is concordant with the schistosity of the underlying and overlying rocks, though the contacts were not observed in the study area.

The upper units of the overturned section of the Gullesfjord group are exposed in the southern part of the map area and locally along the western shore of Gullesfjorden. In the south, a fine-grained, rusty-weathering amphibolite occurs with a cream-colored tremolite-bearing marble comprising ~90% recrystallized calcite, ~7% tremolite, and ~3% phlogopite. In thin section, idiomorphic tremolite poikiloblasts are colorless and contain inclusions of calcite. Pleochroic (colorless to pale brown) phlogopite porphyroblasts are aligned with the amphibole grains and give the marble a lepidoblastic fabric.

Above the marble and rusty amphibolite is a zone of strongly sheared Gullesfjord gneiss and a coarse-grained, dark green-black, schistose amphibolite comprising ~75% hornblende and ~20% plagioclase, with minor biotite, quartz, rutile, and zoisite. Hornblende grains range from xenomorphic, with abundant inclusions of plagioclase, to elongate, subidioblastic, the latter of which impart a faintly nematoblastic fabric to the rock. The amphibolite was intruded by the adjacent Gullesfjord gneiss and contains

granitic veins (Tveten, personal communication 2010). These contact relations require that the amphibolite is part of the basement complex rather than a cover unit. The unit's position structurally above the metasediments is discussed below, but it is likely a xenolith that acted as a zone of weakness in the Gullesfjord gneiss along which thrusting occurred.

The uppermost unit of the Gullesfjord group is an orthoquartzite that occurs in lenses along the western shore of Gullesfjorden (Fig. 9). Samples from a roadside outcrop (Fig. 2: UTM33, E532114 N7609667) were collected for petrographic and isotopic analysis (discussed below). The rock is composed of ~95% roughly equigranular, recrystallized quartz grains and ~5% muscovite, which occurs as a bimodal distribution of larger (~250-600 µm) and smaller (~50-75 µm) grains. All of the muscovite is roughly aligned forming a lepidoblastic fabric in the rock and imparting a flaggy appearance in outcrop and hand sample.

The contact between this quartzite and the adjacent gneiss is not exposed in the study area, and its isolated occurrence has led previous workers to interpret it to be a xenolith within the 2.6 Ga Gullesfjord gneiss. Recent LA-ICP-MS analysis (Steven Braun, Vanderbilt University) of detrital zircons extracted from a sample collected at the same outcrop as described in the previous paragraph yield a wide range of ages, the vast majority of which (~90%) were 1100 and 1350 Ma. These detrital grains are not only 1.2 to 1.5 billion years younger than the Archean gneiss, but also cannot have been derived from any known plutonic rocks in the West Troms, Lofoten, or Ofoten basement. This clearly requires that the quartzite, along with the rest of the units comprising the Gullesfjord group, was emplaced along a series of thrust faults.

Vassvika Group – Tveten (personal communication 2007) mapped a sequence of metasedimentary rocks extending from the southern shore of Gullesfjorden directly east of Forøya, eastward to the head of Austerfjorden where they appear to be continuous with the upper units of the Austerfjord group (Fig. 9). This sequence is herein referred to as the Vassvika group, for exposures along the shoreline of the cove called Vassvika and along the steep ridge to the east called Vassvikegga (Fig. 5). At their eastern extent, the units occupy a position in the nose of the Austerfjord anticline. West of there, the rocks become subvertical, and at their westernmost exposures at Vassvika they are overturned and dip steeply to the south. The sequence is described below from presumed stratigraphic bottom to top (south to north). The southern contact of the sequence with the subjacent gneiss was not directly observed in the field; near Gullesfjorden the rocks are vegetatively covered and the dangerously steep and narrow terrain along Vassvikegga was not mapped by the present author. Tveten (personal communication 2008) reported that the contact is tectonic in nature based on his observation of strong fabrics in the rocks near it, and the fact that the foliation in the gneiss to the south had been swept into concordance with the boundary.

The lowest unit in the sequence is lithologically similar to the biotite gneiss on Forøya and along the eastern shore of Gullesfjorden (Tveten, personal communication 2010). This unit was only observed by the present author in patchy exposures near the lake south of Vassvika (Fig. 5).

Above the biotite gneiss are quartzose garnet mica schist and biotite-rich quartzite that are observed along the shore near Vassvika. The quartzose garnet mica schist contains muscovite, biotite, and recrystallized quartz ribbons that define the schistosity of

the rock. Biotite and quartz are present in roughly subequal proportions composing ~70% of the rock. Coarse (1.5 to 2 mm), undeformed biotite grains and slightly undulatory muscovite (~20%) occur with graphite inclusions along cleavage planes. Some quartz grains have undulose extinction. Subidio- to idioblastic garnets with inclusions of quartz and graphite compose ~10% of the mode. A few garnets have been rotated and preserve evidence of an earlier foliation (Fig. 10). Microcline, plagioclase, and opaque mineral grains constitute roughly one percent of the rock.

Above the quartzose garnet mica schist is a fine-grained, biotite-rich quartzite comprising >90% quartz. The contact between the two units is obscured by rubble and vegetation. Biotite grains averaging a few tens of microns in length compose ~7% of the rock, and are very strongly aligned to form an intense lepidoblastic and nematoblastic texture. Poikiloblastic muscovite grains (averaging ~400 µm) enclosing quartz grains make up about one percent of the rock. The randomly oriented muscovite grains overgrew the dominant schistosity of the rock.

The next unit in the sequence, exposed along Vassvikegga, is a several-hundred-meter thick lens of granitic gneiss with a foliation defined by the alignment of biotite and flattened quartz and feldspar grains. The gneiss comprises ~40% quartz, ~50% microcline, ~5% plagioclase, and ~3% biotite. Hornblende, nearly completely altered to biotite, and epidote with cores of allanite are present in trace amounts. The contacts between the gneiss and the adjacent metasedimentary units are not exposed in the only area where the unit was observed along Vassvikegga; the orientation of the rock fabric, however, is parallel to the overall east-west trend of the metasedimentary sequence. Its exotic position amongst the metasedimentary layers of the Vassvika group rocks, coupled
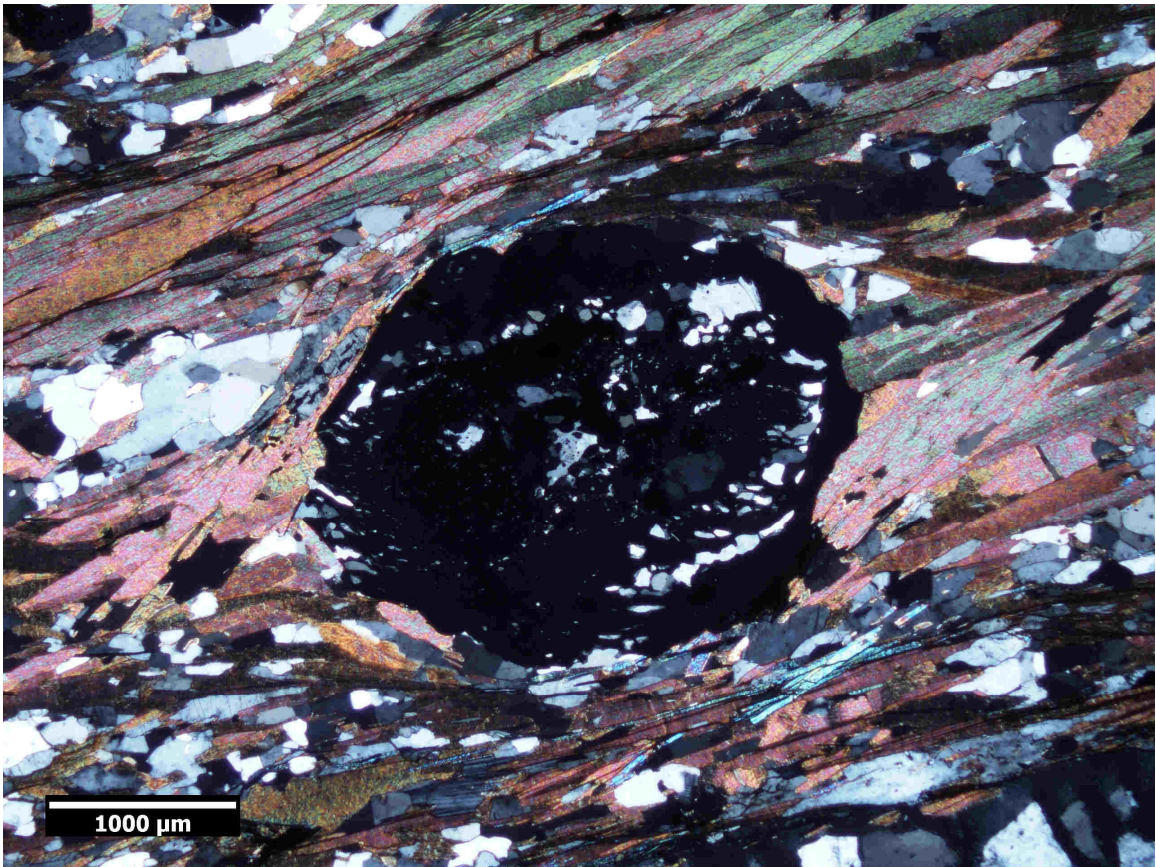
Figure 10. Photomicrograph of a garnet porphyroblast in the quartzose garnet-mica schist of the Vassvika group. Inclusion trails defined by quartz grains were rolled as the garnet grew. The internal and external fabrics are not traceable across grain boundary, indicating post-crystallization rotation of the garnet. Thin section cut parallel to stretching lineation and perpendicular to foliation. Cross-polarized light.

with its similar position to that occupied by the lenses of granite within the Gullesfjord group led the author to interpret it as a fault-emplaced sliver of basement.

Above the tectonic gneiss sliver is a schistose amphibolite. Hornblende and biotite occur in subequal amounts, together composing ~60% of the rock, and their alignment defines a well developed lepidoblastic fabric. Subidio- to idiomorphic amphibole porphyroblasts up to 2 cm in length have a poikiloblastic texture with inclusions of small grains of quartz, plagioclase, epidote, sphene, and calcite. The inclusions in the hornblende grains are aligned with the schistosity of the rock. In some grains, the curvi-planar trails have been inclined up to ~30 degrees to the external fabric into which they merge, indicating synmetamorphic rotation (Fig 11). A few of the amphibole grains are partially altered to biotite. Polygonal quartz grains compose ~25% of the rock. Feldspar grains, mostly plagioclase with minor microcline (~1%), compose another ~10 to 15%, and subidio- to idioblastic epidote and zoisite constitute the remainder of the rock volume.

Above the amphibolite is another sliver of granite exposed on the eastern shore of Vassvika and along Vassvikegga (Fig. 5). Quartz and feldspar (predominantly plagioclase) occur in roughly equal amounts as equigranular, polygonal grains and compose ~75% of the rock. Undeformed grains of biotite (~15% by volume) define the mesoscopic schistosity of the rock. Muscovite (~7%) occurs as randomly oriented porphyroblasts. Minor amounts of epidote, zoisite, apatite, and opaque grains form the remainder of the rock.

Within the sheared granite lens are two <10 meter thick layers of strongly deformed amphibolite (not shown at the map scale) comprising ~60% hornblende, ~30%

38
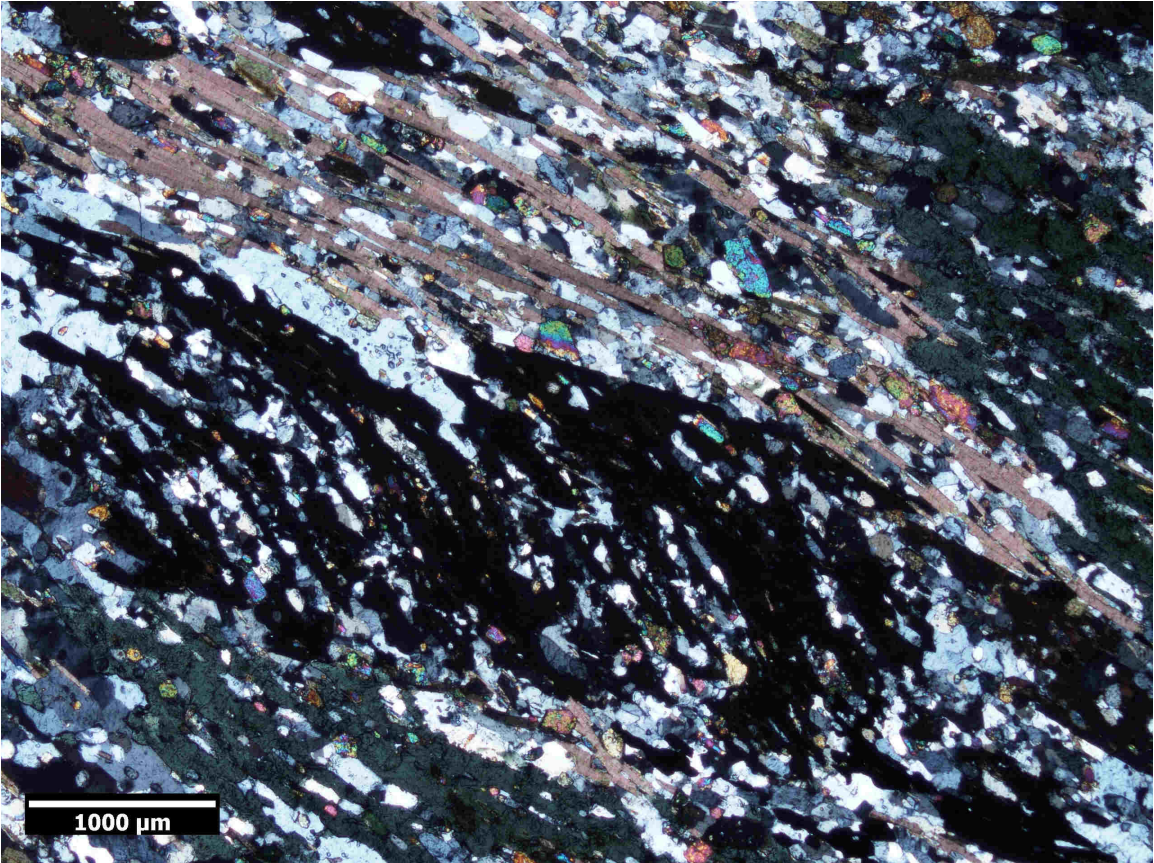
Figure 11. Photomicrograph of the schistose amphibolite from the Vassvika group. The large hornblende porphyroblast (extinct grain in center of photo) contains inclusion trails defined by quartz, plagioclase, epidote, sphene, and calcite that have been rotated, but can be traced into parallelism with the external schistosity of the rock. Cross-polarized light.

plagioclase, ~5% biotite (mostly all altered to chlorite), with accessory quartz, rutile, calcite and opaques composing the remaining ~5%.

The largest, most continuous unit above the granite sliver is an amphibole-bearing biotite schist. Parallel biotite grains (~30% by volume) define the schistosity. At the top of the unit near its contact with the basement gneiss, the rock has an S-C composite planar fabric defined by biotite grains wrapped around sigma-type plagioclase porphyroclasts (Fig. 12). The S-C fabric indicates a pre-folding, tops-east (thrusting) shear sense. Plagioclase (~40%) occurs as both porphyroclasts with recrystallized tails and in layers that alternate with layers of biotite. Quartz (~25%) and plagioclase form layers (0.5-mm-thick) between those of biotite (0.5-mm-thick). Subidiomorphic hornblende porphyroblasts (~700 µm) in the biotite layers constitute <5% of the rock. Calcite, apatite, and opaques are present in trace amounts. A few grains of biotite have been altered to chlorite along cleavage planes.

About 20 meters from the structural top of this unit, the amphibole-bearing biotite schist is interbedded with a tremolite-bearing, quartzose marble. There are two layers of marble – a lower one about two meters thick, separated by two meters of schist from an upper one less than 20 meters thick. The marble contains ~50% calcite with ~40% quartz. The alignment of tremolite poikiloblasts (up to 5mm in length) with small inclusions of calcite and quartz (~10% of the rock volume), imparts a nematoblastic fabric (Fig. 13). Faintly pleochroic (colorless to very pale brown) porphyroblasts of phlogopite are present in trace amounts.

At the structural top of the amphibole-bearing biotite schist is granitic gneiss. The contact is obscured by vegetation, but both rocks have intensely developed fabrics near
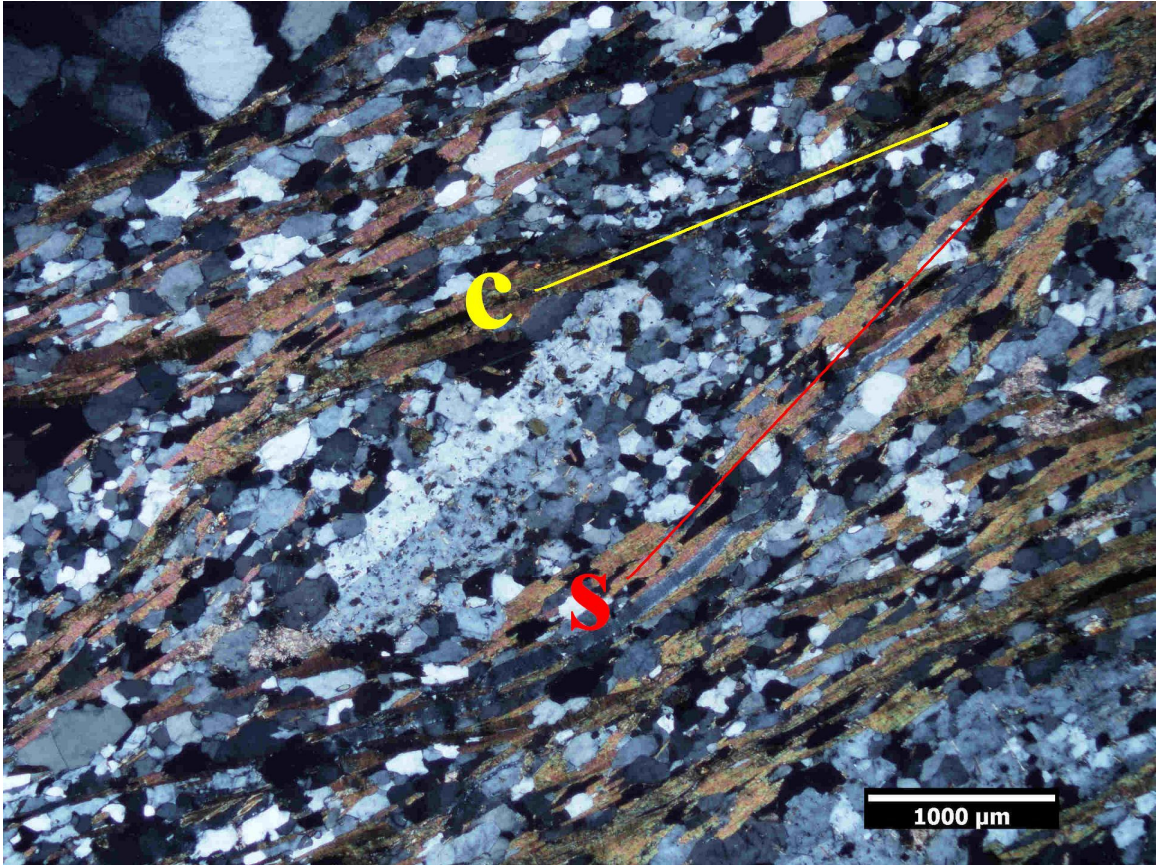
Figure 12. Photomicrograph of partially recrystallized sigma-type plagioclase porphyroclast (grain at center with albite twins) in amphibole-bearing biotite schist from the overturned panel of the Vassvika group. Biotite grains that grew along the boundaries of the porphyroclast define a composite planar fabric (Red line = S-plane; Yellow line = C-plane). Structural analysis (see text) indicates the unit was overturned, such that in its upright orientation the asymmetry of the tails would indicate tops-east (thrust) movement. Thin section cut parallel to stretching lineation and perpendicular to foliation. Cross-polarized light.
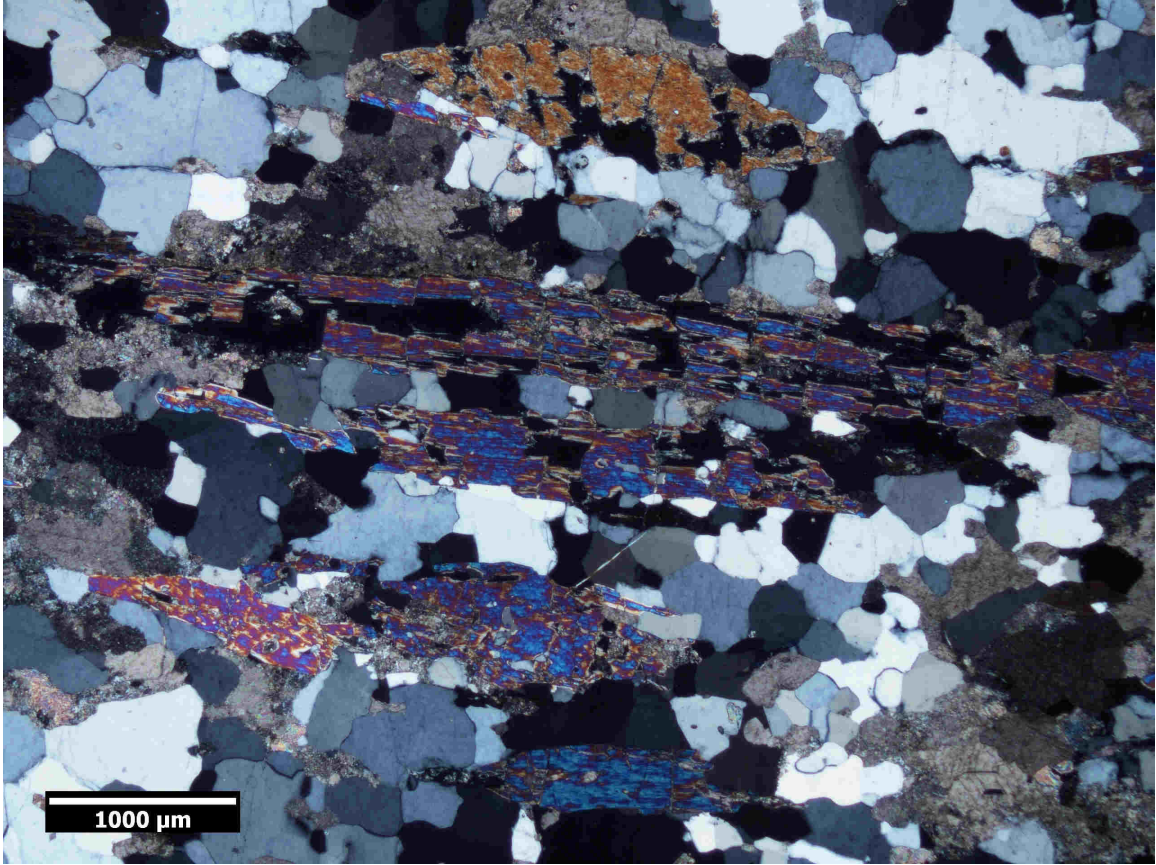
Figure 13. Photomicrograph of parallel amphibole porphyroblasts in tremolite-bearing, quartzose marble. Thin section cut parallel to mineral lineation and perpendicular to foliation. Cross-polarized light.

the boundary. Petrographic examination of the gneiss revealed a fine- to medium-grained groundmass of quartz and feldspar. Two-millimeter-thick poly-crystalline quartz ribbons and recrystallized mica (muscovite, ~10%; biotite, 2%) define the strong mylonitic foliation. The formation of quartz ribbons suggests deformation at medium- to high-grade temperatures (400-700°C; Passchier and Trouw, 1996). Quartz (~45% of the rock) commonly has undulose extinction, subgrains, and deformation lamellae. Microcline (~40% of the rock) constitutes most of the groundmass. Plagioclase composes ~3% of the groundmass.

Along the steep ridge about 100 meters north of the boundary between the schist and gneiss is recrystallized micaceous quartzite that ranges in thickness from ~5 to 20 meters. The quartzite comprises equigranular quartz (~90%), microcline (~5%), and muscovite (~5%). The consistently strong mylonitic fabric in this nearly 100-meter-thick zone is interpreted to reflect the ductile imbrication of the gneiss and the quartzite during the final emplacement of Gullesfjord gneiss above the duplexed allochthonous metasedimentary rocks (Fig. 14). The strong mylonitic fabric at the contact with the amphibole-bearing biotite schist gradually disappears away from the contact, giving way to very weakly foliated Gullesfjord gneiss (Fig. 15).

Austerfjord Group – The Austerfjord group metasedimentary rocks were first described and named by Hakkinen (1977) where they are exposed in an antiform at the head and south of Austerfjorden (Fig. 5). The present author did not map the Austerfjord group in detail, and, therefore, cannot contribute much in addition to the fine degree of detail already documented by Hakkinen (1977). The units and their inclusive lithologies are
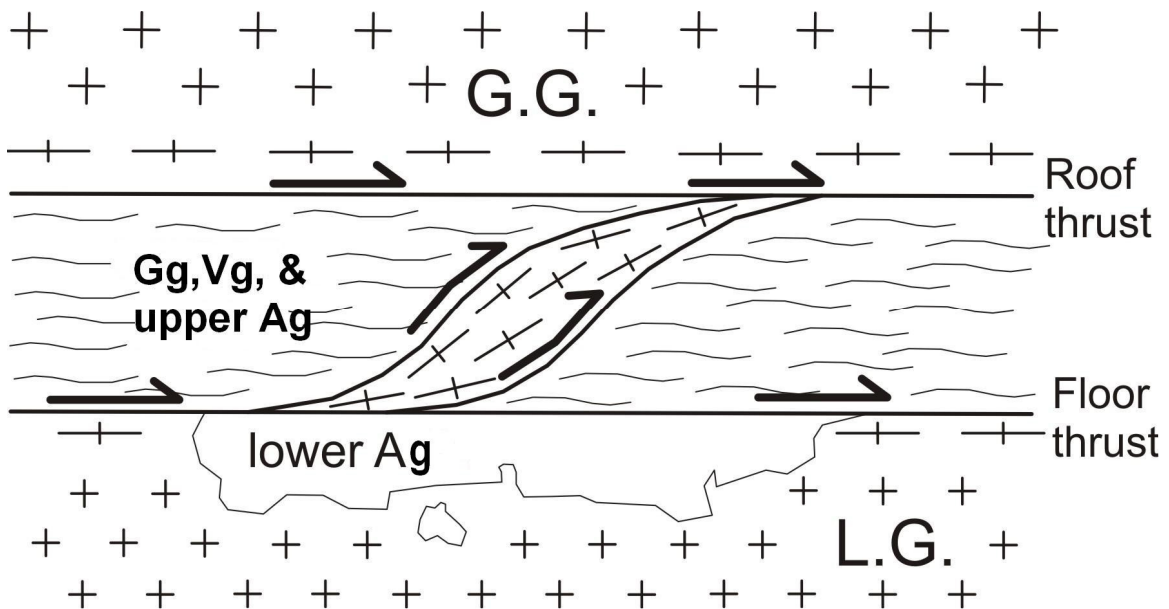
Figure 14. Schematic cross-section illustrating the structural configuration of the Gullesfjord-Austerfjord duplex. The duplex comprises units of the Gullesfjord group (Gg), Vassvika group (Vg), and upper Austerfjord group (upper Ag) interleaved with basement gneiss. Beneath the floor thrust to the duplex is Lødingen granite gneiss (L.G.), and the xenolithic units of the lower Austerfjord group (lower Ag) it intruded (discussed below). Gullesfjord granodiorite gneiss (G.G.) was emplaced above the duplex along the roof thrust (discussed in Structural Geology section below).
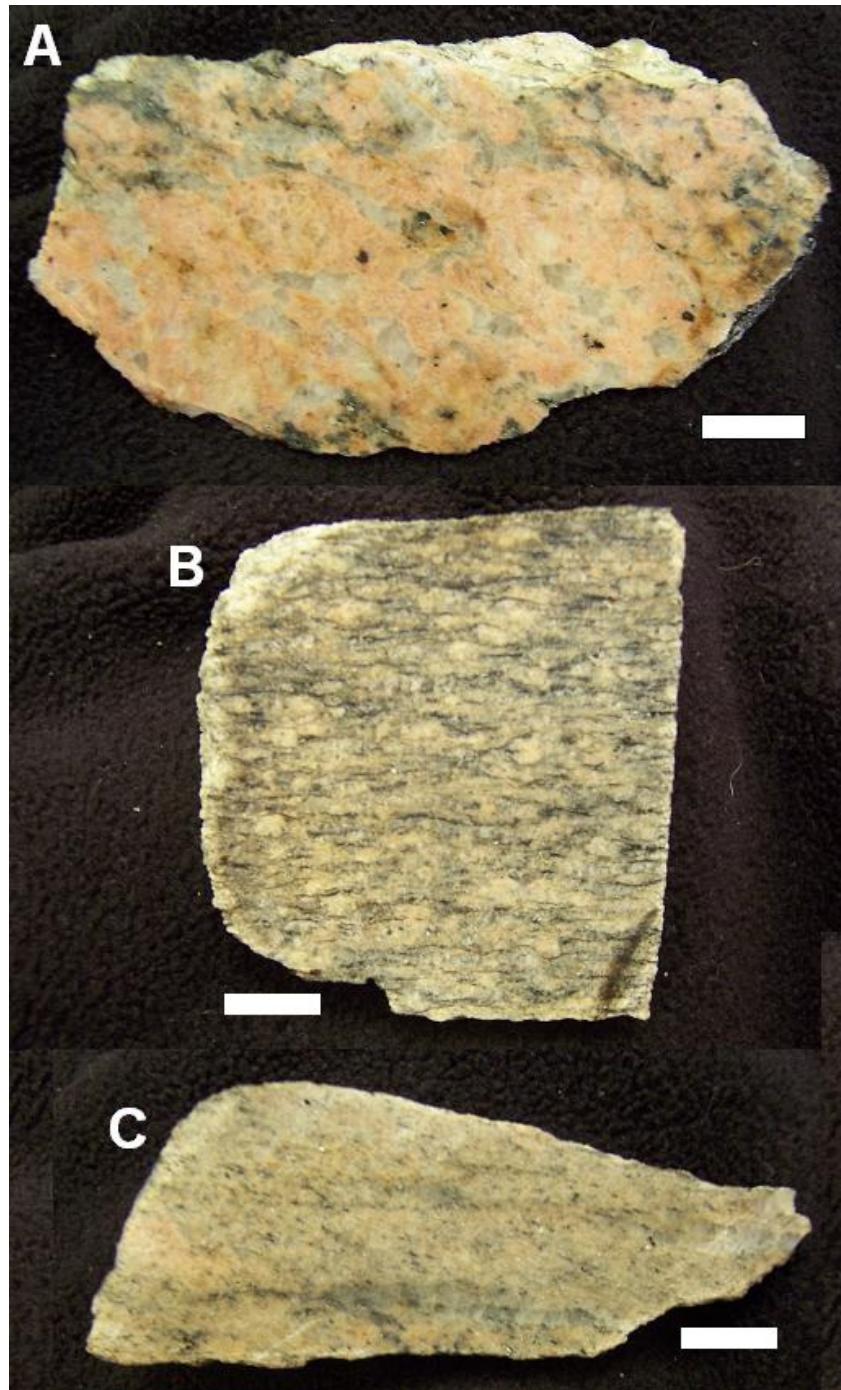
Figure 15. Photos of progressively developed mylonitic foliation within Gullesfjord gneiss approaching the Gullesfjord-Austerfjord shear zone along Vassvikegga from A) ~600 m north of, B) ~150 m north of, and C) at the thrust fault boundary. Slabs (B and C) cut perpendicular to foliation (horizontal in photo) and parallel to elongation lineation. Scale bars are 1 cm.

outlined in Table 4. Key to the present thesis, however, is the relationship of the Austerfjord group to the basement upon which it presently resides. Erosional levels have exposed the core of the Austerfjord antiform, which is formed by the Lødingen granitic gneiss that Hakkinen (1977) interpreted to have intruded the sequence. Rykkelid (1992) interpreted the contact between the granite and the lower schists as depositional, though field observations clearly document an intrusive relationship (Fig. 16).

At the base of the lower Austerfjord group south of Middagsfjellet and farther south near Snøfjellet (Fig. 9), Rykkelid (1992) reported several exposures of metaconglomerate and cross-bedded sub-arkoses, which Hakkinen (1977) apparently did not recognize. Rykkelid interpreted the coarse-grained, metasiliciclastic rocks to be in depositional contact with the subjacent granitic gneiss. The author observed metaconglomerate at Snøfjellet (UTM33 E541386 N7605970) and in the area northeast of Fiskefjorden (Fig. 9). The metaconglomerate contains deformed pebbles of arkosic composition up to 10 cm in length. Petrographic examination of the rock revealed a matrix of similar composition, but with substantially higher contents of clinopyroxene, garnet, and epidote. Biotite and muscovite contents were fairly high in the matrix of a few samples (up to ~10% by volume). Minor amounts of hornblende were only found in the matrix of the rock. Contrary to Rykkelid's (1992) report of a depositional contact at Snøfjellet, however, the author observed a clear intrusive relationship between the metaconglomerate and the adjacent Lødingen granite (Fig. 17). The sedimentary protolith of this metaconglomerate must have once shared a depositional contact with some basement rocks, but it is clear that the metaconglomerate is preserved as xenoliths within younger plutonic basement rock(s).

Austerfjord Group			
Lithology	**Mineralogy**		
	Major	**Minor**	
Quartzite	qtz, sericite, microcline, albite	biotite, clinozoisite, sphene, opaq	Allochthonous (not intruded by Lødingen granite)
Quartzo-feldspathic schist	qtz (>50%), feldspar, biotite, chl, hbl	clinozoisite, garnet	
Fine-grained biotite schist	biotite, qtz, plag	amphibole, musc, epid, sphene, secondary chl	
Iron-stained amphibolite	hornblende and plagioclase	biotite, qtz, epid-clinozoisite, secondary chl and calcite	
Tremolite-bearing marble	calcite, tremolite	sphene, epid, clinozoisite, phlogopite, chl, musc, apatite	
Calcareous schist	abundant calcite with amphibole, biotite, qtz, microcline, sphene, opaques, and minor relict garnet		
Biotite-rich amphibolite	equal amounts hbl and biotite	qtz, feldspar, epid, clinozoisite, sphene, secondary chl and calcite	
Garnet-musc. schist	musc, large garnets, qtz, biotite	plag, apatite, tourmaline, zircon, clinozoisite, opaq, pyrite, hbl	
Biotite schist, minor amphibolite	biotite + hbl (40%), qtz (30%), plag (10%)	microcline, sphene, clinozoisite, zircon, opaq	
Sericite quartzite	qtz, musc, sericite	opaq, biotite, chl, microcline, clino-zoisite, epid, apatite, zircon, relict garnet	
Garnet amphibolite	roughly equal amounts of fine-grained hbl and plag	biotite, epid-clinozoisite, sphene, apatite, opaq, plag, musc, qtz, calcite, garnet	
Intercalated with marble	calcite	dol, qtz, biotite, musc, clinozoisite, apatite	
Chl-biotite schist	biotite, chlorite, quartz	pyrite	Intruded by Lødingen granite
Kyanite-garnet-biotite schist	biotite, garnet, kyanite, musc, sericite, qtz, plag	epid (w/allanite core), clinozoisite, tourm, rounded zircon, topaz	
Biotite schist, finely laminated	biotite, qtz, plag, microcline	musc, hbl, epidote, tourm, calcite, chl, graphite, relict garnet	
Meta-conglomerate	qtz, microcline, clinopyroxene, garnet	biotite, epid, musc, plag, hbl	

Table 4. Units of the Austerfjord group. Thick black lines delineate the seven major units and thin black lines delineate distinctive lithologies present within some units. Red line represents the fault that separates allochthonous units (structurally above) from xenolithic units (structurally below). Summarized from Hakkinen (1977). Description of metaconglomerate from Rykkelid (1992) and the present study. Heights of boxes do not imply any vertical scale.
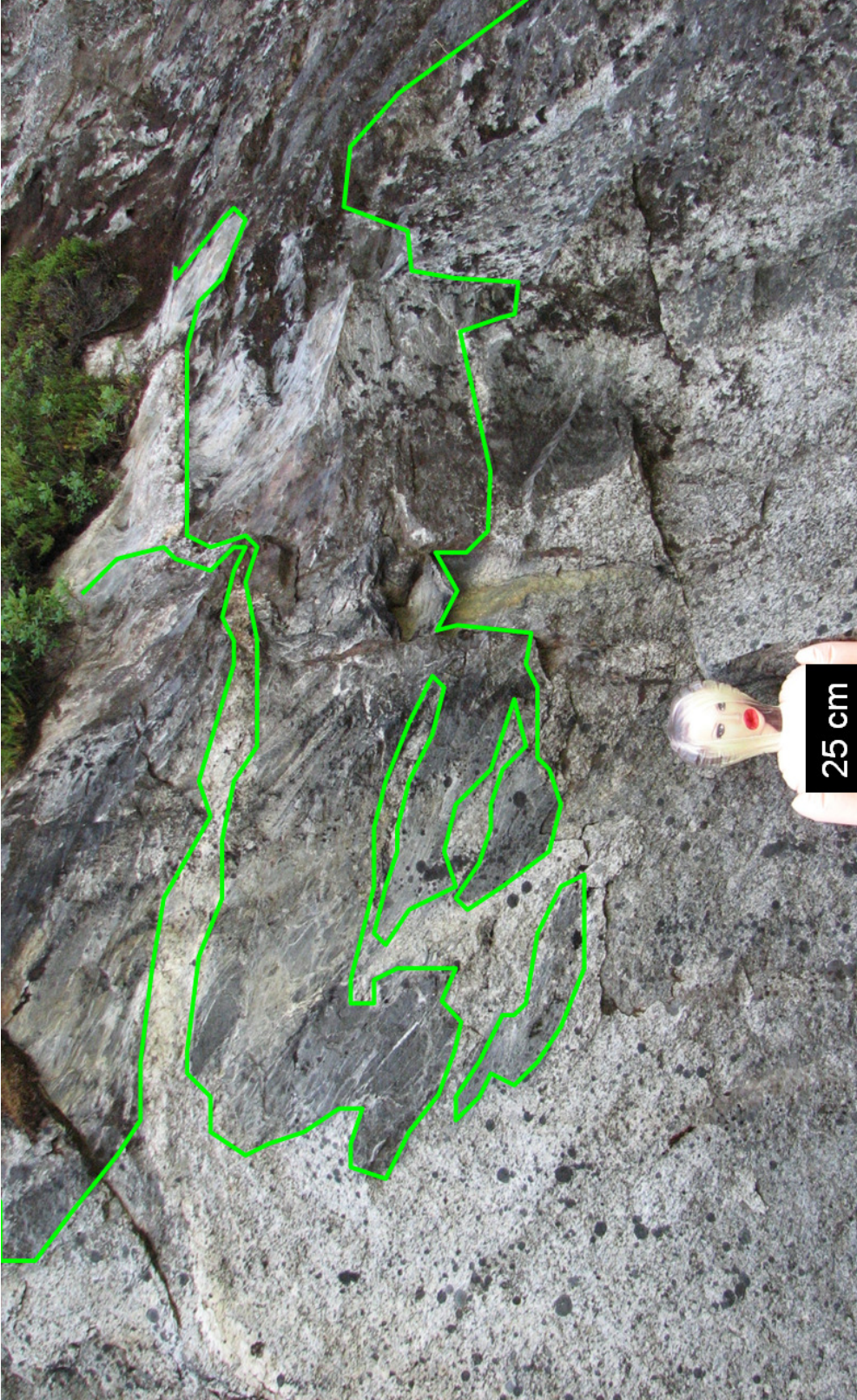
Figure 16. Photo (looking south) of the intrusive contact between the finely-laminated biotite schist of the lower Austerfjord group and the granitic gneiss exposed in the core of the Austerfjord antiform in a roadside outcrop at the head of Austerfjorden (UTM33, E542756 N7614278). The green line highlights apophyses and a small xenolith of biotite schist intruded by the granite.
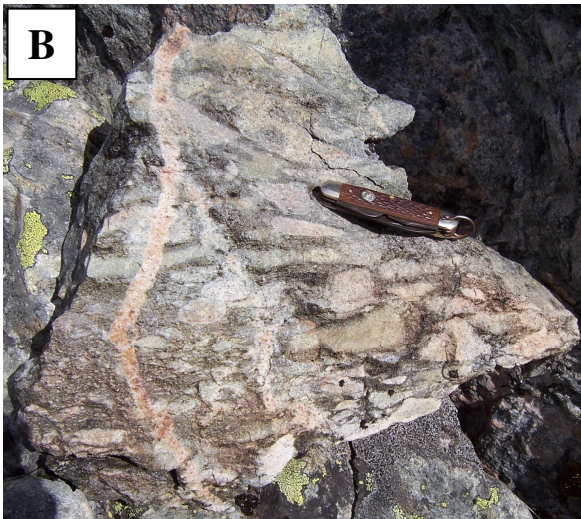
Figure 17. Deformed metaconglomerate (A and B) near Snøfjellet and (C) northeast of Fiskefjorden (Fig. 9). Note that the vein in B cuts deformed pebbles. The clasts in the outcrop surface in C have a higher resistance to weathering than the matrix and stand out in relief. Hammer is 35 cm long, knife is 9 cm long, and hammer head is 10 cm long.

Field and map relations clearly document that the three lowest units of the Austerfjord group (Table 4) have been intruded by the Lødingen granite, and, in fact, are all xenolithic enclaves. The allochthonous rocks of the Vassvika group, which clearly correspond to the upper units of the Austerfjord group (c.f. Figures 9 and 18), have been coincidentally juxtaposed by a thrust fault with the underlying xenolithic metasedimentary units, giving the appearance of a continuous sequence of metasedimentary rocks within the Austerfjord antiform (Figs. 18 and 19: cross-sections A-A' and B-B'). This interpretation is supported by the fact that the western limb of the Austerfjord antiform south of the intersection of the Austerfjord and Vassvika groups, contains only rocks of the lower three units (Fig. 5). The distribution of Hakkinen's (1977) field stations implies that his interpretation of the contact between the upper Austerfjord group metasediments and the overlying Gullesfjord gneiss were limited to exposures directly west of Austerfjorden; a contact that now is documented to extend westward along the northern contact between the Vassvika/upper Austerfjord group rocks and the Gullesfjord gneiss (Tveten, personal communication 2007).

In the eastern limb of the Austerfjord antiform, Hakkinen (1977) mapped a sliver of granite that he interpreted to be a sliver of the Gullesfjord gneiss of the upper plate of the Austerfjord thrust stranded above Austerfjord group rocks (Fig. 3E). He stated that the contact with the metasediments was poorly exposed, but documented that the internal fabric of the gneiss is concordant with that of the adjacent, east-dipping Austerfjord group rocks. Topographic profiles and geologic cross-sections (Fig. 19: sections A-A' and B-B') through this sliver of gneiss illustrate that a subhorizontal thrust surface beneath a klippe is less geometrically probable than anastomosing upper (eastern) and

50
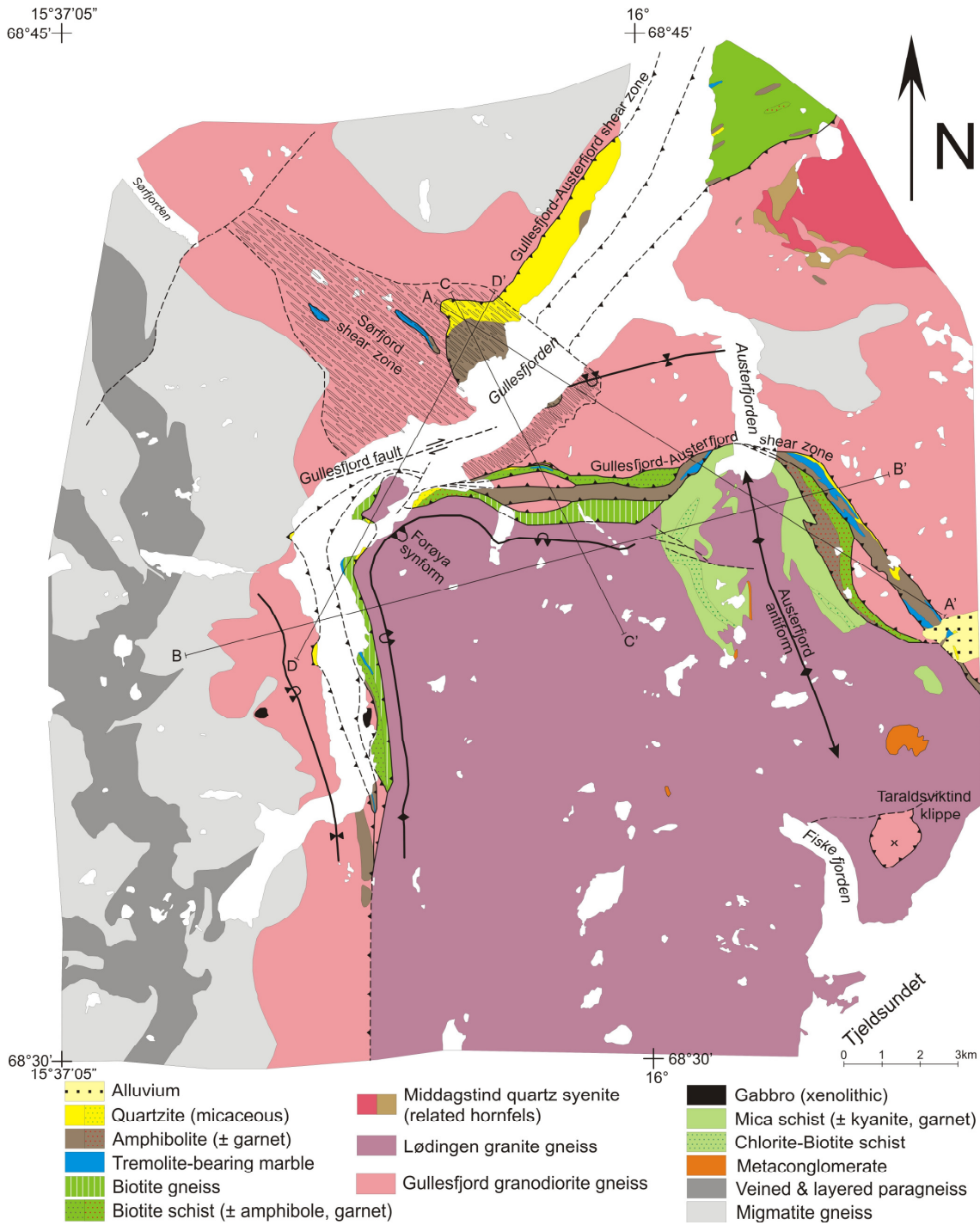
Figure 18. Lithotectonic map of central Hinnøy. Modified from Hakkinen (1977), Rykkelid (1992), Tveten (personal communication 2008), and the present study. Cross-sections are presented in Figure 19.

51
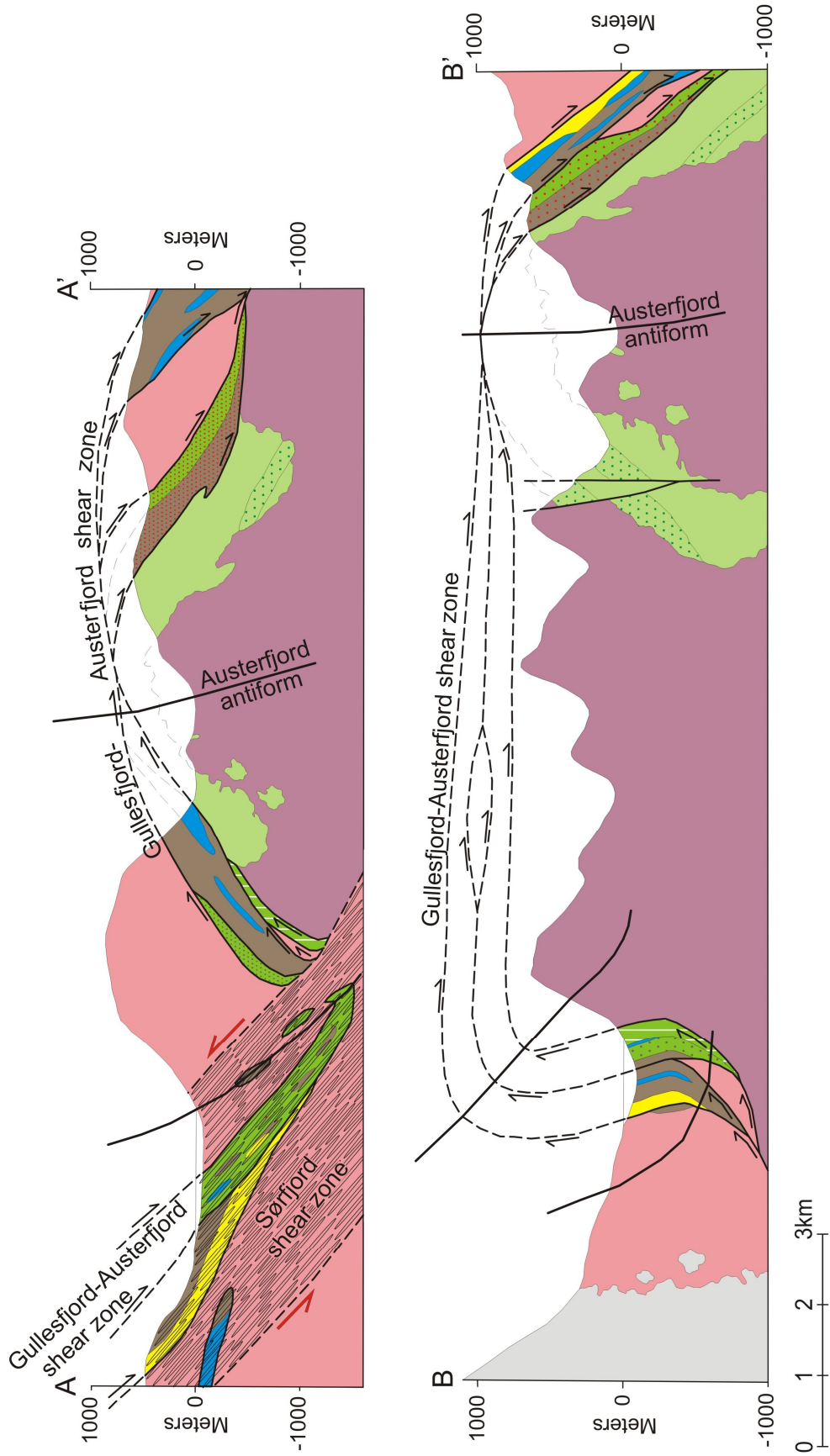
Figure 19. Structural cross-sections of the study area. Section lines and lithologic symbols shown in Figure 18. Black arrows and T (toward) and A (away) indicate direction of movement within, out of, or into the plane of the section, respectively. Red arrows indicate sense of movement in the Sørfjorden shear zone. Horizontal scale is the same for all cross-sections.

52
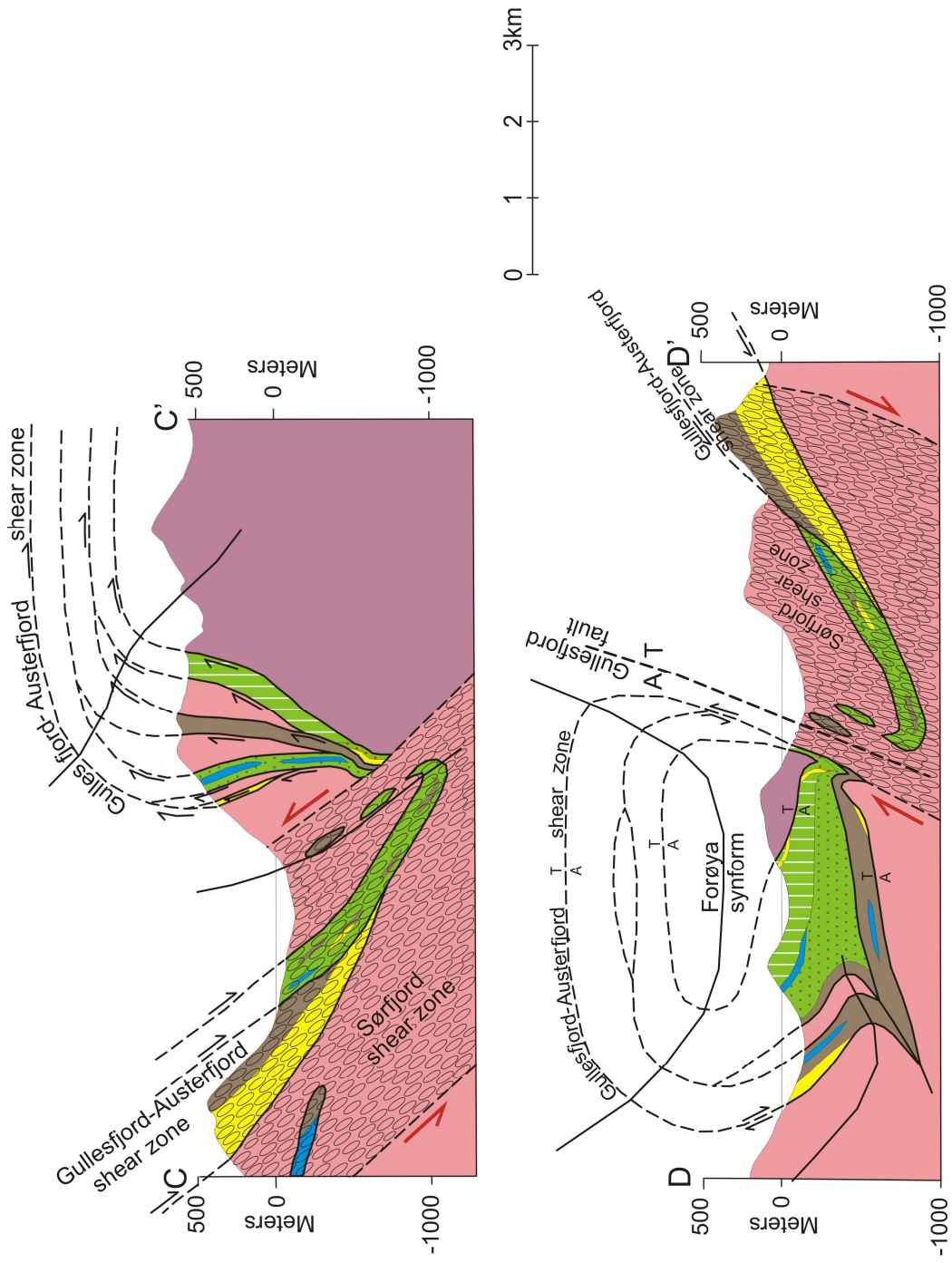
Figure 19 (continued)

53

lower (western) thrusts. Though the contact between the gneiss and metasediments would show evidence of deformation in either case, the author favors the latter interpretation based on similar slivers of tectonized granite within the Vassvika metasedimentary sequence, where such a duplexed geometry is herein documented (Fig. 18).

Metamorphism

The earliest regional metamorphic events recognized in Lofoten-Vesterålen basement rocks accompanied the emplacement of the AMCG suite at ca. 1800 Ma (Griffin et al., 1978). High-grade metamorphism produced amphibolite-facies assemblages in the rocks of central and northwestern Hinnøy, and granulite-facies assemblages further west on Langøy and southwest Hinnøy. Griffin et al. (1978) described an orthopyroxene isograd that is the boundary between the two zones (Fig. 1). Previous workers have documented evidence that the rocks of eastern Hinnøy next experienced prograde amphibolite facies metamorphism related to the peak Scandian phase of the Caledonian orogeny (Hakkinen, 1977; Griffin et al., 1978; Bartley, 1980; Rykkelid, 1992). Later, Corfu (2004a) documented that Leknes group metasedimentary rocks experienced a Middle Ordovician amphibolite facies metamorphic event. Steltenpohl et al. (2003b and 2006) also found relicts of Middle Ordovician metamorphism in some Lofoten-Vesterålen rocks. Regionally, Middle Ordovician metamorphism and deformation is well documented in the exotic (Laurentian/Taconic?) Uppermost Allochthon (Yoshinobu et al., 2002; Roberts, 2003; Barnes et al., 2007), but the nature and extent of this event in Lofoten-Vesterålen is only fragmentary as this report was written.

The quartzofeldspathic gneisses of central Hinnøy offer little diagnostic information concerning metamorphic pressure-temperature relations in rocks of the

Lofoten-Vesterålen region. Commonly, the granitic gneisses comprise quartz, microcline, plagioclase, biotite, muscovite, and epidote. Trace amounts of hornblende and rare garnet relicts occur in some samples. Hakkinen (1977) interpreted that the petrographically determined anorthite content of plagioclase (oligoclase to andesine) combined with the presence of epidote-zoisite minerals in the rocks of western Hinnøy indicate recrystallization in the medium-pressure range of the amphibolite facies.

Aluminous pelitic rocks of the Gullesfjord, Vassvika, and upper and lower Austerfjord groups contain mineral assemblages that most reliably allow inferences to be made of the conditions of metamorphism. The assemblage quartz – biotite – muscovite – garnet – graphite in a metapelite from the Vassvika group is indicative of the lower amphibolite-facies. No aluminosilicate minerals were observed in any of the rocks from within the Gullesfjord-Austerfjord shear zone, but Hakkinen (1977) reported kyanite in the garnet mica schists of the lower Austerfjord group. Hakkinen (1977) interpreted the presence or absence of aluminosilicate in these rocks to be compositionally controlled, such that their local occurrence or absence did not serve as an indication of mineral isograds, a problem well documented in pelitic rocks of the Ofoten nappe stack directly to the east (Steltenpohl and Bartley, 1984 and 1987).

Mineral assemblages within the marbles are of mainly two types; tremolite – calcite – phlogopite ± quartz ± dolomite is found within the Gullesfjord and Vassvika groups, and tremolite – actinolite – calcite – dolomite – muscovite – epidote-clinozoisite occurs within the upper Austerfjord sequence (Hakkinen, 1977). The former assemblage indicates equilibration under epidote-amphibolite facies conditions (Blatt and Tracy,

1995); Hakkinen (1977) interpreted the latter assemblage to indicate metamorphism and recrystallization under upper-greenschist to lower-amphibolite facies conditions.

Calcic plagioclase and hornblende in the upper Austerfjord group amphibolites indicates amphibolite facies metamorphism, which is consistent with the metamorphic conditions deduced from rocks in the Lofoten-Ofoten region (Hakkinen, 1977; Steltenpohl and Bartley, 1987). No estimates were made of anorthite content in plagioclase of the amphibolites of the Gullesfjord or Vassvika groups for the present study. Hakkinen (1977), Tveten (personal communication 2010), and the present author document the presence of almandine garnet in textural equilibrium with hornblende within amphibolites of the all three sequences of metasedimentary rocks on central Hinnøy, which is consistent with mid- to upper-amphibolite facies metamorphic conditions.

Rykkelid (1992) reported the mineral assemblage potassium feldspar + garnet + clinopyroxene within the metaconglomerate at the structural base of the lower Austerfjord group, and he interpreted it to indicate uppermost amphibolite facies conditions of metamorphism, perhaps approaching the granulite facies. Metaconglomerate examined during the present study farther to the southeast (Fig. 18), also contains the mineral assemblage quartz – microcline – clinopyroxene – epidote ± garnet. Clear intrusive contact relations with the enveloping Lødingen granite (Fig. 17), however, indicate that these bodies are xenoliths within the basement complex, such that metamorphism predated the Caledonian event. Hakkinen (1977) reported an isolated occurrence of sillimanite in the veined and layered gneiss north of the present study area, which clearly records uppermost amphibolite-facies metamorphism. The present author

observed a mafic pod at the base of the Gullesfjord group that contained the mineral assemblage garnet – clinopyroxene – calcite. These localized high-grade assemblages were only found in rocks of the basement complex, and, therefore, are all interpreted as surviving vestiges of pre-Caledonian metamorphism.

Structural Geology

The basement in Lofoten-Vesterålen has long been noted for its lack of strong fabric elements related to Caledonian deformation (Griffin et al., 1978). The structures and fabrics in the allochthons lying toward the east in the Ofoten region progressively disappear westward and structurally downward into the Lofoten basement, despite its deepest structural position within the core of the mountain belt (Tull, 1977; Bartley, 1981; Hodges et al., 1982; Steltenpohl et al., 2004). Earlier workers interpreted this as evidence for Lofoten being an exotic terrane that docked with Baltica during the late-Caledonian, thus allowing it to have remained at a high structural level and to have escaped temperatures, pressures, and fluid influx required to penetratively deform it (e.g., Hakkinen, 1977). The current consensus, however, is that the Lofoten basement was already the western edge of Baltica during Caledonian times, and that deformation was limited to the shallow levels where metamorphic fluids from dehydration reactions in the overriding allochthonous rocks were able to percolate downward into the rigid, anhydrous granulitic basement (Bartley, 1982a).

A major problem in deciphering the tectonic history in Lofoten is the difficulty, and expense (i.e., isotopic age dating), in differentiating structures that formed during the Caledonian from those formed earlier. The recent recognition of Middle-Ordovician metamorphism and deformation further complicates deciphering what structures and fabrics resulted from the Scandian event. The Lofoten terrane is mainly a granite plutonic

basement block, with fabrics and structures that can look alike, but have the potential to have formed from the Archaean into the Tertiary. The only way to absolutely distinguish which structures are Caledonian in these plutonic rocks is to date appropriate materials isotopically (Hames and Andresen, 1996; Corfu, 2004a; Steltenpohl et al., 2004). Once a Caledonian age is documented, one can then trace those structures and fabrics along strike until they are no longer recognizable. Combined with the fact that the majority of these shear zones juxtapose granite next to granite, this becomes a difficult pursuit. Workers have, therefore, recognized that metasedimentary packages present distinctive mapping units and that they commonly are bound by Caledonian shear zones. It is this relationship that led to the present investigation that focuses on three such metasedimentary packages on central Hinnøy, which can partially be connected eastward to the Caledonian allochthons.

Structures and fabrics in the field area that are interpreted to have formed as the result of pre-Caledonian deformation and metamorphism are mostly inferred by their discordance with structures of known Caledonian age. For example, the Austerfjord thrust is continuous with Caledonian structures that deform the nappe stack on the mainland to the east (Hakkinen, 1977; Hodges et al., 1982). Likewise, as will be discussed below, ages determined from $^{40}Ar/^{39}Ar$ analyses of muscovite were integrated with results from the structural analysis to aid in identifying Caledonian structures and fabrics. Pre-Caledonian structures that were recognized are as follows: compositional banding in dated Archaean and Palaeoproterozoic migmatites (Hakkinen, 1977; Griffin et al., 1978); intrusive contacts between the unfoliated 1.7 Ga Middagstind quartz syenite and foliated Gullesfjord gneiss, Hesjevann assemblage, and Kvæfjord group wall rocks

60

(Bartley, 1981); foliated xenoliths of metaconglomerate with deformed clasts cross-cut by undeformed granitic veins (Fig. 17); and intrusive contacts between the 1.8 Ga Lødingen granite and biotite schists of the lower Austerfjord group (Fig. 16). The notation, D_0, is used to refer to all features related to pre-Caledonian deformation; however, temporal correlations among these structures are not implied.

Structural Analysis

Structural data collected during the present study were compiled with the data sets of Hakkinen (1977) and Tveten (personal communication 2008) in order to evaluate structures across most of central Hinnøy. A structural form line map was constructed from the orientations of the dominant metamorphic foliations to aid in recognition and characterization of Caledonian structures (Fig. 20). An analysis of the form line map led to the delineation of four subareas to highlight possible rock volumes affected by Caledonian deformation. Figures 21 and 22 depict these subdivisions and include lower-hemispherical stereographic projections (equal area) of structural measurements collected in each subarea (poles to foliation planes and mineral/stretching lineations, respectively). Structural analysis indicates that these data support two principal Caledonian phases of deformation, D_2 folds and shear zones that have reoriented previously formed D_1 thrust faults. D_1 and D_2 are notations used here to refer to the local sequence of deformation and for suggesting possible correlations to regional Caledonian deformational phases recognized by other workers. The following notations are used to refer to structures formed during the D_1 and D_2 deformational phases:
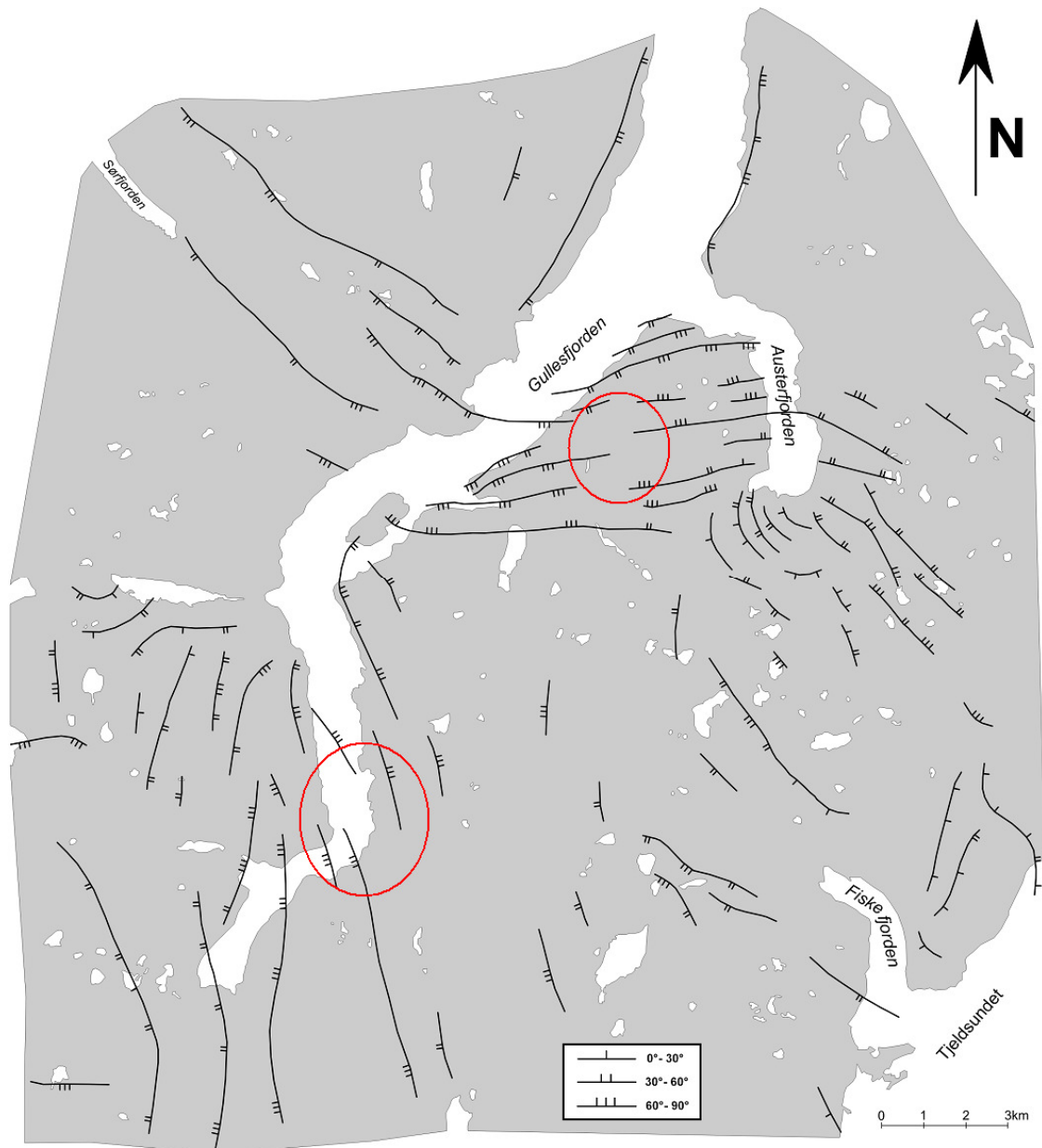
Figure 20. Structural form line map of the structural grain in rocks of central Hinnøy. Constructed from data collected by the author and from Tveten (personal communication 2008) and Hakkinen (1977). Black lines parallel the visual best-fit trends of metamorphic folia. Tick marks indicate the direction of dip. Number of tick marks indicates relative amount of dip (see legend). Red circles highlight inflection points of structural overturning associated with the interaction of the D_1 Gullesfjord-Austerfjord shear zone and D_2 Sørfjord shear zone (see text).
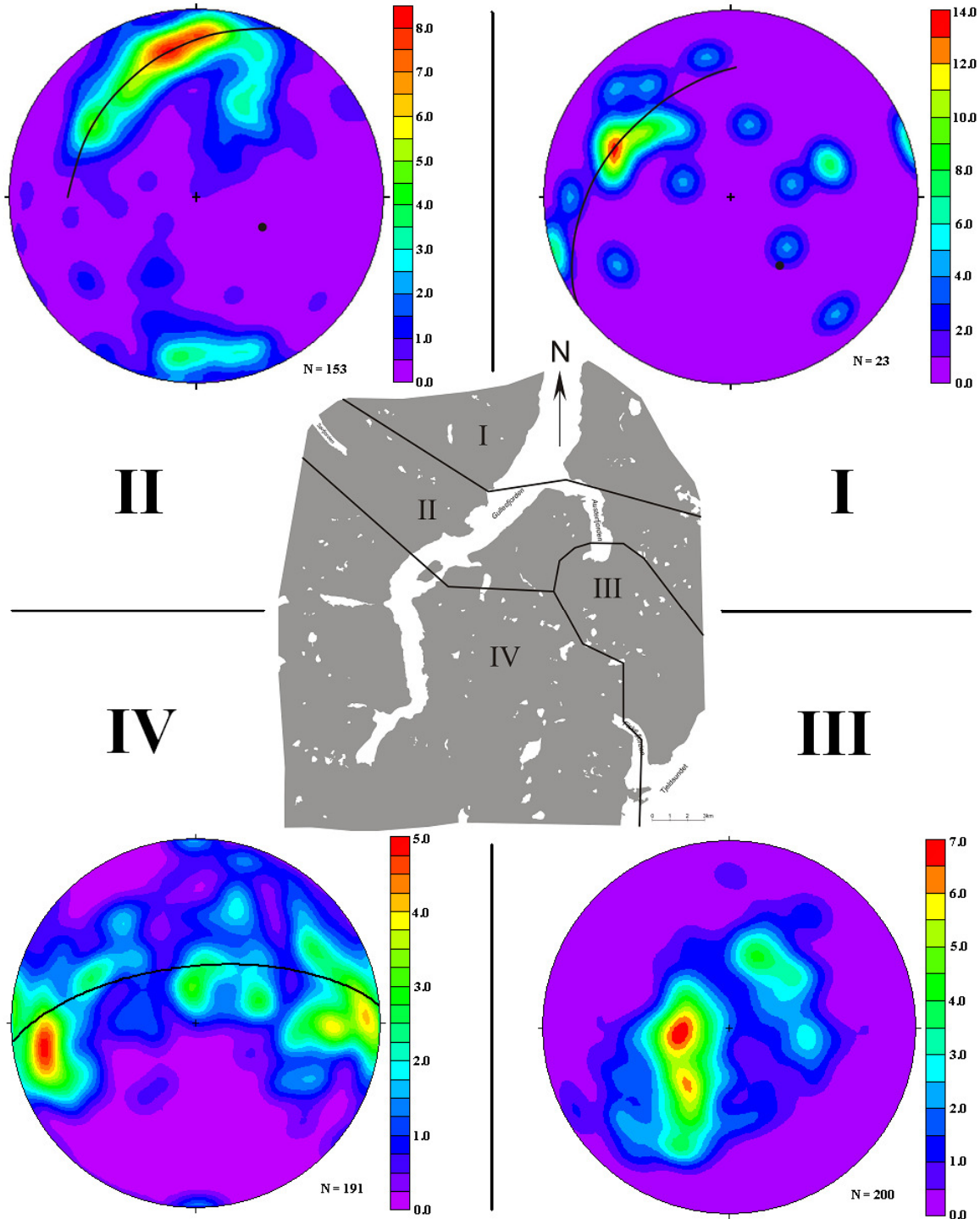
Figure 21. Contoured lower-hemisphere stereoplots of poles to foliation from each subarea. Plots include data from the present study, Tveten (personal communication 2008; mostly in the eastern part of subarea I and western part of subarea IV), and Hakkinen (1977; mostly in the northern part of subarea III). Scale bars are graded in % per % area. Visually estimated best-fit partial girdles and π-axes are shown for subareas I and II. Computer-generated best-fit great circle girdle is shown for data from subarea IV.
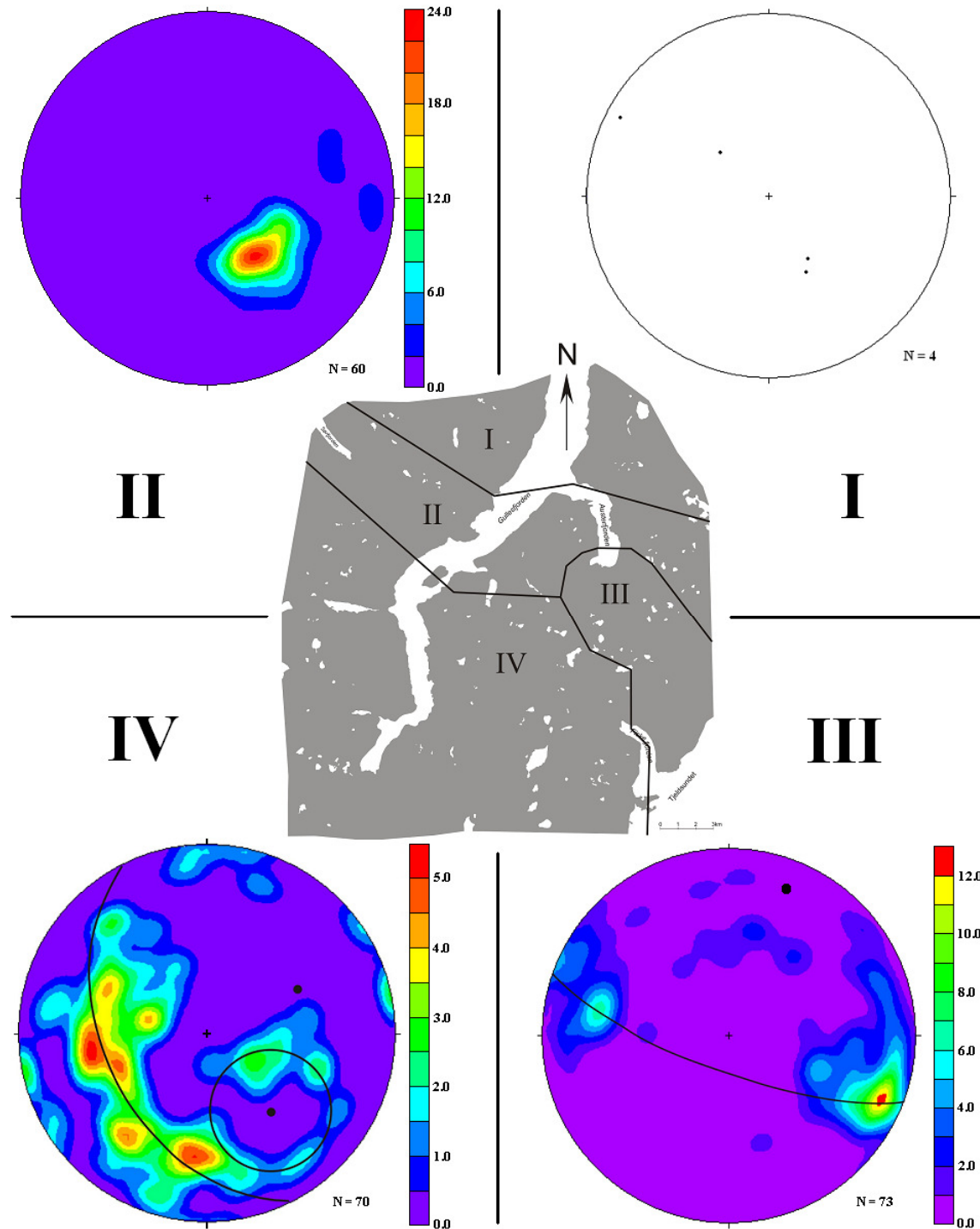
Figure 22. Contoured lower-hemisphere stereoplots of mineral and stretching lineations from each subarea. Plots include data from the present study, Tveten (personal communication 2008; mostly in the eastern part of subarea I and western part of subarea IV), and Hakkinen (1977; mostly in the northern part of subarea III). Scale bars are graded in % per % area. Visually estimated best-fit great circle girdles/π-axes and small circle/cone axis are shown for subareas III and IV.

S_1 – metamorphic foliation and coplanar mylonitic
foliation in D_1 shear zones

L_1 – mineral and elongation lineations associated
with D_1 thrusting

F_1 – asymmetric folds and crenulations within
D_1 shear zones

L_2 – elongation lineations in D_2 shear zones

F_2 – folding of S_1 about F_2 axis parallel to L_2

Based on the present analysis, four macroscopic structures are recognized on central Hinnøy (Fig. 18): 1) the north-northwest trending, doubly-plunging Austerfjord antiform; 2) the Gullesfjord-Austerfjord shear zone, which partly coincides with the Austerfjord thrust of Hakkinen (1977) and the Gullesfjord shear zone of Rykkelid (1992); 3) the Sørfjord shear zone; and 4) the Forøya synform, a northwest-closing sheath-fold. The list above indicates the relative timing of development of these macroscopic structures as has been deduced during the present study, that is, 1) formed first and 4) formed last. For convenience, however, the following structural analysis is written to emphasize the relationships between these structures that led the present author to develop this relative chronological framework for the structural evolution of the rocks on central Hinnøy.

Deformation D_1 – The first phase of Caledonian deformation recognized on central Hinnøy is characterized by development of a metamorphic foliation in granitic gneisses and metasedimentary rocks formed under amphibolite-facies metamorphic conditions. The peak of metamorphism was accompanied, but was outlasted, by D_1 deformation that

produced a coplanar mylonitic foliation in tops-east-directed shear zones and led to the development of east-vergent asymmetric folds and mineral and elongation lineations parallel to the direction of transport.

The Austerfjord thrust has long been recognized as a Caledonian structure traceable westward from the Ofoten nappe stack (Hakkinen, 1977; Hodges et al., 1982; Tull et al., 1985) and, thus, serves as a Caledonian "benchmark" for establishing temporal relationships between structures in the study area. Rykkelid (1992) inferred a Caledonian age for the Gullesfjord shear zone based on parallelism with the Austerfjord thrust, though he did not recognize their physical connection. The present author's field observations and petrographic and structural analysis document the following five lines of evidence that link these two shear zones: 1) the physical, map connection, from west to east, of the Gullesfjord, Vassvika, and upper Austerfjord groups; 2) slivers of granitic basement gneiss within all three metasedimentary sequences; 3) they all have mylonites of the same rheological development; 4) all fit within the same relative deformational event – D_1 tops-east thrusting; and 5) $^{40}Ar/^{39}Ar$ muscovite cooling dates document overlapping timing of movement (see below). The name Gullesfjord-Austerfjord shear zone is, therefore, used here to refer to this structural duplex that ranges in thickness from a few hundreds of meters to up to ~2 km. It comprises anastomosing, crystal-plastic thrusts along which the sequences of metasedimentary rocks are interleaved with slivers of granite gneiss, all sandwiched between the floor thrust with the Lødingen basement gneiss and the roof thrust with the Gullesfjord gneiss (Fig. 15). The Gullesfjord-Austerfjord shear zone is macroscopically folded with locally overturned panels,

documenting its earlier relative age with respect to the large-scale D_2 structures in the study area.

Along the western shore of Austerfjorden, mylonites of the Gullesfjord-Austerfjord shear zone are characterized by recrystallized muscovite and flattened quartz grains that wrap around plagioclase and microcline porphyroclasts that are mantled by fine-grained quartz and feldspar (Fig. 23). Hakkinen (1977) inferred east-directed sense of movement along the Austerfjord thrust based on regional Caledonian trends, but at that time little was known about how to deduce shear sense from meso- and microscopic observations. Measurements of the S-C composite planar fabric (Fig. 24) in the nearly 100-meter-thick zone of mylonitic gneiss along the western shore of Austerfjorden (Fig. 18) document slip lines that parallel elongation lineations measured in mylonites of subarea III (Fig. 22). Petrographic examination of the mylonitic gneiss, however, reveals typically symmetrical (orthorhombic symmetry) φ-type feldspar porphyroclasts that do not lend themselves to unequivocal determination of shear sense. A few σ-type plagioclase porphyroclasts indicate oblique dextral, tops-east movement along north-dipping shear planes (Fig. 23).

Granitic mylonites from the Gullesfjord-Austerfjord shear zone contain common kinked albite twins in plagioclase grains (Fig. 23B) and undulose extinction in quartz and feldspar. Evidence for grain boundary migration recrystallization and subgrain rotation recrystallization is also common (Fig. 25). These microstructures indicate dynamic recrystallization at medium-grade temperatures of 400-500°C (Passchier and Trouw, 1996) with retrogression of peak-metamorphic minerals and textures. Microscopic fabric relations in metasedimentary rocks within the Gullesfjord-Austerfjord shear zone also
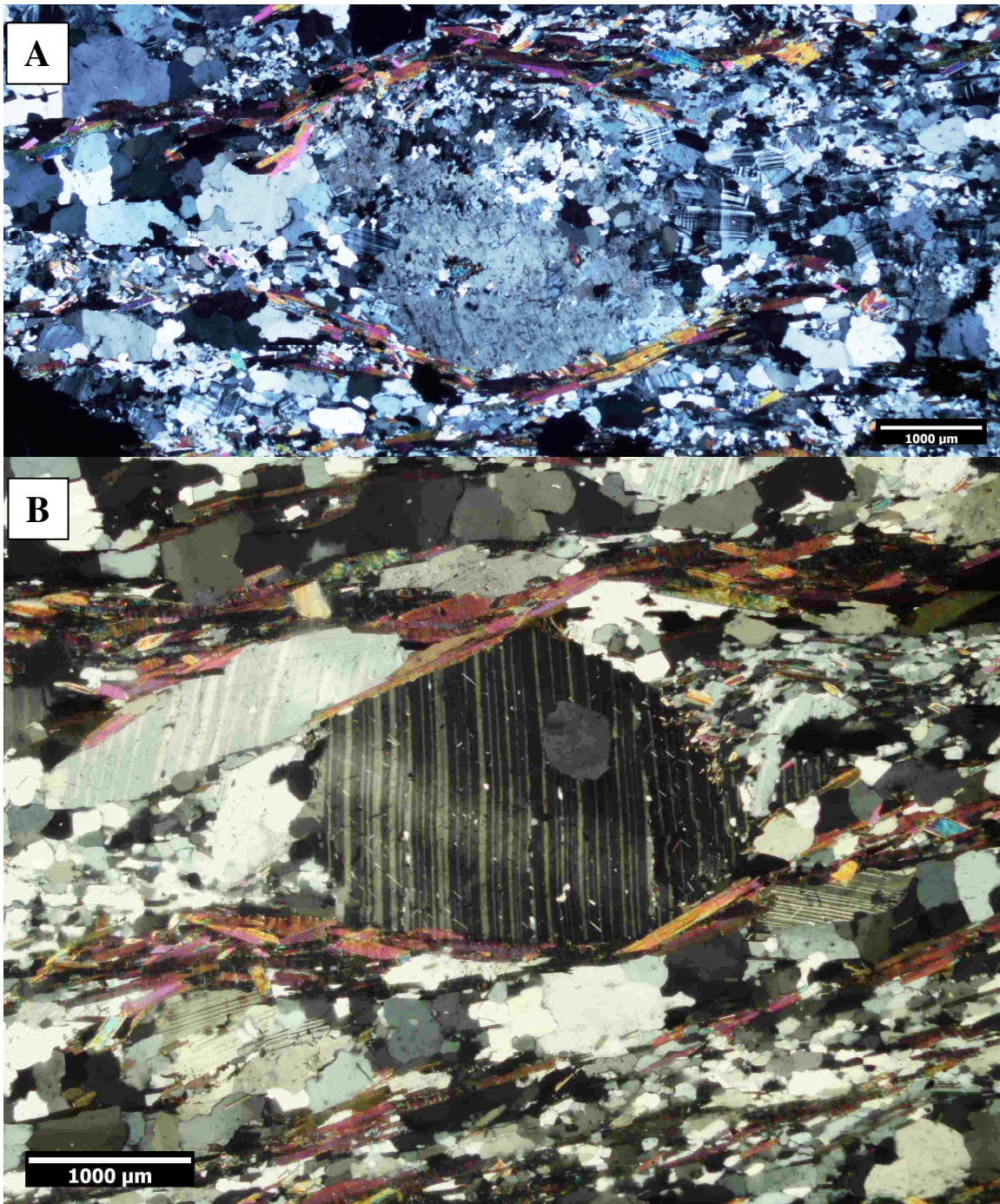
Figure 23. Photomicrographs of granitic mylonite samples (A) JB07-100A and (B) JB07-101 from the Gullesfjord-Austerfjord shear zone along the western shoreline of Austerfjorden. (A) Typical symmetrical (φ-type) mantled porphyroclast. (B) Dextral σ-type plagioclase porphyroclasts. Grain at center contains a weak dextral kink of albite twins. Thin sections cut parallel to elongation lineation and perpendicular to foliation. Cross-polarized light.
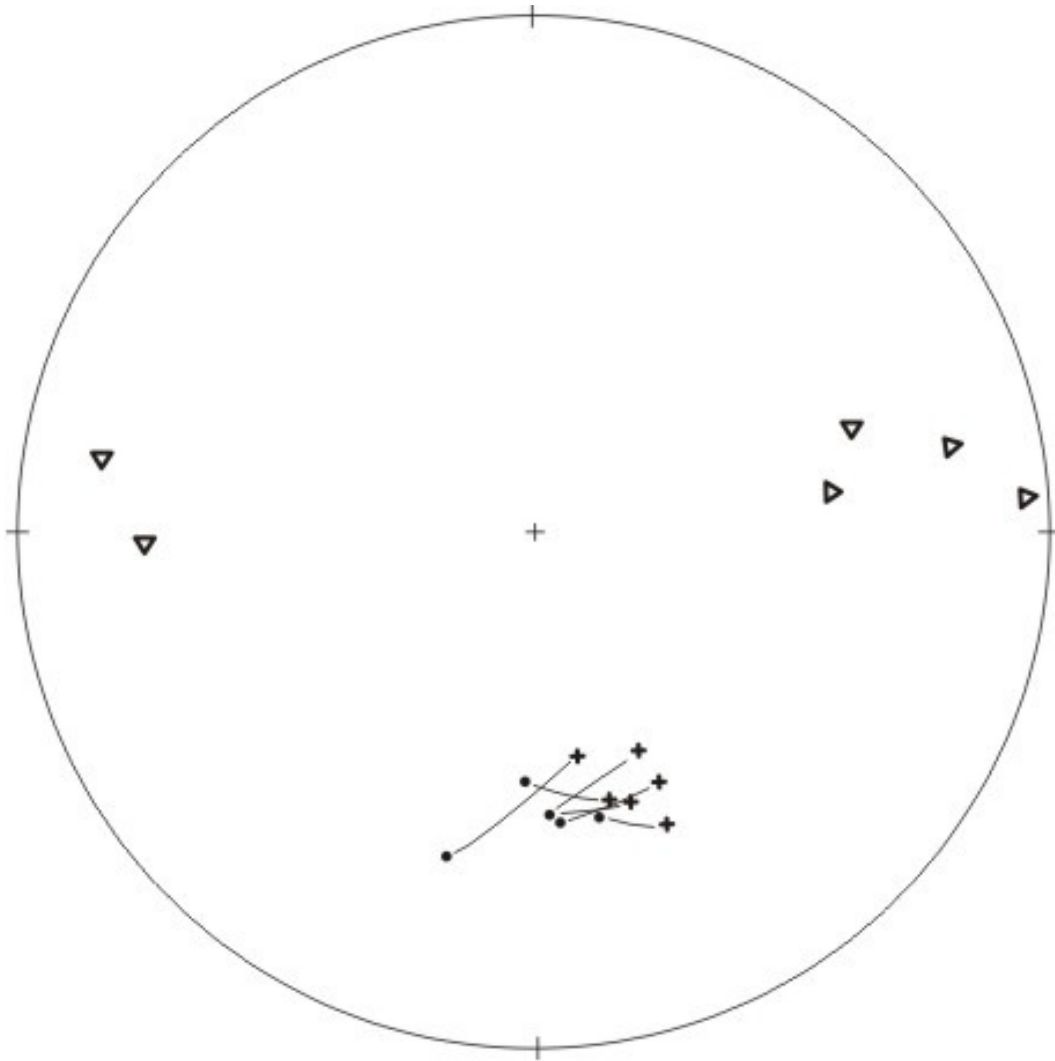
Figure 24. Lower hemisphere stereographic projection of poles to C-planes (•) and S-planes (+) that form the composite planar fabric in the Gullesfjord-Austerfjord shear zone along the western shore of Austerfjorden. Triangles are stereographically determined slip lines from the S-C pairs, which define a weak elliptical point maximum and indicate an oblique dextral, tops-east sense of shear in this north-dipping segment of the shear zone.
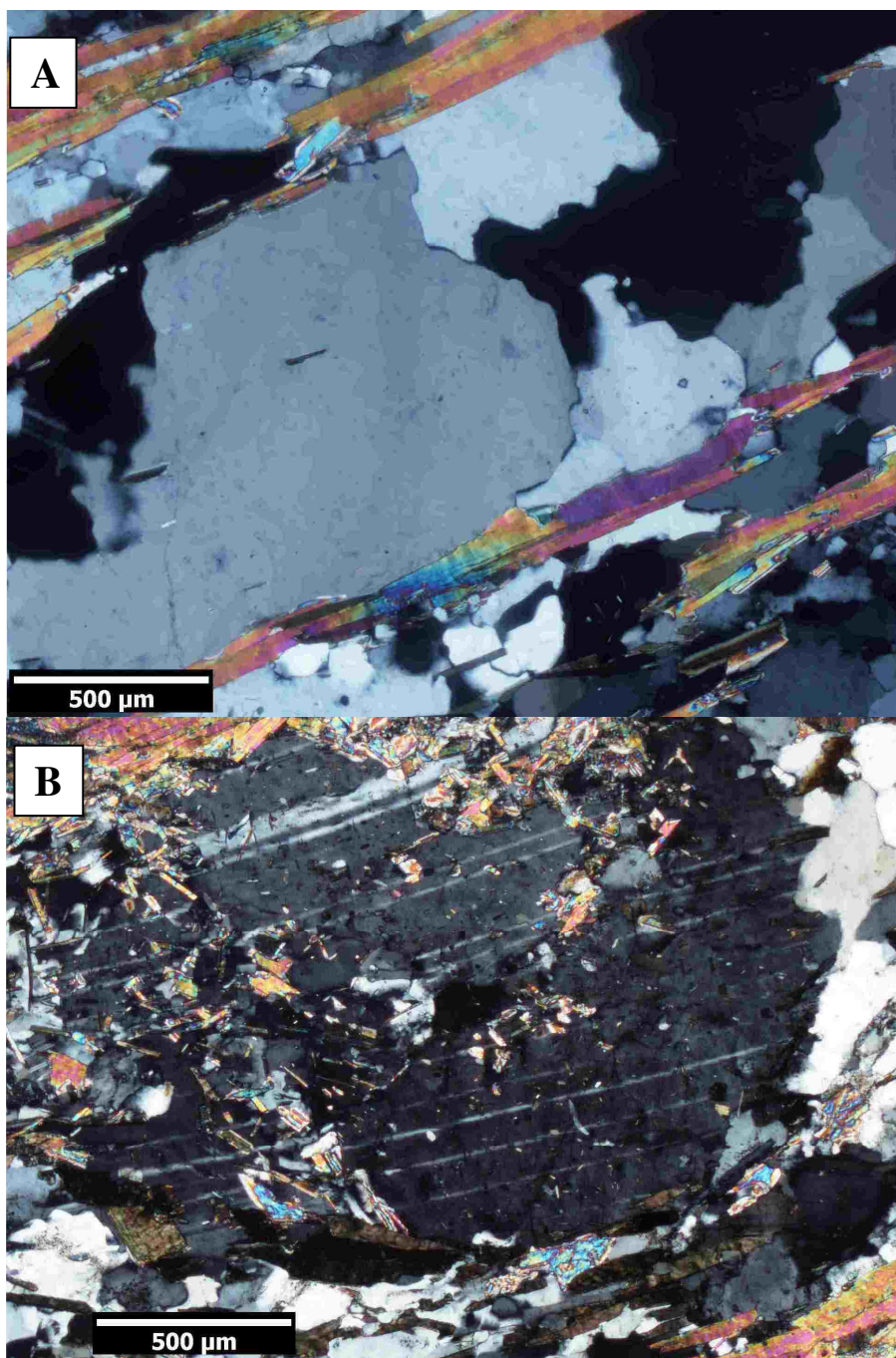
Figure 25. Photomicrographs of granitic mylonites from the Gullesfjord-Austerfjord shear zone along the shore of Austerfjorden. A) Grain boundary bulges document grain boundary migration recrystallization in a quartz ribbon. B) Plagioclase grain with rotated subgrain at top center. Cross-polarized light.

reveal indications of retrogressive deformation (i.e., rotated inclusion trails in garnet porphyroblasts in mica schists of the Vassvika (Fig. 10) and Austerfjord groups (Hakkinen, 1977), and curved inclusion trails in a few hornblende porphyroblasts (Fig. 11) in the Vassvika group amphibolite.

Near Vassvika, the Gullesfjord-Austerfjord shear zone trends east-west and is subvertical to south-dipping. The change in orientation of the shear zone between here and the Austerfjord area is due to D_2 folding (see below). At the northern boundary of this section, which is now the structural bottom of the duplex, the uppermost granitic gneiss is in thrust contact with the amphibole-bearing biotite schist. This roof fault is marked by a subhorizontal quartz and feldspar elongation lineation and a strong mylonitic fabric defined by the alignment of recrystallized muscovite grains and 1-2 mm wide poly-crystalline quartz ribbons (Fig. 26A). No unequivocal asymmetry was observed in the mylonitized granite; however, kinematic indicators were found in the schist, in the form of σ-type plagioclase porphyroclasts (Fig. 14) that indicate dextral, tops-east motion. Amphibole mineral lineations in marble (Fig. 13) and amphibolite of the Vassvika group also parallel the elongation lineation present in the gneiss and schist.

Farther to the west (Fig. 18), there is a >90° bend in the outcrop trace of the Gullesfjord-Austerfjord shear zone around the hinge of a large D_2 synform at Forøya (discussed below). South of this bend the shear zone trends north-south and dips to the east (Fig. 20). Neither bounding surface of the shear zone was found to be exposed along this segment of the duplex. Quartzite along western Gullesfjorden (Fig. 18) is strongly foliated and has an elongation lineation that plunges moderately down-dip to the east, but microscopically the rock has an annealed fabric devoid of stored elastic strain (i.e., the

71
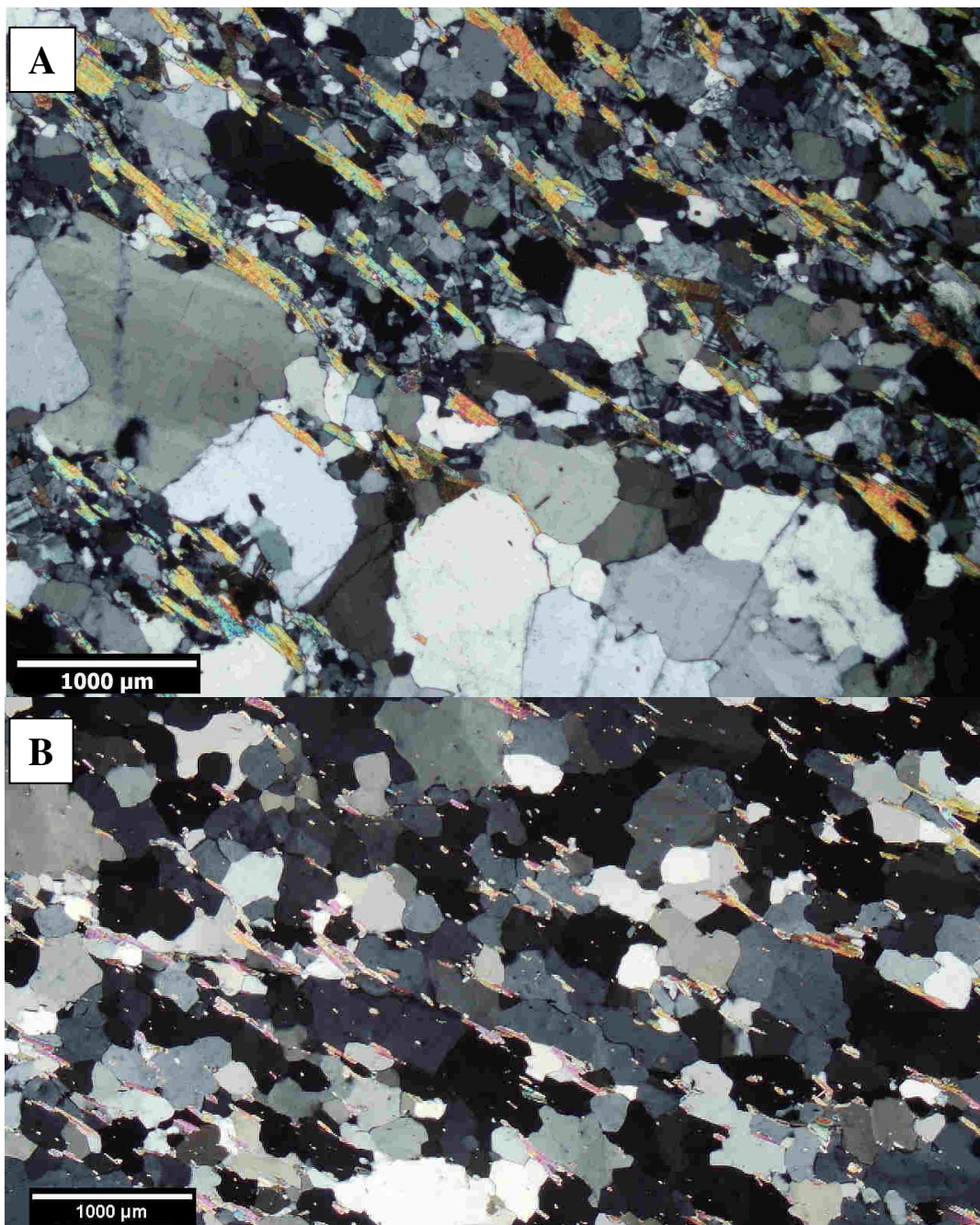
Figure 26. Photomicrographs of roof thrust mylonites of the Gullesfjord-Austerfjord shear zone. (A) Granitic mylonite from the present structural base of the duplex east of Vassvika. Note aligned muscovite grains and poly-crystalline quartz ribbon that define the foliation. (B) Sample JB07-13, a recrystallized quartzite from the western side of Gullesfjorden. Note bimodal size distribution of muscovite grains and the annealed fabric with abundant triple-point junctions between quartz grains. Thin sections cut parallel to elongation lineation and perpendicular to foliation. Cross-polarized light.

fabric is metamorphic rather than mylonitic) and no unequivocal kinematic indicators were observed (Fig. 26B).

The Gullesfjord-Austerfjord duplex dramatically thins, and, over the crest of the Austerfjord antiform, merges into a single fault strand (Figs. 18 and 19). The Austerfjord antiform is herein defined by the domed schistosity of the rocks of the lower Austerfjord group and the foliation in the Lødingen granite gneiss (Figs. 18 and 19: cross-sections A-A' and B-B'). The form line map in Figure 20 demonstrates that this antiformal structure is doubly-plunging and extends north-northwest to south-southeast from Austerfjorden to Fiskefjorden. The mylonitic foliation in the Gullesfjord-Austerfjord shear zone curves around the nose of this structure near the head of Austerfjorden and diverges westward from it to the southwest of Austerfjorden (Fig. 20). A plot of planar fabrics from subarea III (Fig. 21), a mixture of D_0 and D_1 folia, results in a homogenized distribution such that the Austerfjord antiform *sensu stricto* and the plunging antiformal fold defined by the rocks within the Gullesfjord-Austerfjord shear zone are hard to differentiate. A plot of foliation measurements from the rocks deformed within the Gullesfjord-Austerfjord shear zone documents that the structure is folded about a N47°E, 44° plunging axis (Fig. 27), which differs from the north-northwest trend of the Austerfjord antiform.

The southern crest of the Austerfjord dome, near Fiskefjorden, plunges gently to the south-southeast. A klippe of granitic gneiss (Gullesfjord?) is present at the top of Taraldsviktind (Figs. 18 and 28). Tveten (personal communication 2009) reports that the base of the gneiss is a subhorizontal fault that separates it from Lødingen granite gneiss below. Along this boundary are mesoscale lenses of deformed metaconglomerate, similar to those described above, that likely served as a zone of weakness exploited by the
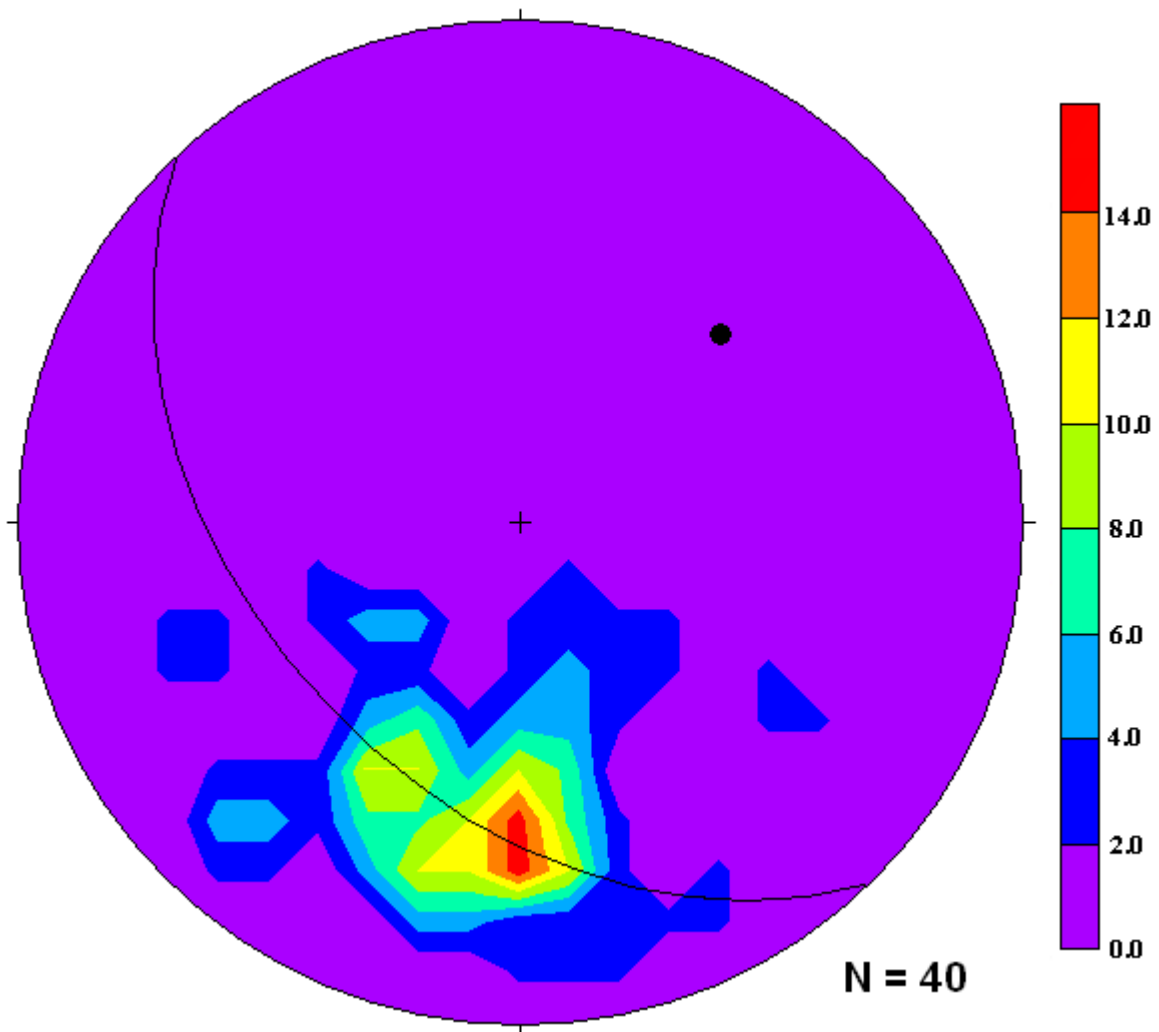
Figure 27. Contoured lower hemisphere stereoplot of poles to schistosity in the Vassvika and upper Austerfjord groups and mylonitic foliation in the Gullesfjord gneiss within the Gullesfjord-Austerfjord shear zone near the head of Austerfjord. The visually-estimated great circle girdle and π-axis (N47°E, 44°) indicate a moderately-plunging northeastern trend for the anticline about which the shear zone was folded. Contour interval is 2% per 1% area.

Figure 28. Photo (looking southwest) of the klippe of Gullesfjord(?) gneiss at the top of Taraldsviktind (Fig. 18 for location). Red arrow indicates the subhorizontal fault boundary separating the upper gneiss from the lower Lødingen gneiss.

developing shear zone. The present author interprets that the Taraldsviktind klippe is Gullesfjord gneiss and the underlying, subhorizontal shear zone projects into the Gullesfjord-Austerfjord shear zone via warping by later folds (Fig. 19: cross-section B-B').

Several lines of evidence indicate that the Austerfjord antiform is not a Caledonian structure, but rather formed during some pre-Caledonian, D_0, event. Connecting the Vassvika group to the upper Austerfjord group indicates that the Gullesfjord-Austerfjord shear zone is contorted over its crest, resulting in the odd fold interference geometry that is described below under D_2. It is clear that the Austerfjord antiform was present before the Gullesfjord-Austerfjord shear zone formed because the former structure is decapitated and the latter duplex is thinned above the crest. This pre-Caledonian dome may have formed as part of the system of northwest-southeast oriented Palaeoproterozoic folds and shear zones that characterize the West Troms Basement Complex directly to the northeast (Bergh et al., 2007b). The present author hypothesizes, therefore, that the Austerfjord antiform formed in the Palaeoproterozoic, and the unusual geometry of the Caledonian allochthons in this area reflects their emplacement upon this inherited structural grain. That elongation lineations in subarea III describe a partial great circle girdle with a π-axis oriented N20°E, 15° (Fig. 22), generally consistent with the axis indicated in Figure 27, also illustrates the influence that this D_0 antiform had on the geometry of subsequent D_1 structures formed in subarea III.

In subarea III (Fig. 21), the Gullesfjord-Austerfjord shear zone is folded at the meso- and macroscopic scales. Along the western shore of Austerfjorden, the mylonitic foliation is crenulated and asymmetrically folded by rootless intrafolial folds. Figure 29 is
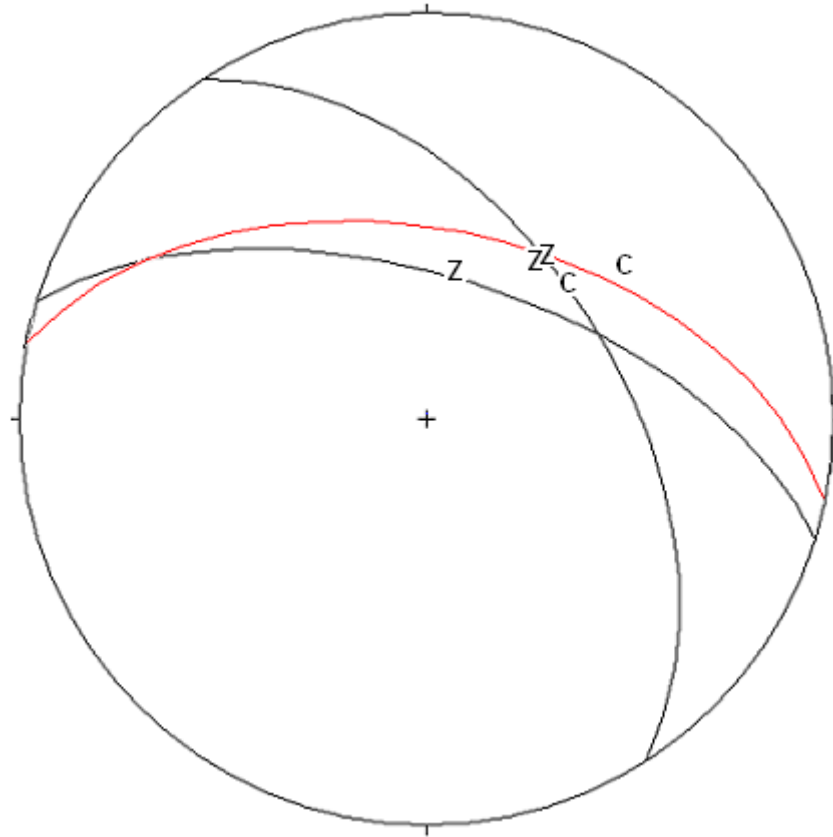
Figure 29. Stereoplot of asymmetric Z-fold axes (Z) and crenulation lineations (C) within the plane of mylonitic foliation (red great circle) in the Gullesfjord-Austerfjord shear zone along the western shore of Austerfjorden indicating slightly oblique, dextral (tops-east) sense of shear. Black great circles represent the orientations of the limbs of the macroscopic Z-fold in the eastern limb of the Austerfjord anticline (Fig. 18) and define a β-axis that roughly parallels the axes of the mesoscopic Z-folds and crenulations in the shear zone to the north.

a stereoplot of crenulation lineations and axes of concentric Z-folds measured along this shoreline section. The average orientation of these axes (N36°E, 49°) is roughly ninety degrees, within the plane of the mylonitic foliation (Fig. 29), from the elongation lineations (Fig. 22: subarea III), indicating dextral, tops-east shearing. At the structural base of the Gullesfjord-Austerfjord duplexes in the eastern limb of the Austerfjord antiform, the floor thrust between the upper and lower Austerfjord group is folded (Fig. 18) about a N64°E, 51° axis, roughly parallel to the average of axes of Z-folds and crenulation lineations in Figure 29. These geometric and vergence relations further support that the Gullesfjord-Austerfjord duplex is a tops-east thrust that was subsequently reoriented by D_2 shears and folds described below.

Deformation D_2 – The second phase of Caledonian deformation recognized on central Hinnøy, D_2, is characterized by tops-to-the-northwest movement along the Sørfjord shear zone, which produced a prominent southeast-plunging pencil lineation (L_2) and a macroscopic sheath fold and related back folds (folds parallel to orogenic trend but verging westward, opposite of typical Scandian vergence) that overturned segments of the Gullesfjord-Austerfjord shear zone. The Sørfjord shear zone (subarea II; Fig. 21) is marked primarily by a zone of strong L-tectonite that extends from the head of Sørfjorden to the southeastern shore of Gullesfjorden, where it plunges beneath the Vassvika group rocks (Fig. 18). Where the Sørfjord shear zone has deformed granitic rocks, they rarely exhibit any vestige of a planar fabric. Rather, an intense pencil lineation is defined by rod-shaped aggregates of stretched quartz and microcline (Fig. 7). The pencil gneiss is very distinctive due to its fine grain size and remarkable, thoroughly homogenized

appearance, which sets it apart from the otherwise coarsely crystalline and massive meta-plutonic rocks in the basement.

Microstructures in Sørfjord shear zone mylonites document amphibolite facies conditions that outlasted D_2 mylonitization, implying the presence of a late-stage thermal dome in this area. The L-tectonite has a thoroughly annealed fabric, with nearly ubiquitous triple-point junctions at boundaries between predominantly strain-free quartz and feldspar grains (Fig. 30). The effects of static recrystallization in the granitic L-tectonite have obliterated clues that might aid in bracketing the conditions of deformation that produced the linear fabric (Fig. 30). Post-kinematic temperature conditions were clearly increased locally in this area, at least as high as 500°C to allow for grain boundary migration recrystallization as a mechanism of grain boundary area reduction to rearrange boundaries to form the equigranular polygonal fabrics in the rocks. Further evidence for, and a mechanism for the formation of this thermal dome is presented in the $^{40}Ar/^{39}Ar$ and discussion sections, respectively.

The lack of a planar fabric in the Sørfjord shear zone and its gradational boundaries make it difficult to clearly delineate the map extent of the shear zone. The pencil lineation is prevalent in the northern and central parts of the study area, especially in subarea II (Fig. 22). The orientation of the pencil lineation corresponds to a strong point maximum of measured elongation lineations oriented at S50°E, 53° (Fig. 22). Planar fabric measurements within the shear zone collected in subareas I and II define partial girdles on stereoplots with π-axes (S65°E, 56° and S47°E, 52°, respectively: Fig. 21) that closely correspond to the signature pencil lineation of the Sørfjord shear zone. Elongation and mineral lineations in the Gullesfjord group metasediments northwest of
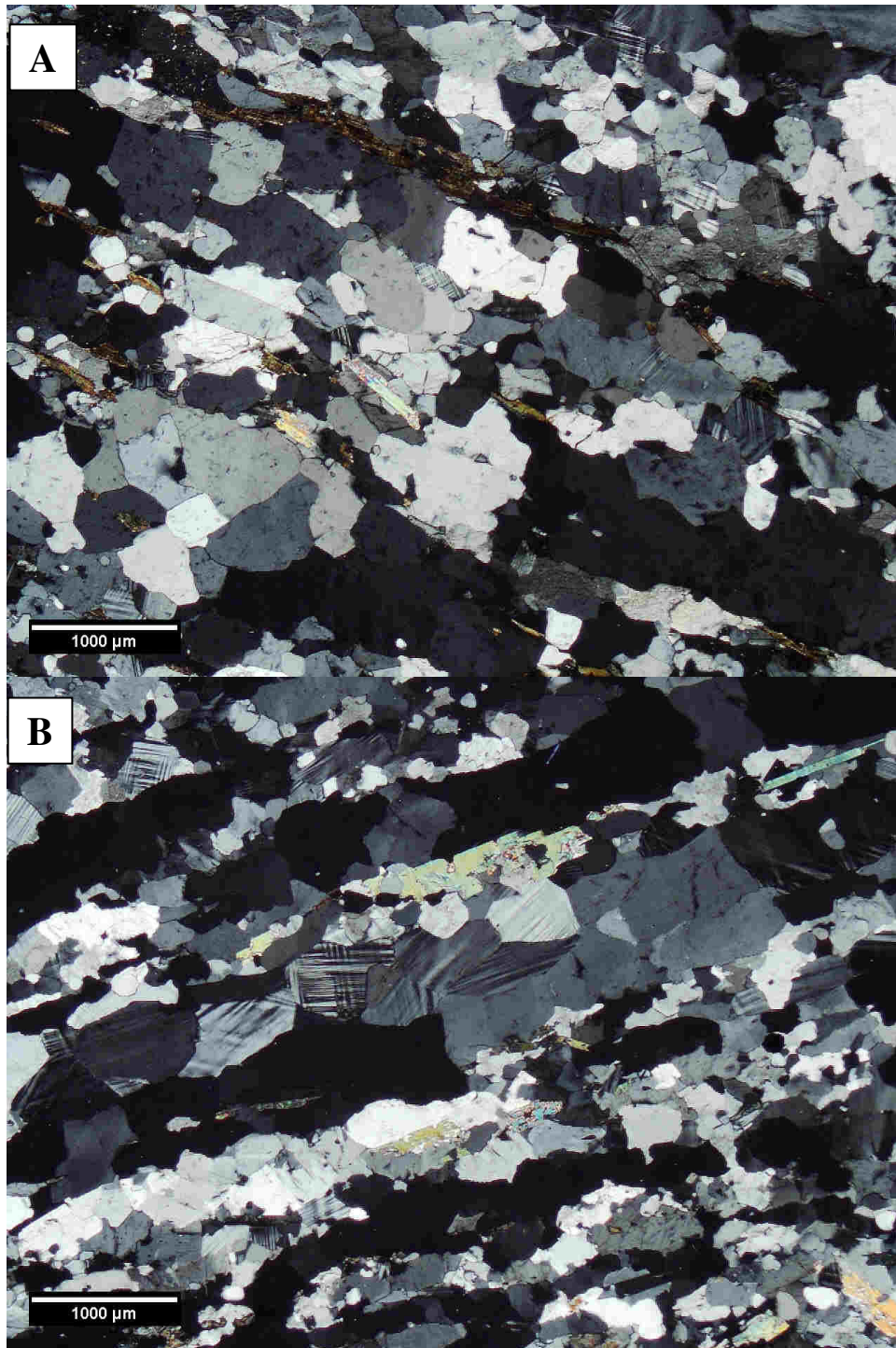
Figure 30. Photomicrographs of Sørfjord shear zone L-tectonite samples TK07-23 (A) and TK07-40 (B). Both samples have an annealed fabric as indicated by the polygonal quartz and feldspar grains typically meeting at ~120° triple junctions. Thin sections cut parallel to pencil lineation. Cross-polarized light.

Gullesfjorden within the Sørfjord shear zone also coincide with this trend. Clearly, all units affected by the shear zone have fabric elements that are strongly drawn into parallelism with it.

Mylonites of the Sørfjord shear zone do not offer any kinematic indicators to unequivocally document the sense of shear, but their high-temperature annealed micro-structures do require intensely plastic, syn-metamorphic conditions of deformation. Taken alone, the mylonites' pencil-shaped aggregates would appear to record purely constrictional strains. Field observations and map and geometric relations do, however, document sympathetic meso- and macroscopic folds that record consistent tops-northwest sense of simple shear movement in this zone.

Near Vassvika, macroscopic structural relationships best illustrate the relative chronology of structures on central Hinnøy. The Gullesfjord-Austerfjord shear zone is swept into the Sørfjord shear zone east of Vassvika (Fig. 20), explaining the former's overturned orientation between Gullesfjorden and Austerfjorden. Construction of four differently oriented lines of cross sections was required in order to unravel the rather peculiar geometry of the Gullesfjord-Austerfjord shear zone, which, as will be shown, results partly due to overprinting by the Sørfjord shear zone. Cross-section C-C' (Fig. 19) illustrates that the Vassvika group rocks are in the overturned limb of a north-northwest-vergent back fold. Similarly, cross-section B-B' (Fig. 19) demonstrates that, south of Forøya, the east-dipping panel of Gullesfjord group rocks results from its position in the overturned limb of a west-verging back fold. These two structures converge near Forøya (Fig. 9), where the orientations of folia in the Gullesfjord and Vassvika group metasediments and the Gullesfjord and Lødingen gneisses define a southeast-plunging

synform (Fig. 31). Cross-section D-D' (Fig. 19), which is oriented roughly perpendicular to the stereographically determined axis of the Forøya synform (S74°E, 51°), reveals an overall conical, or sheath-fold geometry. The trend of the contacts between the Gullesfjord gneiss and migmatite gneiss flanking the Sørfjord shear zone most likely follows the map scale trace of this sheath fold. Map expressions of the antiformal closures of the back folds and sheath fold apparently have been eroded or faulted away, whereas the synformal counterparts, if any ever existed (see below), likely are in the subsurface (Fig. 19). This sheath fold is interpreted to have developed from continued deformation and amplification of a northeast-southwest trending back fold (Fig. 32), similar to the regional set of back folds recognized directly to the east of the study area (Steltenpohl and Bartley, 1988). The back folds illustrated in cross-sections B-B' and C-C' (Fig. 19) correspond to the "S" and "Z" folds (respectively) of the anvil- shaped basal cross-section of the sheath fold (Fig. 32). The present east-west and north-south trends of the back fold axes resulted from reorientation of the originally northeast-southwest trending back fold as the sheath fold formed (Fig. 32). Axes of tight-to-isoclinal folds in strongly deformed metasedimentary rocks in the limbs of the sheath fold exposed along the eastern shore of Gullesfjorden (Fig. 31) correspond to the flow orientation of the Sørfjord shear zone; the axis of the synform parallels the pencil lineation within the Sørfjord shear zone (Fig. 22, subarea II). Vergence of folds and the intense mineral elongation suggests coeval formation of the sheath fold and Sørfjord shear zone, which is further evidence for highly ductile northwest-directed flow within this shear zone.

Surface exposures indicate that the Sørfjord shear zone did not deform rocks more than 1 km southeast of Gullesfjorden. Poor exposure in the rubble fields and densely
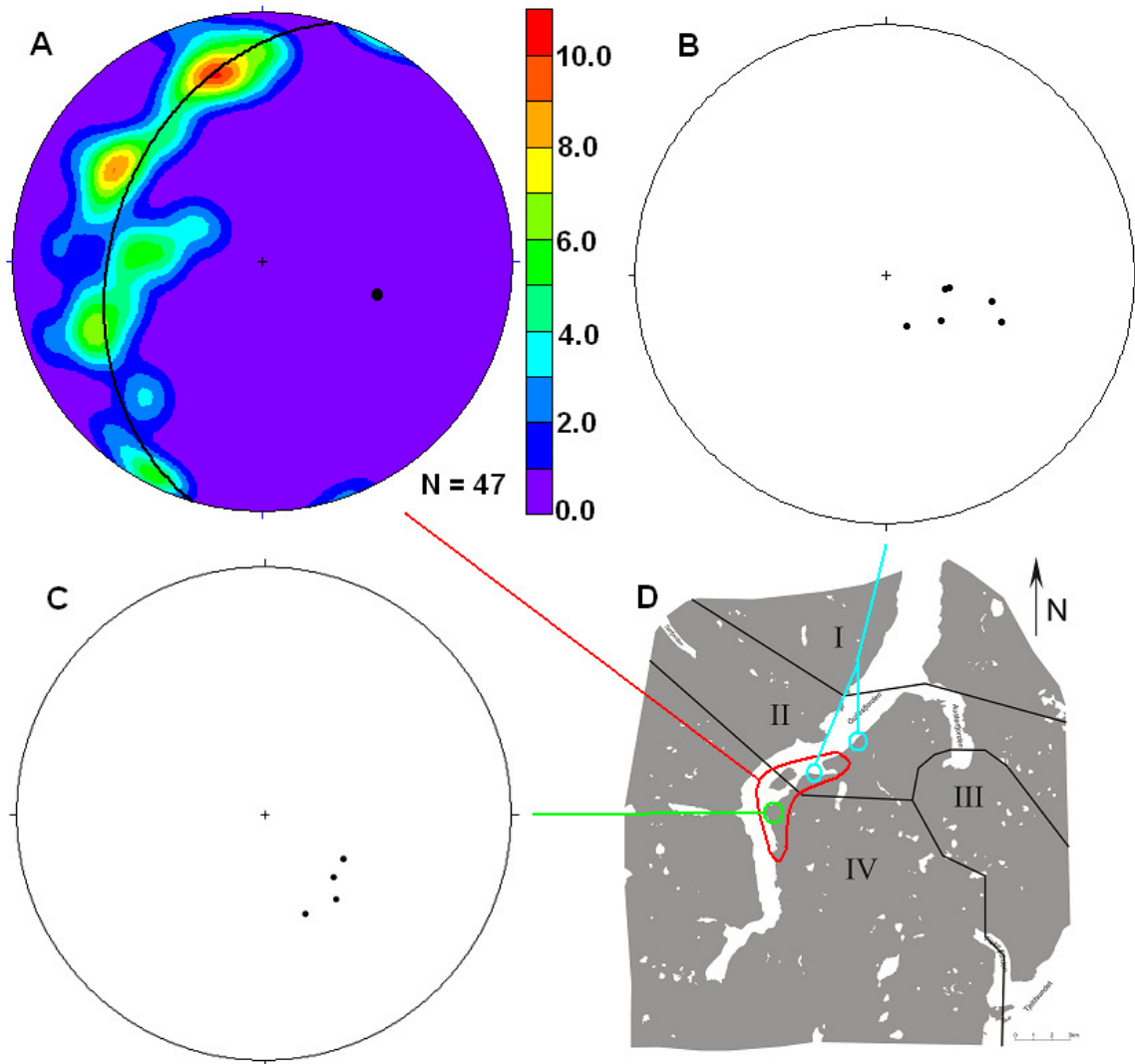
Figure 31. Stereoplots of (A) poles to foliation in the Forøya synform, F_2 fold axes from (B) subarea II and (C) subarea IV. D illustrates the areas from which these structural measurements were obtained. The π-axis indicated in A (S74°E, 51°) closely parallels the axes of mesoscopic folds (B and C) in the limbs of the macroscopic fold and the Sørfjord shear zone elongation lineations (Fig. 22, subarea II). Scale bar in A is graded in % per % area.
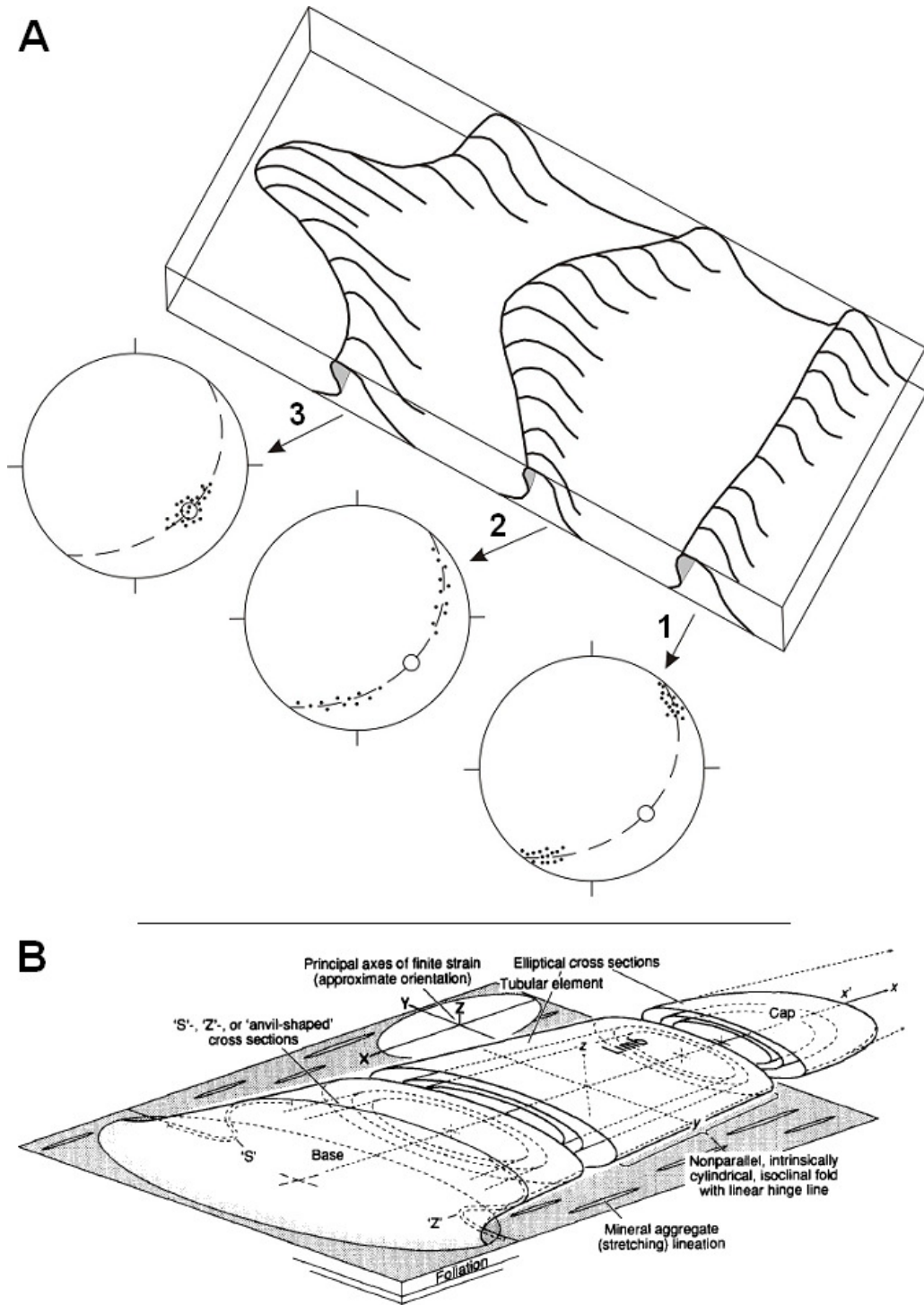
Figure 32. A) Progressive deformation and amplification of cylindrical folds into non-cylindrical then sheath folds through several stages, labeled 1-3. Stereoplots document fold hinge orientations (dots) in each stage. Note how hinges evolve into a down-dip plunging cluster in the final, sheath fold configuration (Modified from Hatcher, 2008). B) Basic geometry of a sheath fold. Note how cross-section changes from anvil-shaped near the base of the fold to elliptical farther out toward the cap (From Mies, 1993).

vegetated valleys of this area obscure the precise location of the boundary of the shear zone, but outcrops of practically unfoliated Gullesfjord gneiss (Fig. 14A) were found ~800 m northeast of Vassvika, between the Sørfjord and Gullesfjord-Austerfjord shear zones (Fig. 18). The author did not map the trace the Sørfjord shear zone to the northwest outside of the study area, but reconnaissance observations suggest its exposure likely ends in the area near the head of Sørfjorden. Possible explanations for termination of the shear zone to the northwest are as follows: it has been eroded away; it domally crests in the study area and plunges out in the subsurface to the northwest; or it was excised along a late, northeast-southwest trending fault recognized in that area by Hakkinen (1977; Fig. 18).

The offset between the axial trace of the Forøya synform and the Sørfjord shear zone east of Forøya is likely due to an apparent late-stage, right-lateral fault within Gullesfjorden, herein called the Gullesfjord fault (Fig. 18). Hakkinen (1977), Bartley (1982b), Steltenpohl (1987), and Tveten (personal communication 2010) all report the presence of late-stage, high-angle faults, some with documented right-slip displacements, in this part of Hinnøy and adjacent Skånland to the east. The trends of these faults are also consistent with Permian to Paleocene rift-related fault-fracture networks recently suggested by Bergh et al. (2007a).

The northeastern arm of Gullesfjord group rocks and related shear zones to the northeast of the Sørfjord shear zone are less well constrained, as little mapping of this area was done for the present study. Hakkinen (1977), Bartley (1981), and unpublished data of Tveten (personal communication 2010) indicate that the contacts between the metasedimentary rocks and Gullesfjord gneiss along this northeastern arm are not well

exposed, which is consistent with the present author's reconnaissance observations. Along the northwest shore of Gullesfjorden, Hakkinen (1977) and Tveten (personal communication 2010) interpreted the southeast-dipping contact between the Gullesfjord group quartzite and Gullesfjord gneiss to be tectonic in nature. Stretching lineations there plunge moderately to the southeast, oblique to dip, but no kinematic indicators were reported (Hakkinen, 1977; Tveten, personal communication 2008). Bartley (1981) and Tveten (personal communication 2010) interpreted the contact between the Gullesfjord group mica schist and the Gullesfjord gneiss along the northeast side of the fjord (Fig. 18) as a tectonic boundary as well. Tveten (personal communication 2010) reports that in this latter area the foliations of the two rocks are swept into concordance near the contact.

Tveten (personal communication 2010) reports that the northeasternmost exposures of the Gullesfjord group rocks are quite similar to the rocks along the southern shore of Gullesfjorden and within the Vassvika group (Fig. 18). Figure 20 shows an east-west trending synformal trace between Gullesfjorden and Austerfjorden. This synform parallels the back-fold to the south (Fig. 19: cross-section C-C'). Given the similar lithologies and structural geometries, the present author interprets this shear zone to be continuous with the Gullesfjord-Austerfjord shear zone beneath Gullesfjorden (Fig. 19: cross-sections A-A', C-C', and D-D'). The Gullesfjord gneiss between Gullesfjorden and the Vassvika group was emplaced along the roof thrust of the Gullesfjord-Austerfjord shear zone. This synform is interpreted to have formed synchronously with the back-fold as a result of tops-northwest movement along the Sørfjord shear zone. The strongly deformed lens of metasediments along the southern shore of Gullesfjorden (Fig. 18),

thus, likely represents a slice of the Gullesfjord group rocks that was segmented by the later formed Sørfjord shear zone at depth.

^{40}Ar/^{39}Ar Thermochronology

<u>Introduction</u>

The recognition of continuity between the Austerfjord thrust and Gullesfjord shear zone demonstrates that the basal Caledonian thrust extends much farther westward into the Lofoten-Vesterålen terrane than was previously thought. The absolute ages of this and related structures require verification through radiometric ages. Sampling for analysis of the age of the Gullesfjord-Austerfjord shear zone, and the newly discovered Sørfjord shear zone, was, therefore, focused on rocks containing the strongest fabrics inferred to be Caledonian based on the present author's mapping and structural analysis. Figure 33 shows the locations for the five analyzed samples relative to these structures. Binocular microscope photomicrographs of the separated minerals, analytical procedures, and analytical results are in Appendix I.

<u>Petrography</u>

Gullesfjord-Austerfjord Shear Zone – Samples JB07-100A and JB07-101 are granitic mylonites of the Gullesfjord-Austerfjord shear zone from coastline exposures along the western shore of Austerfjorden (Fig. 33). Here in the crest of the Austerfjord anticline the shear zone is at its thinnest, marked by a zone of mylonite about 100 meters thick. Samples were taken from the structurally lower half of this zone; JB07-101 from the lowest exposures (UTM33, E543076 N7615195), and JB07-100A from about 20 meters
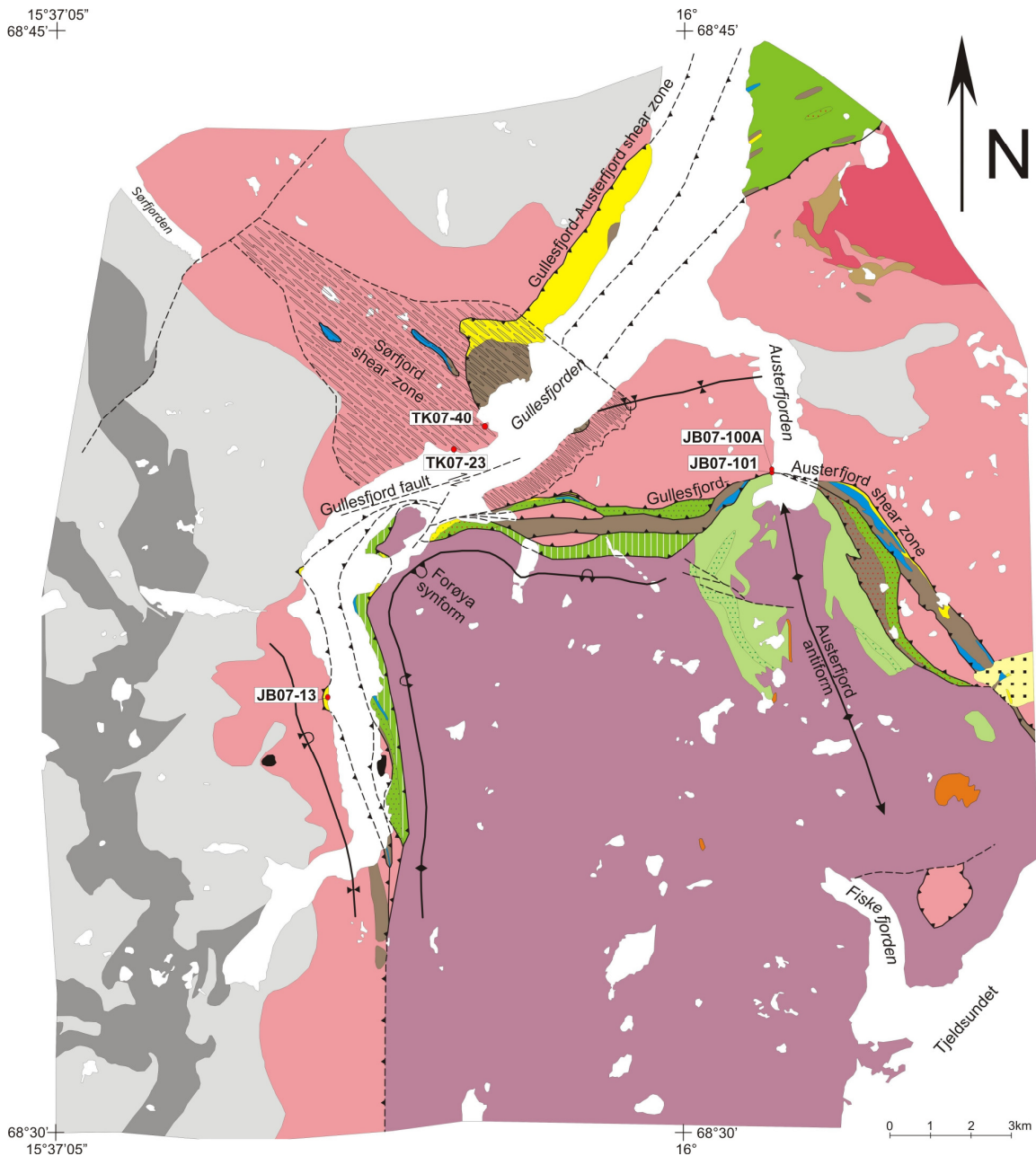
Figure 33. Locations for samples collected for $^{40}Ar/^{39}Ar$ analysis. JB07-13, JB07-100A, and JB07-101 from the Gullesfjord-Austerfjord shear zone; and TK07-23 and TK07-40 from the Sørfjord shear zone. Lithologic and structural symbols are the same as in Figure 18.

north, or up-section (UTM33, E543089 N7615218). Sample JB07-101 is granodioritic in composition with a highly variable grain size distribution. The mylonite's strong planar and linear fabric is defined by the alignment of recrystallized muscovite (~10%) and partially chloritized biotite grains that occur along boundaries of feldspar and flattened quartz grains and gently warp around plagioclase porphyroclasts (Fig. 34A). Most of the quartz grains have undulose extinction and grain boundary bulges (Fig. 25A), and a few have deformation lamellae. Plagioclase grains contain bent and offset twin lamellae. Sharp grain boundaries within the more fine-grained portions indicate static recrystallization. Long dimensions of muscovite grains range from ~200 µm up to 1.5 mm (Fig. 34B), and average roughly 600 µm in length.

Sample JB07-100A is an alkali feldspar-rich granitic mylonite with significantly less plagioclase than sample JB07-101. It also has a highly variable grain size distribution, and its planar fabric is defined by ~1-mm-thick bands of recrystallized quartz and feldspar separated by thin layers of muscovite (Fig. 34B). Porphyroclast development and isolation in this sample was not so pervasive as in sample JB07-101. Porphyroclasts are a mix of plagioclase and microcline grains that occur as recrystallized aggregates or as relict cores with recrystallized mantles. Muscovite makes up about 10% of this sample, and occurs as recrystallized grains with long dimensions ranging from ~200 up to 1.5 mm, and averaging ~500 µm.

Sample JB07-13 is an orthoquartzite from near the western boundary of the Gullesfjord-Austerfjord shear zone, at the top of the overturned Gullesfjord group metasedimentary sequence (Fig. 33; UTM33, E532114 N7609667). It comprises nearly all quartz with minor feldspar, and it has a flaggy appearance with a strong lineation
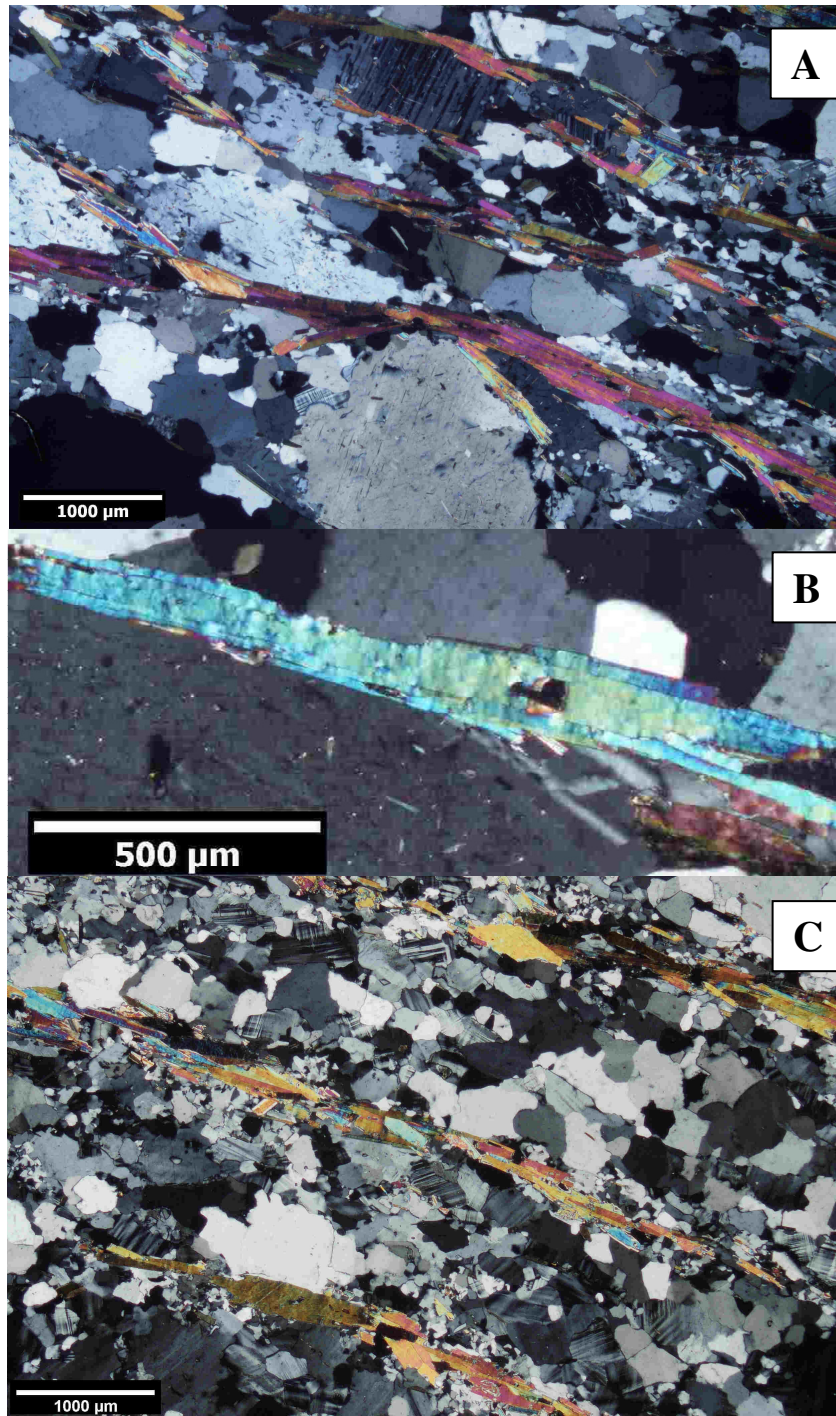
Figure 34. Muscovite in the granitic mylonites from the Gullesfjord-Austerfjord shear zone near Austerfjorden. Sample JB07-101: A) plagioclase porphyroclast in bottom center, mylonitic foliation defined by parallel muscovite and elongate quartz and feldspar grains; and B) large, fabric-forming muscovite grain. Sample JB07-100A: C) mylonitic foliation defined by alternating bands of recrystallized quartz and feldspar grains and thin layers of muscovite. Sections cut parallel to elongation lineation and perpendicular to foliation. Cross-polarized light.

imparted by the alignment of muscovite grains. Muscovite composes ~5% of the sample. The fabric of the rock is nearly completely annealed, with strain-free, polygonal quartz grains and abundant ~120° triple point junctions (Fig. 26B). There is a bimodal size distribution of recrystallized muscovite grains; a smaller, more randomly oriented set (~70 µm) and a larger fabric-forming set (~250-600 µm). The size of the grains isolated during sample preparation (see below) ensured that grains used for geochronological analysis were the larger, fabric-forming grains (see appendix).

Sørfjord Shear Zone – Samples TK07-23 and TK07-40 are mineralogically and texturally identical alkali feldspar-rich granitic L-tectonites from a quarry (UTM33, E535076 N7615773) and a road cut (UTM33, E535878 N7616456), respectively, from along the north shore of Gullesfjorden (Fig. 33). The samples were collected about 1 km from one another within the core of the ~5-km-wide Sørfjord shear zone. Here, the rocks rarely contain a planar fabric (Fig. 7), but are intensely lineated. The strong pencil lineation is defined by the rod-shaped quartz and feldspar composites, in which grains boundaries meet at 120° triple point junctions (Fig. 30). Samples TK07-23 and TK07-40 contain undeformed muscovite porphyroblasts (~1% by volume of both samples) with average long dimensions averaging roughly 400 and 600 µm in length, respectively. Muscovite grains typically have a poikiloblastic texture with quartz inclusions. The long dimensions of some of the muscovite grains parallel the linear fabric of the rocks, but many grains are randomly oriented, suggesting that metamorphic conditions outlasted deformation in this zone.

^{40}Ar/^{39}Ar Methods

The five samples were crushed by hand and sieved. The size fractions taken from the 80-100 mesh sieves were found to be preferable for the spectrometric analysis of muscovite. Samples were then run through the Frantz magnetic separator to concentrate the muscovite. Approximately 50 to 100 muscovite grains were hand picked from each sample using a binocular microscope and were prepared for ^{40}Ar/^{39}Ar analysis in the Auburn Noble Isotope Mass Analysis Laboratory (ANIMAL). Ten grains from each sample were analyzed using Single Crystal Total Fusion techniques. Further information concerning ^{40}Ar/^{39}Ar methods and raw data are included in the appendix.

^{40}Ar/^{39}Ar Results

The Single Crystal Total Fusion analyses of ten muscovite grains from each sample yielded mid- to late-Devonian mean ages ranging from 391 to 372 Ma (Fig. 35). Analysis of single crystals selected at random produced a statistically representative array of intercrystalline ages of each sample. The results are described from oldest to youngest.

Gullesfjord-Austerfjord Shear Zone – Muscovite from sample JB07-101 from the structurally lowest portion of the Gullesfjord-Austerfjord shear zone yielded a mean age of 391.4 ± 1.7 Ma (n = 9; MSWD = 1.2). For sample JB07-101, one grain that yielded an age of 420.9 ± 2.9 Ma differed from the mean of nine other samples by more than two standard deviations and was omitted from calculation of the mean. Sample JB07-100A, from 20 meters structurally higher, has a mean age of 384.8 Ma.
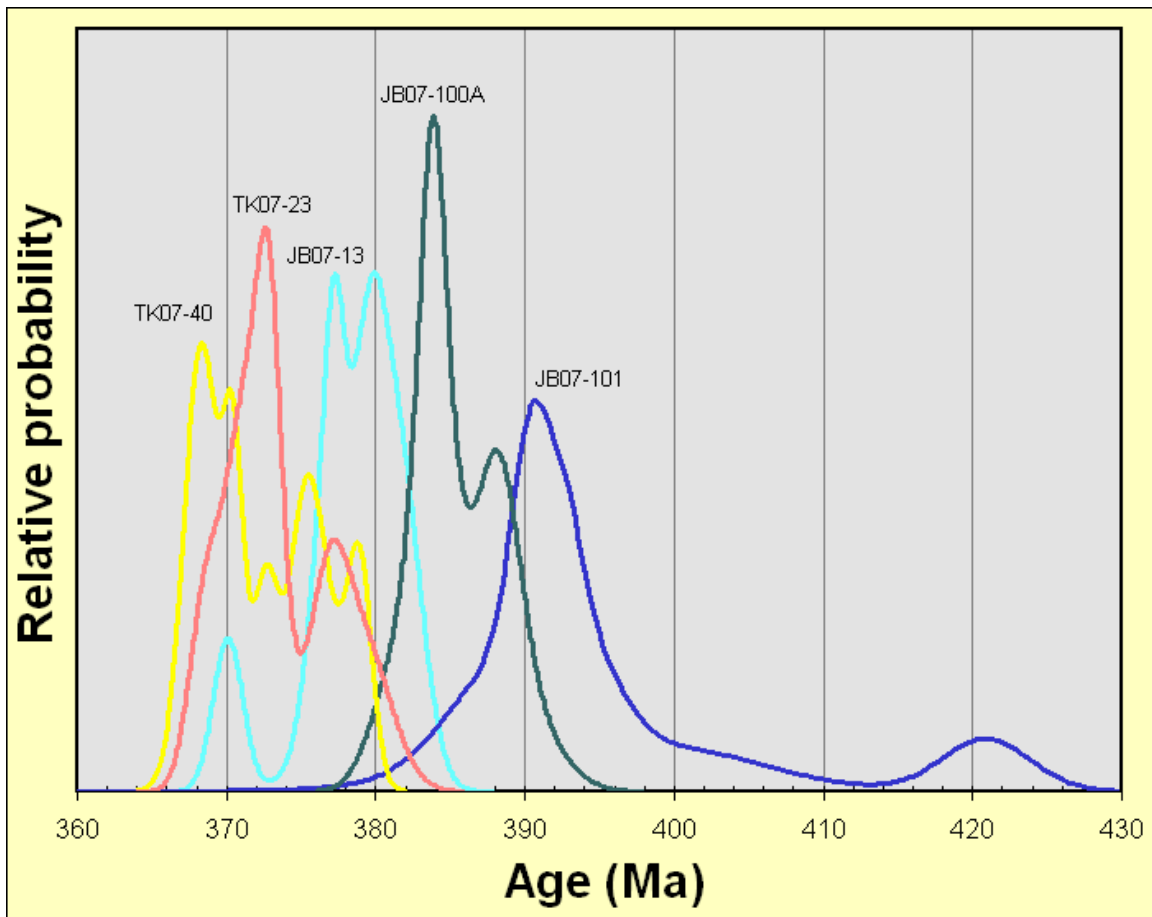
Figure 35. Probability density curves created from the Single Crystal Total Fusion data from samples from the Gullesfjord-Austerfjord shear zone (samples JB07-100A, JB07-101, and JB07-13) and the Sørfjord shear zone (samples TK07-23 and TK07-40). Age population distributions were constructed for 1σ at 95% confidence level.

Muscovite from the quartzite from near the western boundary of the Gullesfjord-Austerfjord shear zone, sample JB07-13, yielded a mean age of 378.8 Ma. One grain, which yielded an age of 370.1 ± 1.0 Ma, was omitted from the mean age calculation because the age differed from the mean of nine other samples by more than two standard deviations.

Sørfjord Shear Zone – Muscovite from samples TK07-23 and TK07-40, from the core of the Sørfjord shear zone, yielded the youngest mean ages of 372.5 and 372.4 Ma, respectively. Sample TK07-40 has a MSWD of 17 (see appendix) indicating the muscovite in the sample has geologic age variability with some crystals as old as ca. 380 Ma and some as young as ca. 368 Ma.

Interpretation of ^{40}Ar/^{39}Ar Results

Results of ^{40}Ar/^{39}Ar analyses are discussed from oldest to youngest in both the context of the ages of the structures they represent relative to one another, and the thermal histories of the rocks as evidenced by petrographic analysis of their internal fabrics. Figure 36 illustrates the structural positions of the five samples within the major shear zones on central Hinnøy.

Structural data document that the metasedimentary rocks and basement slivers of the Austerfjord, Vassvika, and Gullesfjord groups, as well as the Gullesfjord gneiss above the roof thrust to the Gullesfjord-Austerfjord duplex were emplaced prior to back fold and sheath fold formation related to movement along the Sørfjord shear zone (Fig 19).
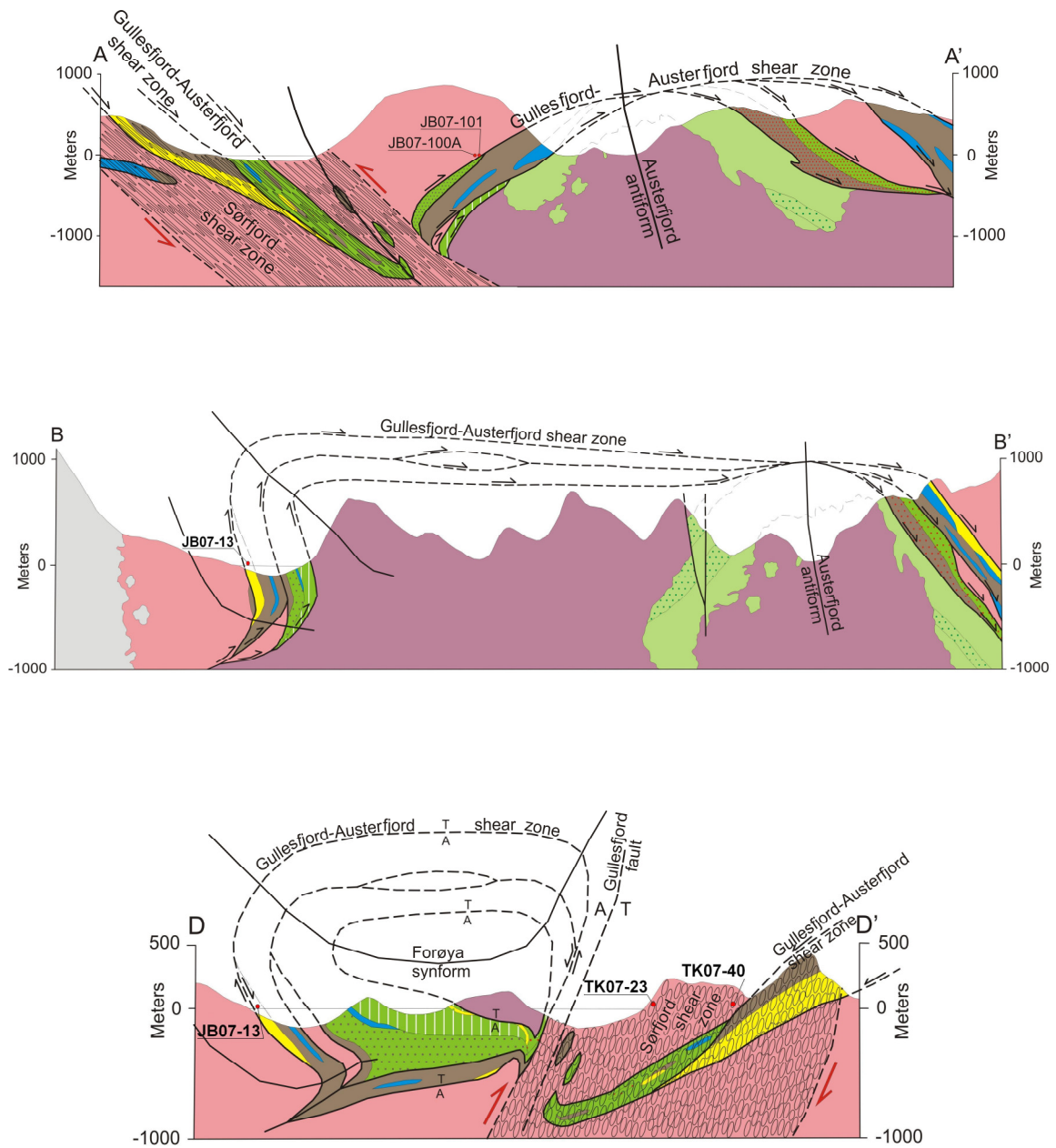
Figure 36. Cross-sections A, B, and D (from Figure 19) illustrating the structural positions of samples (projected onto the planes of the sections) relative to the major shear zones. Section A-A': samples from the Gullesfjord-Austerfjord shear zone from the nose of the Austerfjord anticline (Fig. 33). Section B-B': sample from the Gullesfjord-Austerfjord shear zone in the overturned limb of the north-south trending back-fold. Section D-D': sample from the Gullesfjord-Austerfjord shear zone in the limb of the sheath-fold (Forøya synform) and samples from the core of the Sørfjord shear zone.

^{40}Ar/^{39}Ar cooling ages of muscovite from mylonitic rocks sampled from within these shear zones corroborates the relative timing sequence of deformation based on the structural analysis.

The oldest ages (ranging from 381-420 Ma) are from samples collected from a section of the D$_1$ Gullesfjord-Austerfjord shear zone farthest from the Sørfjord shear zone, and, therefore were least affected by movement along the D$_2$ Sørfjord shear zone. Dynamic recrystallization appears to have been dominant over static recrystallization, indicating uplift soon after deformation ceased (Fig. 25). Complete recrystallization was never attained as documented by the predominance of stored elastic strain in bent and offset plagioclase twin lamellae and undulose extinction in quartz and feldspar grains. The presence of muscovite grains much larger than the size fraction obtained from the sieves (e.g., Fig. 34B) suggests that some of the grains analyzed were likely fragments of larger grains, which would be expected to have older cores and younger rims due to the cylindrical diffusion geometry of the muscovite crystal structure (Hames and Bowring, 1994). A nominal 350°C closure temperature is only justified for single-generation assemblages with a ~100-200 µm diameter grain size (Hames and Bowring, 1994). The larger grains, therefore, may have cores with ages representing argon retention upon passage above a higher-temperature isotherm (up to about 500°C: Hames and Andresen, 1996). This might explain the presence of the 420 Ma grain in sample JB07-101, an age that is consistent with the peak of the Scandian phase of the Caledonian orogeny. Hames and Andresen (1996) reported similar findings on muscovites from farther west in Lofoten.

Sample JB07-13 was collected from the westernmost exposures of the Gullesfjord-Austerfjord shear zone. The younger, 370-382 Ma, age range of this sample plots between the oldest ages from the Gullesfjord-Austerfjord shear zone to the east and the younger, 368-379 Ma ages from the core of the Sørfjord shear zone (Fig. 35). The affects of static recrystallization produced a completely annealed fabric in the quartzite, indicating that rocks in this section of the Gullesfjord-Austerfjord shear zone experienced elevated temperatures after movement along the zone had ceased. This was likely a result of burial beneath the upright limb of the back fold, as illustrated in cross-sections B-B' and D-D' (Fig. 36). The muscovite grain from sample JB07-13 that yielded the youngest age (370 Ma) that was excluded from the mean age calculation might be explained by the possibility of its being a rim fragment of one of the fabric-forming grains from the sample that records recrystallization during only the latest stage of elevated temperature above that of argon retention for muscovite (~350°C). The young age is also consistent with cooling ages from the core of the Sørfjord shear zone and may likely represent resetting during D_2 deformation. Another explanation for the younger ages from the western portion of the Gullesfjord-Austerfjord shear zone lies in the difference in average grain size between granitic mylonites from the Austerfjord area and the quartzite from Gullesfjorden. Considering nominal parameters for argon diffusion in muscovite (Hames and Bowring, 1994) and the cooling model of Dodson (1973), a difference in closure temperature of ~25°C would be expected for grains sizes of 0.6 mm vs. 0.3 mm resulting in a 5-10 m.y. shift.

The youngest ages were obtained from samples TK07-23 and TK07-40 (368-379 Ma) from the core of the Sørfjord shear zone (Fig. 36). These rocks have the most

completely annealed fabrics of all analyzed samples. Such a strong fabric must have been produced by intense, syn-high temperature deformation, but the near absence of stored elastic strain energy in the mineral grains is interpreted to indicate the rocks experienced a period of burial at elevated temperatures during which the mylonitic rock fabric was annealed. This allowed cooling by ~380-370 Ma. The poikiloblastic texture of the muscovite porphyroblasts is also compatible with the interpretation that argon isotopic closure occurred in at least some of the grains after the period of intense deformation in this zone. Several muscovite grains in these L-tectonites are up to 2mm in length, which suggests that the younger ages cannot be attributed to the same negative cooling age shift as is postulated as a possible explanation for the younger Gullesfjord-Austerfjord shear zone ages from sample JB07-13.

The relatively older ages of samples JB07-100A and JB07-101 are interpreted to record cooling from the earliest movement along that zone (in the cores of its largest grains) to their passage through the ~350°C isotherm (in the smaller grains and rims of the larger grains). Ages of muscovite from sample JB07-13 record cooling after having been overturned by movement along the Sørfjord shear zone, which resulted in a domal elevation of the ~350°C isotherm in this localized area.

Discussion and Conclusions

Field investigation and laboratory analysis of rocks on central Hinnøy has led to two significant discoveries concerning the Caledonian structural and tectonic evolution of this region: 1) the Austerfjord thrust and Gullesfjord shear zone are the same structural feature, the Gullesfjord-Austerfjord shear zone, comprising several thrusts within a wide zone of deformation; and 2) the Sørfjord shear zone and related back folds that document tops-northwest, late-Caledonian extensional transport.

The recognition that the Gullesfjord-Austerfjord shear zone involves rocks of extra-Lofoten origin (i.e., 1.1-1.3 Ga, Laurentian derived, allochthonous metasiliciclastic rocks of the Gullesfjord group), contradicts previous interpretations that implicated the Austerfjord thrust as a relatively minor Caledonian structure (e.g., Hodges et al., 1982). $^{40}Ar/^{39}Ar$ muscovite ages from the Austerfjord area (420 to 380 Ma) demonstrate that faults within the Gullesfjord-Austerfjord shear zone experienced movement during the peak Scandian contractional event through Early Devonian extension. These thermo-chronological findings, and map and field relations documented in the present study support Rykkelid's (1992) model involving the late-stage, out-of-sequence thrusting of basement over the metasedimentary rocks and slivers of granite within the duplex that led to the present configuration of these rocks being sandwiched between thick slabs of allochthonous granitic basement gneiss.

Subsequent movement along the Sørfjord shear zone, and synchronous back folding of the Gullesfjord-Austerfjord shear zone prior to cooling by 380-370 Ma, represents the earliest documented stage of west-vergent, extensional deformation in the arctic Norwegian Caledonides. The high-temperature mylonitic fabrics developed within this macro-scale sheath fold also indicate that high-grade conditions of deformation persisted in this area into the Early Devonian.

The presence of near synchronous, both east- and west-vergent Caledonian structures on central Hinnøy requires that ideas about the timing and styles of contraction and extension in the northern portions of the Scandinavian Caledonides be reevaluated. Large-scale and rapid extension beginning in the Devonian is well documented in southwest Norway (Andersen and Jamtveit, 1990; Walsh et al., 2007). The presence of Devonian extensional structures in north Norway, however, has been suggested (Steltenpohl and Bartley, 1988; Klein et al., 1999; Steltenpohl et al., 2009) and debated (Fossen and Rykkelid, 1992; Steltenpohl and Bartley, 1993). Two main models for Devonian extension throughout Scandinavia have been proposed. Fossen (1992) and Fossen and Rykkelid (1992) suggest that Devonian extension was caused by rifting in the core of the mountain belt, which resulted in west-vergent, hinterland-directed structures in the Scandinavia (Baltica) and east-vergent, hinterland-directed structures in Greenland (Laurentia). Andersen (1993) suggests, however, that over-thickening of the crust during the Early Devonian led to thermal upwelling, which caused both foreland- and hinterland-directed (east- and west-vergent, respectively) extensional movements (Fig. 37). East-vergence is the signature of Caledonian thrusting, and, therefore, if Devonian
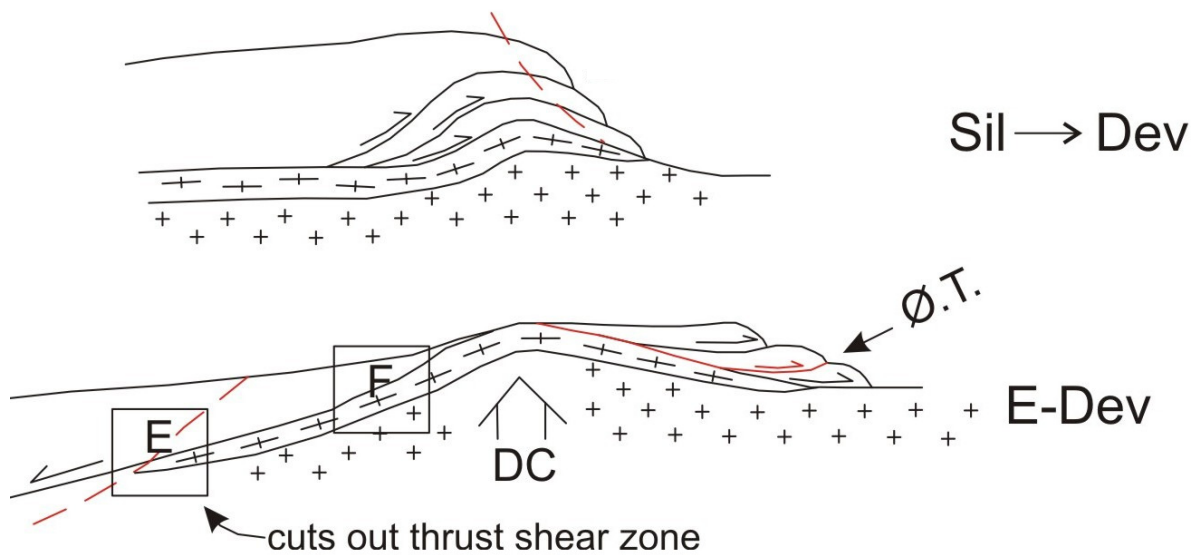
Figure 37. Schematic drawing that illustrates the formation of a thermal dome in response to the thickening of the nappe pile during Siluro-Devonian collision. The dashed red line in the top frame represents incipient, gravity-driven, foreland-directed extensional movement along the Øse thrust (Ø.T.). In the second frame, exhumation of the Devonian core (DC) is facilitated by extension in the foreland (right) and hinterland (left). E = Eidsfjord shear zone (tops-west movement); F = Fiskefjord shear zone (remnant, tops-east contractional shear zone; Mager, 2005).

foreland-directed extensional structures exist in north Norway, the key to differentiating them lies in thermochronological verification.

Anderson et al. (2008) report late-stage tops-east, out-of-sequence thrusting along the Øse thrust within the lower parts of the Ofoten nappe stack on mainland Norway directly east of the present study area. ^{40}Ar/^{39}Ar dates from the Øse thrust suggest timing of movement was in the middle-late Devonian (ca. 395-375 Ma). These ages overlap those documented herein on central Hinnøy. The out-of-sequence thrust style documented for the Øse thrust (Barker, 1989; Anderson et al., 1992) resembles the latest stage of thrusting along the Austerfjord thrust on Hinnøy (Rykkelid, 1992). The present author suggests that these late-stage, east-directed thrusts may represent foreland-directed extensional-collapse-driven movement. The west-directed Sørfjord shear zone appears to be a hinterland-directed counterpart that formed synchronously as a thermal core-complex dome formed in the lower plate, with the upper plate stretching over it and translated tops-west and tops-east. The earliest extensional structures would likely exploit and reactivate preexisting Caledonian contractional shear zones (tops-east thrusts), compatible with well documented low-angle normal faults world-wide (Axen, 1993). Fossen and Rykkelid (1992) and Lanphier (1996) documented evidence for tops-west kinematic indicators that overprint previously formed top-east thrusts in the Ofoten Nappe stack. A similar reactivation of tops-east contractional fabrics recently was documented west of Hinnøy in the Eidsfjord shear zone, which also records Early Devonian movement (Moecher and Steltenpohl, 2009; Steltenpohl et al., 2010). Back folds (Steltenpohl and Bartley, 1988) affecting both the upper and lower plates following

the peak of crustal thickening is documented even farther west in Lofoten, further supporting Devonian tops-west extensional-driven movements (Klein et al., 1999).

The complex geometry of shear zones and folds on central Hinnøy likely results from the hypothetical position of these structures within the hinge of a domal Devonian core-complex, separating east- and west-directed Devonian extensional movements. Thermochronological analyses have played an integral role in establishing the ideas presented in this thesis, and will facilitate continued refinement of models addressing timing of both Caledonian contraction and extension in the arctic Caledonides. Throughout the course of this research, it has become evident that many long-known problems still exist, including some to which no consensus has been reached (e.g., ages, provenance, and correlations of metasupracrustal/metasedimentary rocks; and ages and extents of basement rocks in Lofoten-Vesterålen). Future focused sampling and thermo-chronological analyses of metasiliciclastic and metaplutonic rocks will significantly aid in further unraveling the geologic history of this part of the Scandinavian Caledonides.

References

Andersen, T.B., 1993, The role of extensional tectonics in the Caledonides of south Norway: Discussion: Journal of Structural Geology, v. 15, n. 11, p. 1379-1380.

Andersen, T.B. and Jamtveit, B., 1990, Uplift of deep crust during orogenic extensional collapse: A model based on field studies in the Sogn-Sunnfjord region of Western Norway: Tectonics, v. 9, p. 1097-1111.

Anderson, M.W., Barker, A.J., Bennett, D.G., and Dallmeyer, R.D., 1992, A tectonic model for Scandian terrane accretion in the northern Scandinavian Caledonides: Journal of the Geological Society of London, v. 149, p. 1-15.

Anderson, M.W., Hames, W.E., and Stokes, A., 2008, The anatomy of a major late-stage thrust in the Caledonian crust of northern Scandinavia: 33rd International Geological Congress, Oslo, Norway, Abstracts Volume.

Andresen, A. and Tull, J.F., 1983, The age of the Lødingen granite and its possible regional significance: Norsk Geologisk Tidsskrift, v. 63, p. 269-276.

Axen, G., 1993, Ramp-flat detachment faulting and low-angle normal reactivation of the Tule Springs thrust, southern Nevada: Geological Society of America Bulletin, v. 105, p. 1076-1090.

Barker, A.J., 1989, Metamorphic evolution of the Caledonian nappes of north central Scandinavia, *in* Gayer, R.A. ed., The Caledonide Geology of Scandinavia: London, Graham and Trotman, p. 192-204.

Barnes, C.G., Frost, C.D., Yoshinobu, A.S., McArthur, K., Barnes, M.A., Allen, C.M., Nordgulen, Ø., and Prestvik, T., 2007, Timing of sedimentation, metamorphism, and plutonism in the Helgeland Nappe Complex, north-central Norwegian Caledonides: Geosphere, v. 3, n. 6, p. 683-703.

Bartley, J.M., 1980, Structural geology, metamorphism, and Rb/Sr geochronology of east Hinnøy, north Norway: Ph.D. thesis, Massachusetts Institute of Technology, Cambridge, Massachusetts, 263 p.

Bartley, J.M., 1981, Field relations, metamorphism, and age of the Middagstind Quartz Syenite: Norsk Geologisk Tidsskrift, v. 61, p. 237-248.

Bartley, J.M., 1982a, Limited basement involvement in Caledonian deformation, Hinnøy, north Norway, and tectonic implications: Tectonophysics, v. 83, p. 185-203.

Bartley, J.M., 1982b, Mesozoic high-angle faults, east Hinnøy, north Norway: Norsk Geologisk Tiddskrift, v. 61, p. 291-296.

Bergh, S.G., Eig, K., Kløvjan, O.S., Henningsen, T., Olesen, O., and Hansen, J.A., 2007a, The Lofoten-Vesterålen continental margin: a multiphase Mesozoic-Palaeogene rifted shelf as shown by offshore-onshore brittle fault-fracture analysis: Norwegian Journal of Geology, v. 87, p. 29-58.

Bergh, S.G., Kullerud, K., Corfu, F., Armitage, P.E.B., Davidsen, B., Johansen, H.W., Pettersen, T., and Knudsen, S., 2007b, Low-grade sedimentary rocks on Vanna, north Norway: a new occurrence of a Palaeoproterozoic (2.2-2.4 Ga) cover succession in northern Fennoscandia: Norwegian Journal of Geology, v. 87, p. 301-318.

Bingen, B., Nordgulen, Ø., and Viola, G., 2008, A four-phase model for the Sveco-norwegian orogeny, SW Scandinavia: Norwegian Journal of Geology, v. 88, p. 43-72.

Björklund, L.J.O., 1987, Basement-cover relationships and regional correlations of the Caledonian nappes, eastern Hinnøy, north Norway: Norsk Geologisk Tidsskrift, v. 67, p. 3-14.

Blatt, H. and Tracy, R.J., 1995, Petrology: Igneous, Sedimentary, and Metamorphic, 2nd ed.: W.H. Freeman and Company, New York, 529 p.

Cawood, P.A., Nemchin, A.A., Smith, M., and Loewy, S., 2003, Source of the Dalradian Supergroup constrained by U-Pb dating of detrital zircon and implication for East Laurentian margin: Journal of the Geological Society of London, v. 160, p. 231-246.

Coker, J.E., Steltenpohl, M.G., Andresen, A., and Kunk, M.J., 1995, An $^{40}Ar/^{39}Ar$ thermochronology of the Ofoten-Troms region: Implications for terrane amalgamation and extensional collapse of the northern Scandinavian Caledonides: Tectonics, v. 14, n. 2, p. 435-447.

Corfu, F., 2004a, U-Pb geochronology of the Leknes Group: an exotic Early Caledonian metasedimentary assemblage stranded on Lofoten basement, northern Norway: Journal of the Geological Society of London, v. 161, p. 619-627.

Corfu, F., 2004b, U-Pb age, setting and tectonic significance of the anorthosite-mangerite-charnockite-granite suite, Lofoten-Vesterålen, Norway: Journal of Petrology, v. 45, n. 9, p. 1799-1819.

Corfu, F., 2007, Multistage metamorphic evolution and nature of the amphibolite-granulite facies transition in Lofoten-Vesterålen, Norway, revealed by U-Pb in accessory minerals: Chemical Geology, v. 241, p. 108-128.

Cox, S.G., Griffin, P.F., Adams, C.S., DeMille, D., and Riis, E., 2003, Reusable ultrahigh vacuum viewport bakeable to 240 C: Review of Scientific Instruments, v. 74, n. 6, p. 3185-3187.

Cross, W.G., 1951, Two-directional focusing of charged particles with a sector-shaped, uniform magnetic field: Reviews of Scientific Instruments, v. 22, p.717-722.

Dodson, M.H., 1973, Closure temperature in cooling geochronological and petrological systems: Contributions to Mineralogy and Petrology, v. 40, n. 3, p. 259-274.

Fossen, H., 1992, The role of extensional tectonics in the Caledonides of South Norway: Journal of Structural Geology, v. 14, p. 1033-1046.

Fossen, H. and Rykkelid, E., 1992, Postcollisional extension of the Caledonide orogen in Scandinavia: Structural expressions and tectonic significance: Geology, v. 20, p. 737-740.

Graham, D.J. and Midgley, N.G., 2000, Graphical representation of particle shape using triangular diagrams: an excel spreadsheet method: Earth Surface Processes and Landforms, v. 25, p. 1473-1477.

Griffin, W.L., Heier, K.S., Taylor, P.N., and Weigand, P.W., 1974, General geology, age and chemistry of the Raftsund mangerite intrusion, Lofoten-Vesterålen: Norges Geologiske Undersøkelse, v. 312, p. 1-30.

Griffin, W.L., Taylor, P.N., Hakkinen, J.W., Heier, K.S., Iden, I.K., Krogh, E.J., Malm, O., Olsen, K.I., Ormassen, D.E., and Tveten, E., 1978, Archean and Proterozoic crustal evolution of Lofoten-Vesterålen, north Norway: Journal of the Geological Society of London, v. 135, p. 629–647.

Gustavson, M., 1974, Berggrunnskart Narvik, 1:250,000: Norges Geologiske Under-søkelse, Trondheim.

Hakkinen, J.W., 1977, Structural geology and metamorphic history of western Hinnøy and adjacent parts of eastern Hinnøy, north Norway: Ph.D. thesis, Rice University, Houston, TX, USA, 161 p.

Hames, W.E., and Bowring, S.A., 1994, An empirical study of the argon diffusion geometry in muscovite: Earth and Planetary Science Letters, v. 124, p. 161-169.

Hames, W.E. and Andresen, A., 1996, Timing of Paleozoic orogeny and extension in the continental shelf of north-central Norway as indicated by laser ^{40}Ar/^{39}Ar muscovite dating: Geology, v. 24, no. 11, p. 1005-1008.

Hatcher, R.D., 2008, Nature of the Talladega front in the Sylacauga, Alabama area, *in* Higgins, M.W., Crawford, R.F., and Hatcher, R.D., Alternative interpretations of the Talladega slate belt, Alabama and Georgia: Field Trip Guidebook for the 45th Annual Meeting of The Alabama Geological Society: Tuscaloosa, Alabama, p. 30-42.

Heier, K.S. and Compston, W., 1969, Interpretation of Rb-Sr age patterns in high grade metamorphic rocks, north Norway: Norsk Geologisk Tidsskrift, v. 49, p. 257-283.

Hodges, K.V., Bartley, J.M., and Burchfiel, B.C., 1982, Structural evolution of an A-type subduction zone, Lofoten-Rombak area, northern Scandinavian Caledonides: Tectonics, v. 1, no. 5, p. 441-462.

Kautsky, G., 1987, Geologic map of pre-Quaternary rocks of northern Fennoscandia, 1:1,000,000: Geologic Surveys of Finland, Norway, and Sweden, Helsinki, Finland.

Key, T.B., Steltenpohl, M.G., Hames, W.E., Andresen, A., and Ball, J.B., 2007, Reconciling metamorphic timing between Precambrian basement and Caledonian allochthonous cover in the Lofoten terrane, north Norway: Geological Society of America Abstracts with Programs, v. 39, n. 6, p. 229.

Klein, A., Steltenpohl, M.G., Hames, W.E., and Andresen, A., 1999, Ductile and brittle extension in the southern Lofoten archipelago, north Norway: implications for differences in tectonic style along an ancient collisional margin: American Journal of Science, v. 299, p. 69-89.

Krogh, E., 1976, Origin and metamorphism of iron formation and associated rocks, Lofoten-Vesterålen, north Norway, The Vestpollitind Fe-Mn deposit: Lithos, v. 9.

Lanphier, A.Y., 1996, Geological transects from the base of the Ofoten nappe complex into the Precambrian Baltic basement, Ofoten, north Norway, and their implications for Caledonian tectonics, Unpublished M.S. thesis, Auburn University, Auburn, Alabama, 93 p.

Ludwig, K.R., 2003, User's manual for Isoplot, v. 3.0, a geochronological toolkit for Microsoft Excel: Berkeley Geochronological Center, Special Publication n. 4.

Mager, S., 2005, The late- to post-Caledonian extensional history of northwest Hinnøy, north Norway: M.S. Thesis, Auburn University, Auburn, Alabama, 98 p.

McDougall, I. and Harrison, T.M., 1999, Geochronology and Thermochronology by the $^{40}Ar/^{39}Ar$ Method, 2nd ed.: Oxford University Press, Oxford, 269 p.

Mies, J.W., 1993, Structural analysis of sheath folds in the Sylacauga Marble Group, Talladega slate belt, Southern Appalachians: Journal of Structural Geology, v. 15, n. 8, p. 983-993.

Moecher, D.P. and Steltenpohl, M.G., 2009, Direct calculation of rupture depth for an exhumed paleoseismogenic fault from mylonitic pseudotachylyte: Geology, v. 37; no. 11; p. 999-1002.

Northrup, C.J., 1997, Timing Structural Assembly, Metamorphism, and Cooling of Caledonian Nappes in the Ofoten-Efjorden Area, North Norway: Tectonic Insights from U-Pb and $^{40}Ar/^{39}Ar$ Geochronology: Journal of Geology, p. 565-582.

Passchier, C.W. and Trouw, R.A.J., 1996, Microtectonics: Springer-Verlag, Berlin, 289 p.

Renne, P.R., Swisher, C.C., Deino, A.L., Karner, D.B., Owens, T.L., and DePaolo, D.J., 1998, Intercalibration of standards, absolute ages and uncertainties in $^{40}Ar/^{39}Ar$ dating: Chemical Geology, v. 145, n. 1-2, p. 117-152.

Roberts, D., 2003, The Scandinavian Caledonides: Event chronology, paleogeographic settings and likely modern analogues: Tectonophysics, v. 365, p. 283-299.

Rykkelid, E., 1992, Contractional and extensional structures in the Caledonides: Sc.D. thesis, University of Oslo, Oslo, Norway, 176 p.

Steltenpohl, M.G., 1987, Tectonostratigraphy and tectonic evolution of the Skånland area, north Norway: Norges Geologiske Undersøkelse, Bulletin 409, p. 1-19.

Steltenpohl, M.G. and Bartley, J.M., 1984, Kyanite grade metamorphism in the Evenes and Bogen Groups, Ofoten, north Norway: Norsk Geologisk Tiddskrift, v. 64, p. 21-26.

Steltenpohl, M.G. and Bartley, J.M., 1987, Thermobarometric profile through the Caledonian nappe stack of western Ofoten, north Norway: Contributions to Mineralogy and Petrology, v. 96, p. 93 103.

Steltenpohl, M.G. and Bartley, J.M., 1988, Cross folds and back folds in the Ofoten-Tysfjord area, north Norway, and their significance for Caledonian tectonics: Geological Society of America Bulletin, v. 100, p. 140-151.

Steltenpohl, M.G. and Bartley, J.M., 1993, Comment on "Postcollisional extension of the Caledonide orogen in Scandinavia: Structural expressions and tectonic significance": Geology, v. 21, p. 476-477.

Steltenpohl, M.G., Andresen, A., Lindstrøm, M., Gromet, P., and Steltenpohl, L.W., 2003a, The role of felsic and mafic igneous rocks in deciphering the evolution of thrust-stacked terranes: an example from the north Norwegian Caledonides: American Journal of Science, v. 303, p.149-185.

Steltenpohl, M.G., Hames, W.E., Andresen, A., and Markl, G., 2003b, New Caledonian eclogite province in Norway and potential Laurentian (Taconic) and Baltic links: Geology, v. 31, no. 11, p. 985-988.

Steltenpohl, M.G., Hames, W.E., and Andresen, A., 2004, The Silurian to Permian history of a metamorphic core complex in Lofoten, northern Scandinavian Caledonides: Tectonics, v. 23, p. 1-23.

Steltenpohl, M.G., Kassos, G., and Andresen, A., 2006, Retrograded eclogite-facies pseudotachylytes as deep-crustal paleoseismic faults within continental basement of Lofoten, north Norway: Geosphere, v. 2, no. 1, p. 61-72.

Steltenpohl, M.G., Carter, B.T., Andresen, A., and Zeltner, D.L., 2009, ^{40}Ar/^{39}Ar Thermochronology of Late- and Postorogenic Extension in the Caledonides of North-Central Norway: The Journal of Geology, v. 117, p. 399-414.

Steltenpohl, M.G., Ball, J.B., Moecher, D.P., and Andresen, A., 2010, The Eidsfjord detachment: an Early Devonian, paleoseismogenic low-angle normal detachment fault exposed in Lofoten-Vesterålen, north Norway: Norges Geologisk Forening (Geological Society of Norway), Nordic Geologic Winter Meeting, Abstracts and Proceedings, no. 1, p 186-189.

Stephens, M.B., Kullerud, K., Claesson, S., 1993, Early Caledonian tectonothermal evolution in outboard terranes, central Scandinavian Caledonides; new constraints from U-Pb zircon dates: Journal of the Geological Society of London, v. 150, no. 1, p. 51-56.

Taylor. P.N., 1974, Isotope geology and related geochemical studies of ancient high-grade metamorphic basement complexes: Lofoten and Vesterålen, north Norway: Ph.D. thesis, University of Oxford.

Tull, J.F., 1973, The Geology and Structure of Vestvågøy in Lofoten, North Norway: Ph.D Thesis, Rice University, Houston, Texas.

Tull, J.F., 1977, Geology and Structure of Vestågøy, Lofoten, North Norway: Norges Geologiske Undersøkelse, Bulletin 333, 59 p.

Tull, J.F., Bartley, J.M., Hodges, K.V., Andresen, A., Steltenpohl, M.G., and White, J.M., 1985, The Caledonides in the Ofoten region (68-69°N), north Norway: Key aspects of tectonic evolution, *in* Gee, D.G., and Sturt, B.A., (eds.), The

Caledonide Orogen in Scandinavia and Related Areas, Wiley Interscience, New York, p. 553-569.

Tveten, E., 1978, Geologisk kart over Norge, berggrunnskart Svolvær 1:250,000: Norges Geologiske Undersøkelse, Trondheim.

Van Winkle, S.W., Steltenpohl, M.G., and Andresen, A., 1996, Basement-cover relations and Caledonian tectonostratigraphy of Sandsøya, Grytøya, Åkerøya, and Kjøtta, Western Gneiss Region, north Norway: Norges Geologiske Undersøkelse, Bulletin 431, p. 67-69.

Vogt, T., 1941, Trekk av Narvik – Ofoten traktens geologi: Norges Geologiske Under-søkelse, v. 21, p. 198-213.

Wade, S.J.R., 1985, Radiogenic isotope studies of crust-forming processes in the Lofoten-Vesterålen Province of north Norway: Ph.D. thesis, University of Oxford.

Walsh, E.O., Hacker, B.R., Gans, P.B., Grove, M., and Gehrels, G., 2007, Protolith ages and exhumation histories of (ultra)high-pressure rocks across the Western Gneiss Region, Norway: Geological Society of America Bulletin, v. 119, p. 289-301.

Yoshinobu, A.S., Barnes, C.G., Nordgulen, Ø., Prestvik, T., Fanning, M., and Pedersen, R.B., 2002, Ordovician magmatism, deformation, and exhumation in the Caledonides of central Norway: An orphan of the Taconic orogeny?: Geology, v. 30, p. 883-886.

Appendix I

This appendix contains argon isotope data collected at the Auburn Noble Isotope Mass Analysis Laboratory (ANIMAL) at Auburn University, under the supervision of Dr. W.E. Hames. Muscovite grains were separated from granitic mylonites, JB07-100A and JB07-101; granitic L-tectonites, TK07-23 and TK07-40; and quartzite, JB07-13 and dated by fusion of single crystals. The monitor mineral FC-2 (from a split prepared by New Mexico Tech) was used to determine J-values (see McDougall and Harrison, 1999) with the age of 28.02 Ma assigned to FC-2 (after Renne et al. 1998). All argon data are recorded in moles. Table headings for argon data are reported as follows:

^{40}Ar (*, atm) – Radiogenic ^{40}Ar derived from natural decay of ^{40}K

and the atmosphere;

^{39}Ar (K) – ^{39}Ar derived from ^{39}K by irradiation;

^{38}Ar (Cl, atm) – ^{38}Ar derived from chlorine and the atmosphere;

^{37}Ar (Ca) – ^{37}Ar derived from calcium;

^{36}Ar (atm) – ^{36}Ar derived from the atmosphere.

The following paragraphs contain an analytical description of the ANIMAL facility. The facility is equipped with an ultra-high vacuum, 90-degree sector, 10 cm radius spectrometer optimized for ^{40}Ar/^{39}Ar research (single-crystal and multigrain sample incremental heating). The spectrometer employs second-order focusing (Cross, 1951), and is fitted with a high sensitivity electron-impact source and a single ETP electron multiplier (with signal amplification through a standard pre-amplifier). Analyses

are typically made using a filament current of 2.75 A, and potentials for the source and multiplier of 2000 V and -1300 V, respectively. The total volume of the spectrometer is 400 cc. Resolution in the instrument (with fixed slits for the source and detector) is constrained to ~150, and the high sensitivity and low blank of the instrument permits measurement of 10^{-14} mole samples to within 0.2% precision. Analyses comprise 10 cycles of measurement over the range of masses and half-masses from m/e=40 to m/e=35.5, and baseline corrected values are extrapolated to the time if inlet, or averaged, depending upon signal evolution.

The extraction line for this system utilizes a combination of Varian 'mini' and Nupro pneumatic valves, and Varian turbomolecular and ion pumps. Analysis of samples and blanks is fully automated under computer control. Pumping of residual and sample reactive gases is accomplished through use of SAES AP-10 non-evaporable getters. Pressures in the spectrometer and extraction line, as measured with an ionization gauge, are routinely below ~$5x10^{-9}$ torr. A pipette delivers standard aliquots of air for use in measuring sensitivity and mass discrimination. Typical recent measurements of $^{40}Ar/^{36}Ar$ in air were ~293.

The extraction line is fitted with a 50W Synrad CO_2 IR laser for heating and fusing silicate minerals and glasses. The sample chamber uses a Cu planchet, KBr cover slips, and low-blank UHV ZnS window (manufactured at Auburn University and based on the design of Cox et al., 2003). In the present configuration, this laser system is suitable for incremental heating and fusion analysis of single crystals and multigrain samples. The laser beam delivery system utilizes movable optical mounts and a fixed sample chamber to further minimize volume and improve conductance of the extraction

line. (The time required to inlet, or equilibrate, a 'half-split' of a sample is less than 7 s, and the inlet time for a full sample is ca. 20 s.) Typical blanks for the entire system (4 minute gettering time) are as follows (in moles): ^{40}Ar, 7.6×10^{-17}; ^{39}Ar, 1.3×10^{-17}; ^{38}Ar, 2.8×10^{-18}; ^{37}Ar, 2.0×10^{-18}; ^{36}Ar, 1.2×10^{-18}.

Computer control of the laser, positioning of laser optics, extraction line, mass spectrometer, and data recording is enabled with National Instruments hardware and a Labview program written by lab personnel specifically for ANIMAL. Initial data reduction is accomplished through an in-house Excel spreadsheet, with final reduction using Isoplot (Ludwig, 2003). Figures drawn using Isoplot were constructed using uncertainties of 1σ.

TK07-40 SINGLE CRYSTAL TOTAL FUSION (J-Value = 0.014555) Size range: ~300-600 μm

# P t	$^{40}Ar(*,atm)$	$^{39}Ar(K)$	$^{38}Ar(Cl,atm)$	$^{37}Ar(Ca)$	$^{36}Ar(atm)$	%Rad	R	Age (Ma)	%-sd
1 16 7	2.522E-14 ± 2.84E-17	1.573E-15 ± 3.57E-18	3.66E-18 ± 3.86E-20	1.40E-18 ± 2.40E-19	8.03E-19 ± 6.35E-20	99.1%	15.878	375.1 ± 1.0	0.3%
2 16 7	5.497E-15 ± 6.31E-18	3.386E-16 ± 8.01E-19	1.72E-18 ± 8.93E-20	4.87E-19 ± 1.97E-19	6.61E-19 ± 6.13E-20	96.4%	15.655	370.3 ± 1.6	0.4%
3 16 7	3.596E-14 ± 3.74E-17	2.293E-15 ± 6.64E-18	5.51E-18 ± 7.64E-20	2.72E-18 ± 3.42E-19	1.13E-18 ± 7.30E-20	99.1%	15.536	367.8 ± 1.2	0.3%
4 16 7	3.778E-14 ± 8.07E-17	2.415E-15 ± 3.10E-18	4.02E-18 ± 3.42E-19	3.22E-18 ± 6.56E-19	7.68E-19 ± 5.52E-20	99.4%	15.546	368.0 ± 0.9	0.3%
5 16 7	1.559E-14 ± 2.53E-17	9.672E-16 ± 2.23E-18	2.17E-18 ± 8.22E-20	1.12E-18 ± 3.76E-19	4.87E-19 ± 1.57E-19	99.1%	15.975	377.2 ± 1.6	0.4%
6 16 7	3.875E-14 ± 2.66E-17	2.448E-15 ± 3.32E-18	5.76E-18 ± 1.00E-19	2.69E-18 ± 4.80E-19	1.41E-18 ± 1.04E-19	98.9%	15.661	370.5 ± 0.6	0.2%
7 16 7	1.721E-14 ± 8.22E-18	1.066E-15 ± 1.89E-18	2.62E-18 ± 6.97E-20	1.99E-19 ± 1.64E-18	3.07E-19 ± 5.98E-20	99.5%	16.059	378.9 ± 0.8	0.2%
8 16 7	1.567E-14 ± 1.03E-17	9.751E-16 ± 1.70E-18	2.16E-18 ± 2.66E-20	-1.75E-19 ± 2.79E-19	1.01E-18 ± 6.56E-20	98.1%	15.767	372.7 ± 0.9	0.2%
9 16 7	1.114E-14 ± 1.00E-17	6.862E-16 ± 1.40E-18	1.79E-18 ± 4.46E-20	6.68E-21 ± 1.51E-19	7.69E-19 ± 8.63E-20	98.0%	15.911	375.8 ± 1.2	0.3%
10 16 7	2.046E-14 ± 3.85E-17	1.310E-15 ± 2.18E-18	2.30E-18 ± 5.84E-20	1.04E-18 ± 3.30E-19	1.61E-19 ± 6.27E-20	99.8%	15.586	368.9 ± 1.0	0.3%

Weighted Mean Age: 372.4 ± 2.8 Ma

All uncertainties 1σ
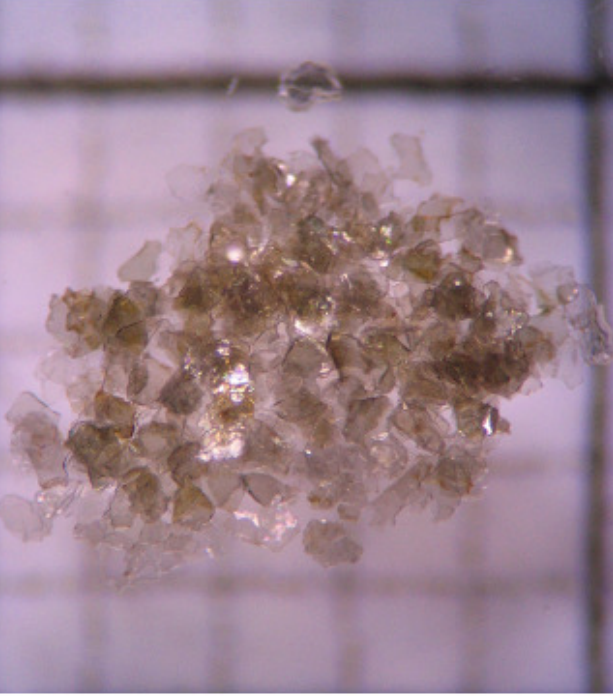
– Analysis number

P – Laser power in % full power

t – Time of laser heating (s)

TK07-23 SINGLE CRYSTAL TOTAL FUSION (J-Value = 0.014555) Size range: ~300-700 µm

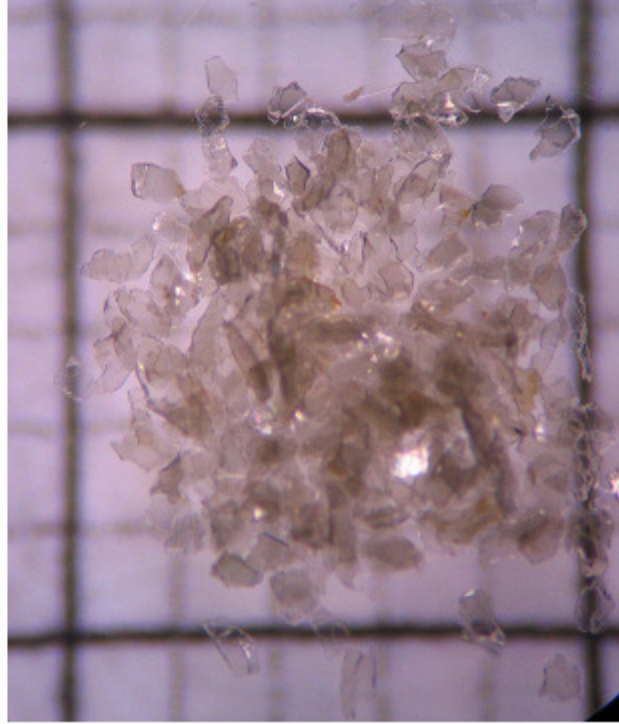| #	P	t	^{40}Ar(*,atm)	^{39}Ar(K)	^{38}Ar(Cl,atm)	^{37}Ar(Ca)	^{36}Ar(atm)	%Rad	R	Age (Ma)	%-sd
11	16	7	1.264E-14 ± 4.15E-17	7.974E-16 ± 4.03E-18	1.85E-18 ± 1.04E-19	1.43E-18 ± 4.17E-19	4.56E-19 ± 1.14E-19	98.9%	15.684	373.8 ± 2.5	0.7%
12	16	7	3.169E-14 ± 3.46E-17	2.015E-15 ± 4.90E-18	5.25E-18 ± 4.73E-20	3.32E-18 ± 5.26E-19	2.02E-18 ± 8.48E-20	98.1%	15.433	368.4 ± 1.0	0.3%
13	16	7	1.751E-14 ± 8.91E-18	1.115E-15 ± 3.73E-18	3.04E-18 ± 9.77E-20	1.85E-18 ± 3.87E-19	3.94E-19 ± 8.05E-20	99.3%	15.598	372.0 ± 1.4	0.4%
14	16	7	1.957E-14 ± 1.78E-17	1.223E-15 ± 5.53E-18	2.90E-18 ± 4.63E-20	1.78E-18 ± 4.37E-19	2.80E-19 ± 7.12E-20	99.6%	15.944	379.4 ± 1.8	0.5%
15	16	7	1.886E-14 ± 1.59E-17	1.199E-15 ± 2.45E-18	2.99E-18 ± 5.37E-20	1.58E-18 ± 3.47E-19	3.57E-19 ± 7.46E-20	99.4%	15.637	372.8 ± 0.9	0.3%
16	16	7	6.181E-14 ± 3.24E-17	3.939E-15 ± 7.44E-18	9.56E-18 ± 9.99E-20	5.05E-18 ± 6.89E-19	6.85E-19 ± 9.46E-20	99.7%	15.640	372.9 ± 0.8	0.2%
17	16	7	4.592E-14 ± 1.99E-17	2.936E-15 ± 6.92E-18	6.48E-18 ± 7.87E-20	3.68E-18 ± 6.20E-19	7.91E-19 ± 9.45E-20	99.5%	15.563	371.2 ± 0.9	0.2%
18	16	7	4.906E-14 ± 2.73E-17	3.093E-15 ± 9.39E-18	7.29E-18 ± 6.42E-20	1.09E-18 ± 4.79E-19	3.35E-19 ± 9.41E-20	99.8%	15.829	376.9 ± 1.2	0.3%
19	16	7	3.951E-14 ± 1.81E-17	2.545E-15 ± 7.34E-18	6.32E-18 ± 7.02E-20	1.77E-18 ± 5.67E-19	2.20E-19 ± 9.00E-20	99.8%	15.502	369.9 ± 1.1	0.3%
20	16	7	3.022E-14 ± 2.59E-17	1.899E-15 ± 1.06E-17	4.28E-18 ± 7.57E-20	1.06E-18 ± 4.76E-19	1.39E-19 ± 8.23E-20	99.9%	15.892	378.3 ± 2.2	0.6%

Weighted Mean Age: 372.5 ± 2.1 Ma

All uncertainties 1σ

– Analysis number
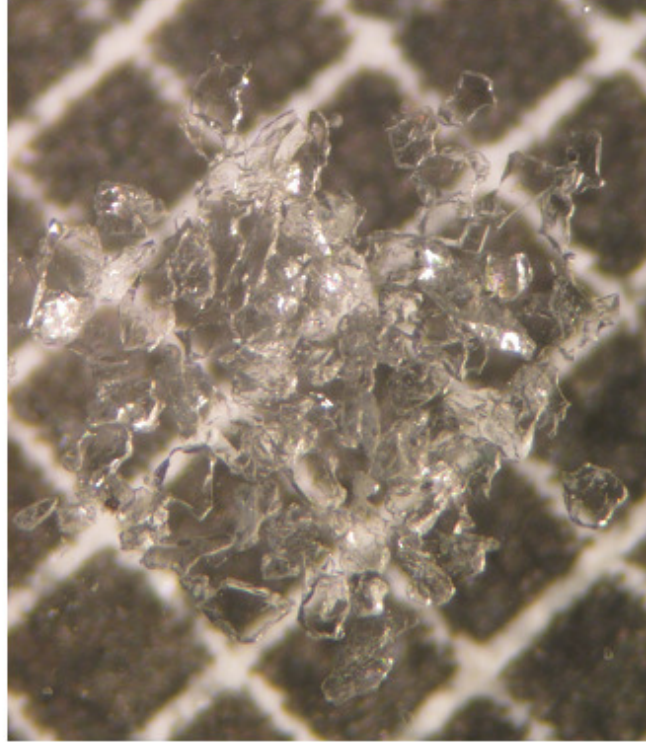P – Laser power in % full power
t – Time of laser heating (s)

JB07-13 SINGLE CRYSTAL TOTAL FUSION (J-Value = 0.014555) Size range: ~250-600 µm

#	P	t	^{40}Ar(*, atm)	^{39}Ar(K)	^{38}Ar(Cl, atm)	^{37}Ar(Ca)	^{36}Ar(atm)	%Rad	R	Age (Ma)	%-sd
61	16	7	1.935E-14 ± 1.50E-17	1.190E-15 ± 1.60E-18	1.79E-18 ± 7.67E-20	7.22E-19 ± 5.3E-19	-1.33E-19 ± -1.56E-19	100.2%	16.293	381.4 ± 1.1	0.3%
62	16	7	2.041E-14 ± 1.88E-17	1.224E-15 ± 1.91E-18	4.20E-18 ± 9.09E-20	3.12E-19 ± 4.9E-19	2.56E-18 ± 1.15E-19	96.3%	16.054	376.3 ± 1.0	0.3%
63	16	7	2.025E-14 ± 5.01E-17	1.251E-15 ± 5.15E-18	1.72E-18 ± 7.47E-20	-5.20E-19 ± 3.85E-19	5.76E-20 ± 1.37E-19	99.9%	16.181	379.0 ± 2.0	0.5%
64	16	7	3.254E-14 ± 5.41E-17	1.988E-15 ± 5.33E-18	4.26E-18 ± 5.50E-20	5.74E-19 ± 4.78E-19	1.52E-19 ± 9.09E-20	99.9%	16.350	382.6 ± 1.2	0.3%
65	16	7	1.980E-14 ± 2.23E-17	1.211E-15 ± 4.18E-18	2.95E-18 ± 7.85E-20	-1.20E-18 ± 4.23E-19	3.99E-19 ± 9.66E-20	99.4%	16.251	380.5 ± 1.5	0.4%
66	16	7	2.556E-14 ± 2.52E-17	1.583E-15 ± 9.07E-18	3.92E-18 ± 6.47E-20	5.82E-19 ± 4.72E-19	1.87E-19 ± 9.50E-20	99.8%	16.114	377.6 ± 2.2	0.6%
67	16	7	2.749E-14 ± 4.13E-17	1.738E-15 ± 3.55E-18	4.47E-18 ± 5.80E-20	7.78E-19 ± 4.73E-19	3.47E-19 ± 8.16E-20	99.6%	15.759	370.1 ± 1.0	0.3%
68	16	7	2.922E-14 ± 1.95E-17	1.803E-15 ± 4.04E-18	4.63E-18 ± 6.17E-20	1.03E-18 ± 5.38E-19	2.46E-19 ± 9.70E-20	99.8%	16.165	378.7 ± 1.0	0.3%
69	16	7	3.959E-14 ± 4.29E-17	2.439E-15 ± 4.50E-18	6.31E-18 ± 6.13E-20	5.65E-18 ± 3.59E-19	8.13E-20 ± 9.38E-20	99.9%	16.225	380.0 ± 0.9	0.2%
70	16	7	2.149E-14 ± 1.07E-17	1.335E-15 ± 1.02E-18	2.34E-18 ± 6.68E-20	-2.97E-20 ± 5.51E-19	-3.97E-21 ± -1.05E-19	100.0%	16.096	377.2 ± 0.6	0.2%

Weighted Mean Age: 378.8 ± 1.6 Ma

All uncertainties 1σ

– Analysis number
P – Laser power in % full power
t – Time of laser heating (s)

JB07-100A SINGLE CRYSTAL TOTAL FUSION (J-Value = 0.014555) Size range; ~300-600 μm

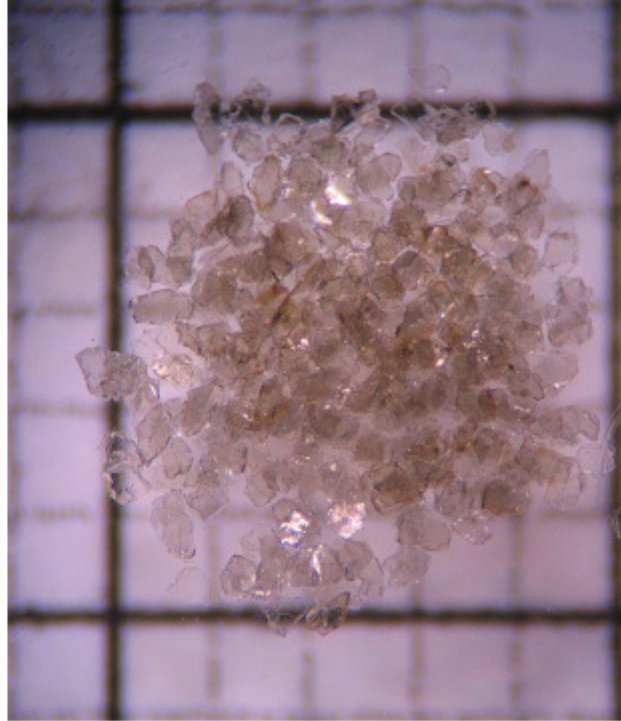| # P t	^{40}Ar(*, atm)	^{39}Ar(K)	^{38}Ar(Cl, atm)	^{37}Ar(Ca)	^{36}Ar(atm)	%Rad	R	Age (Ma)	%-sd
1 16 7	4.310E-14 ± 4.87E-17	2.641E-15 ± 7.46E-18	5.67E-18 ± 1.07E-19	3.09E-17 ± 6.73E-19	1.31E-18 ± 9.48E-20	99.1%	16.172	384.3 ± 1.2	0.3%
2 16 7	1.901E-14 ± 1.75E-17	1.129E-15 ± 6.06E-18	2.36E-18 ± 7.37E-20	1.22E-18 ± 4.49E-19	1.48E-18 ± 9.84E-20	97.7%	16.444	390.1 ± 2.3	0.6%
3 16 7	1.326E-14 ± 1.36E-17	8.160E-16 ± 2.73E-18	2.00E-18 ± 6.97E-20	5.88E-19 ± 3.10E-19	5.90E-19 ± 1.06E-19	98.7%	16.030	381.2 ± 1.6	0.4%
4 16 7	1.145E-14 ± 1.37E-17	6.906E-16 ± 1.61E-18	1.84E-18 ± 8.00E-20	1.39E-18 ± 4.21E-19	5.19E-19 ± 8.18E-20	98.7%	16.361	388.3 ± 1.3	0.3%
5 16 7	6.517E-14 ± 2.66E-17	4.021E-15 ± 7.22E-18	1.02E-17 ± 1.55E-19	6.67E-18 ± 5.00E-19	7.65E-19 ± 9.88E-20	99.7%	16.152	383.9 ± 0.7	0.2%
6 16 7	5.346E-14 ± 1.41E-16	3.283E-15 ± 1.46E-17	7.36E-18 ± 9.21E-20	1.38E-17 ± 2.72E-19	1.55E-18 ± 9.46E-20	99.1%	16.145	383.7 ± 2.0	0.5%
7 16 7	1.847E-14 ± 4.05E-17	1.093E-15 ± 4.24E-18	3.48E-18 ± 1.06E-19	2.39E-18 ± 4.35E-19	2.14E-18 ± 9.07E-20	96.6%	16.321	387.5 ± 1.9	0.5%
8 16 7	3.508E-14 ± 7.86E-17	2.127E-15 ± 6.97E-18	4.58E-18 ± 9.23E-20	9.13E-19 ± 5.52E-19	1.06E-18 ± 9.14E-20	99.1%	16.344	388.0 ± 1.6	0.4%
9 16 7	3.295E-14 ± 2.84E-17	2.030E-15 ± 5.30E-18	4.43E-18 ± 1.04E-19	1.76E-18 ± 5.39E-19	7.10E-19 ± 9.12E-20	99.4%	16.131	383.4 ± 1.1	0.3%
10 16 7	3.474E-14 ± 7.33E-18	2.120E-15 ± 7.44E-18	5.55E-18 ± 7.51E-20	9.20E-19 ± 5.40E-19	1.55E-18 ± 8.79E-20	98.7%	16.173	384.3 ± 1.4	0.4%

Weighted Mean Age: 384.8 ± 1.6 Ma

All uncertainties 1σ

– Analysis number
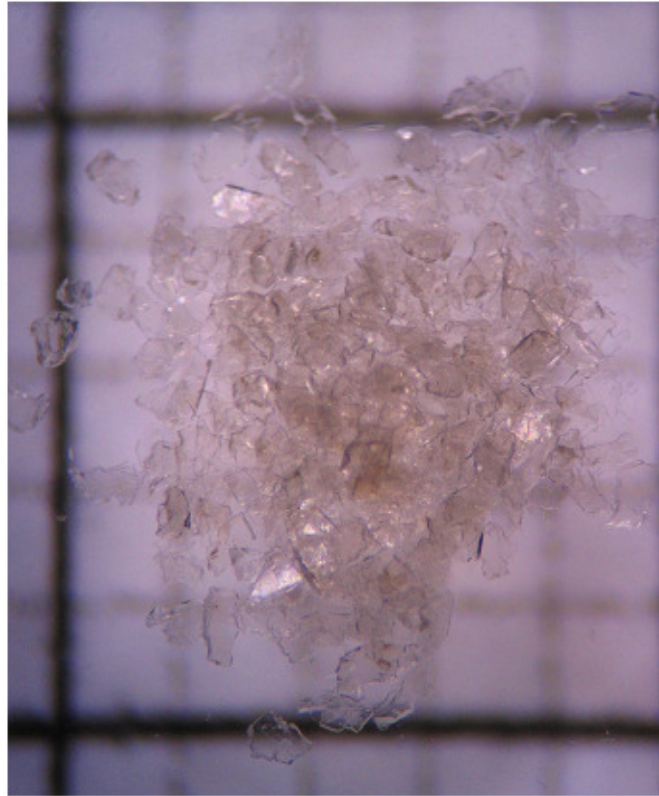P – Laser power in % full power
t – Time of laser heating (s)

JB07-101 SINGLE CRYSTAL TOTAL FUSION (J-Value = 0.014555) Size range: ~300-600 µm

#	P	t	^{40}Ar (*, atm)	^{39}Ar (K)	^{38}Ar (Cl, atm)	^{37}Ar (Ca)	^{36}Ar (atm)	%Rad	R	Age (Ma)	%-sd
91	16	7	1.882E-14 ± 3.48E-16	1.111E-15 ± 2.16E-17	2.91E-18 ± 9.91E-20	-7.90E-18 ± 9.23E-18	5.47E-19 ± 7.85E-20	99.1%	16.7963	395.9 ± 10.7	2.7%
92	16	7	3.487E-14 ± 1.74E-16	2.033E-15 ± 2.49E-17	5.67E-18 ± 1.39E-19	-6.25E-18 ± 4.97E-18	8.84E-19 ± 6.28E-20	99.3%	17.0205	400.6 ± 5.3	1.3%
93	16	7	2.452E-14 ± 2.63E-17	1.466E-15 ± 4.09E-18	2.97E-18 ± 5.59E-20	-6.11E-18 ± 5.93E-18	4.04E-19 ± 5.92E-20	99.5%	16.6443	392.7 ± 1.2	0.3%
94	16	7	1.776E-14 ± 5.72E-17	1.066E-15 ± 7.28E-18	1.82E-18 ± 2.95E-20	-1.07E-17 ± 4.57E-18	9.22E-19 ± 6.65E-20	98.5%	16.4068	387.6 ± 3.0	0.8%
95	16	7	1.184E-14 ± 1.86E-17	6.571E-16 ± 4.31E-18	8.78E-19 ± 2.22E-20	-1.14E-17 ± 4.98E-18	7.53E-20 ± 6.88E-20	99.8%	17.9880	420.9 ± 2.9	0.7%
96	16	7	7.460E-15 ± 1.06E-17	4.497E-16 ± 4.49E-18	6.73E-19 ± 1.88E-20	5.83E-18 ± 5.67E-18	3.09E-19 ± 6.36E-20	98.8%	16.3875	387.2 ± 4.1	1.1%
97	16	7	9.705E-15 ± 1.33E-17	5.809E-16 ± 2.79E-18	1.12E-18 ± 3.08E-20	-5.01E-18 ± 7.55E-18	-2.95E-20 ± 9.19E-20	100.1%	16.7219	394.3 ± 2.3	0.6%
98	16	7	2.643E-14 ± 2.54E-17	1.593E-15 ± 4.13E-18	3.11E-18 ± 7.50E-20	-1.85E-18 ± 4.42E-18	2.98E-19 ± 8.51E-20	99.7%	16.5377	390.4 ± 1.1	0.3%
99	16	7	2.058E-14 ± 2.04E-17	1.230E-15 ± 4.24E-18	2.79E-18 ± 3.66E-20	2.56E-19 ± 5.83E-18	8.53E-19 ± 8.72E-20	98.8%	16.5305	390.3 ± 1.5	0.4%
100	16	7	1.239E-14 ± 2.73E-17	7.399E-16 ± 6.15E-18	1.57E-18 ± 4.43E-20	-4.33E-18 ± 6.25E-18	9.74E-19 ± 6.30E-20	97.7%	16.6236	392.2 ± 3.5	0.9%

Weighted Mean Age: 391.4 ± 1.7 Ma

All uncertainties 1σ

– Analysis number
P – Laser power in % full power
t – Time of laser heating (s)

119